Reshaping of beach nourishments under high angle of wave incidence

Master of Science Thesis

by

Victoria Curto, P.E.

Master of Science Thesis Committee

Prof. dr. ir. M.J.F. (Marcel) Stive	**Chairman TU Delft**
Ir. B.J.A. (Bas) Huisman	**TU Delft and Deltares**
Ir. R. (Roderik) Hoekstra	**Deltares**
Dr. ir. M. (Matthieu) de Schipper	**TU Delft**
Ir. D. P. (Dirk) Rijnsdorp	**TU Delft**

TU Delft Delft University of Technology

Deltares Enabling Delta Life

Preface

The following report presents the Master of Science Thesis titled *"Reshaping Mechanisms of Beach Nourishments under High Angle Wave Conditions"* submitted as a partial fulfillment of the requirements for the degree of Master of Science (MSc) in Civil Engineering, Hydraulic Engineering Track, Coastal Engineering Specialization, taught at Delft University of Technology in Delft, Netherlands.

This MSc Thesis was conducted at and supported by Deltares from May to November 2014 under the main supervision of Ir. Bas Huisman to whom I would like to express my deepest gratitude. I would like to thank him for letting me be part of his PhD research project and specially for trusting his idea in me. As an engineer, it has been an enriching experience to have learned from and with him; I am thankful for his guidance and objective input throughout the entire research process, particularly during the closing phase of my thesis.

I would like to thank the head of my thesis committee Prof. Marcel Stive for giving me the opportunity to work in the NEMO project as a student assistant during my complete tenure at TU Delft, also for his research recommendations, and for his support toward the successful culmination of my MSc thesis. I would also like to thank my committee members Ir. Roderik Hoekstra, Dr. Matthieu de Schipper, and Ir. Dirk Rijnsdorp for their interest and feedback. Deltares as an organization provided me with the necessary tools to complete my project for which I am grateful; more importantly within Deltares, I would like to express my honest gratitude to Ir. Pieter Koen Tonnon, Ir. Gerwin Stam, and Dr. Alessio Giardino for their generous help in overcoming the hurdles faced during numerical modeling.

Lastly, I genuinely want to thank all the friendships I cultivated over the past two years who made the Netherlands feel like home. To my parents, family, and friends from across the Atlantic I want to express my vast appreciation for understanding my decision and for supporting me throughout the process. Moving to the Netherlands and learning hydraulic engineering from the Dutch has been a humbling experience that has made me grow as an engineer as well as a person. For the opportunity, I will always be thankful.

Victoria Curto, P.E.
Delft, November 2014

Abstract

The morphological impact on nourishments of conditions with high oblique wave incidence has been investigated in literature using either a one-line approach or quasy-2D models. These models predict downdrift nourishment migration and the generation of alongshore sand waves for persistent conditions with high oblique wave incidence. However, these models exclude either the effect of wave chronology or use unrealistic nourishment properties.

In this research the reshaping mechanisms of beach nourishments of realistic proportions (i.e. 2 km long and a cross-shore extent of 250m or 1000m) which are exposed to high angle waves are explored using Delft3D. This analysis distinguishes two phases: (1) static sediment transport for time invariant wave climate and (2) evolving nourishment morphology under time varying wave conditions. Model results show that:

- A proper quantification of the degree of downdrift migration could be obtained from the skewness in the initial alongshore sediment transport distribution. Large nourishments under high angle waves result in high skewness and subsequent translation of the feature, while normally incident waves result in symmetric sediment transport distribution with skewness equal to zero and a more classical diffusive response.
- The morphological response of the considered nourishments depends on (1) the moment in time at which a high angle wave event took place and (2) the persistence of the high angle waves within the wave climate. Simulations showed that a period with low-angle waves can rapidly wipe out the instabilities of high-angle wave situations and thus result in a diffusive pattern. However, a longer period with high angle waves will result in smaller net losses from the nourishment area for large scale nourishments.

Extended abstract

Beach nourishments are increasingly employed by coastal zone managers as a mean to mitigate beach erosion. In previous studies, wave action has been found to be one of the dominant factors among waves, tides, and winds influencing nourishment performance. The morphological impact on nourishments under the influence of very oblique waves has been investigated in literature using either a one-line approach or quasy-2D models. These models predict nourishment growth, downdrift nourishment migration, or generation of alongshore sand. However, these models exclude either the effect of wave chronology or use unrealistic nourishment proportions.

In this research, a numerical exploration using process-based wave, circulation, and sediment transport model Delft3D is conducted to assess the reshaping mechanisms of beach nourishments under high wave obliquity. The following variables are considered: angle of wave incidence (normally incidence, low, and high wave obliquity) and realistic nourishment size (2 km long and a cross-shore extent of 250m or 1000m); the analysis distinguishes three phases: (1) initial sediment transport for

time invariant wave climate, (2) evolving nourishment morphology under time invariant wave conditions and (3) evolving nourishment morphology under time varying wave conditions.

Results indicate a proper quantification of the degree of downdrift migration (translation) could be obtained from the skewness in the initial alongshore sediment transport distribution. Large nourishments under high angle waves result in high skewness and subsequent translation of the feature while normally incident waves result in symmetric sediment transport distribution with skewness equal to zero and a more classical diffusive response. Large nourishments under low wave obliquity exhibit a combined response of diffusion and some degree of translation while small nourishments irrespective of wave angle resulted in diffusion. Large skewness values are associated with the refraction-induced wave energy spreading and focusing on the nourishment lee side resulting from shielding effects due to the combination of high wave obliquity and large nourishment size.

Comparison between model results and theoretical S,ϕ-curve show the S,ϕ-curve fails to predict sediment transport rates as Delft3D for high wave obliquity because it cannot represent the refraction-induced transport peaks seen on Delft3D; the deviations are attributed to the assumption of parallel contour lines ignoring the effect of refraction. Therefore, model results prove the value insight process-based model Delft3D provides in the evaluation of nourishment reshaping.

Morphodynamic simulation results show a proper correspondence to the initial sediment transport reshaping predictions. For large nourishments, the reshaping process was found to be depth. For low wave obliquity, diffusion always dominated in shallow water, and translation occurs at deep water after diffusion took place. Under high wave obliquity, translation features include downdrift migration of the crest at deep water, protuberance development on object at downdrift side, and lee erosion.

The morphological response of the considered nourishments depended on (1) the moment in time at which the high angle wave event took place and (2) the persistence of the high angle waves within the wave climate. Simulations showed that for large nourishments a period with low-angle waves can rapidly wipe out the instabilities of high-angle wave situations and thus result in a diffusive pattern. However, a longer period with high angle waves would result in smaller net losses from the nourishment area at the expense of lee erosion.

Key words: beach nourishment, high angle of wave incidence, wave chronology, refraction, Delft3D

Contents

List of figures

List of tables

1 Introduction

1.1 Background

Throughout the world, major cities have developed along the coasts because of the different enriching activities, industries, and growth opportunities associated with the sea such as, navigation, trading, and tourism. Although highly valuable, coastal areas are also vulnerable since such cities are prone to erosion and coastal retreat. The traditional engineering solution to coastal erosion has been the implementation of "hard" structures like seawalls, groins, and breakwaters. However, the erosion problem is then shifted downdrift in addition to the resulting adverse environmental impacts on the ecosystem; hence, worldwide there is a growing need for alternative solutions to coastal erosion (Hamm, et al., 2002).

Beach nourishment is considered a sustainable and environmentally friendly approach to beach erosion, and it is increasingly being applied by coastal zone managers throughout the world. Beach nourishment (example shown on left panel of Figure 1.1) is considered a "soft" engineering solution which consists of compensating the eroded sediment by placing borrowed sand in the nearshore area. The idea is to let sediment transport processes continue their natural course. The design lifetime of commonly employed beach nourishments is approximately five years, upon which a new application is required. In the sandy coast of Zuid-Holland, an unprecedented pilot project call the "Sand Motor" (right panel of Figure 1.1) has been implemented with the goal of providing a solution that fits multiple purposes. One of those purposes is to reduce the frequency of beach nourishing by significantly increasing the size of the nourishment itself.

Figure 1.1 Beach nourishment examples: "Big Beach", Virginia, USA having 91m wide (left) and "Sand Motor", Netherlands having 1000m wide and 2500m long (right). Note photos have different scales with respect to each other (NOAA, 2014) (Rijkswaterstaat, 2013)

Several studies such as, Hamm, et al. (2002), Van Duin, et al. (2004), Hartog, et al. (2008), Benedet, et al. (2007), Davis, et al. (2000), Grunnet, et al. (2005) have been completed with the goal of obtaining a better understanding of the processes and factors that influence the performance of beach nourishments. Such studies include numerical modeling and data analysis based on surveys and documentation of nourishment evolution in time. The intent of these research studies has been to identify key mechanisms in nourishment evolution to improve the design and lifetime of future nourishment projects. Overall, wave action has been found to be one of the dominant factors among waves, tides, and winds influencing nourishment performance (Hartog, et al. 2008; Davis, et al. 2000; Grunnet, et al. 2005).

The angle of wave incidence is a key component in nourishment behavior; it is known that low angle waves are diffusive in character while large angle of wave incident can lead to translation or anti-diffusive (growth) behavior (Ashton & Murray, 2006a; Ashton, et al., 2001; Van den Berg, et al., 2012). Moreover, different sequences of wave conditions have been found to cause different morphodynamic responses, which emphasize the importance of selection of wave conditions in nourishment behavior prediction (Hartog, et al., 2008). Yet, this subject remains an area of research to be further investigated.

The goal of this research is to understand the reshaping mechanisms of beach nourishments of realistic proportions exposed to high angle waves and the morphological nourishment response associated with the time dependency of wave conditions. To accomplish the goal, instantaneous longshore transport rates and morphodynamic simulations have been performed with process-based model Delft3D. The understanding of nourishment reshaping will aid in improving the prediction of morphological development of future beach nourishments particularly of large scale projects such as the Sand Motor.

1.2 Relevance of research

Beach nourishments are equivalent to a protuberance in the alongshore direction; as a results, when a nourishment is implemented, the coastline geometry changes. Since “shoreline orientation is a function of nourishment design” (Hartog, et al. 2008), the angle at which the waves approach the coastline varies along the nourishment perimeter even for a single and fixed wave condition. This is specially the case for large scale nourishments like the Sand Motor.

Studies have shown that oblique incoming waves (>45°) generate instabilities which cause coastline protuberance to grow, translate, or generate an alongshore sand wave (Ashton, et al. 2001; List & Ashton, 2007; Van den Berg, et al. 2012). Even though previous studies have advanced our understanding of nourishment performance, they have not evaluated the reshaping of realistic nourishment proportions (i.e. 2 km long and a cross-shore extent of 250m or 1000m) exposed to a time varying wave climate which comprises a combination of low and high wave obliquity.

Hence, the aim of this research is to evaluate whether there can be net longshore migration of nourishments for areas which experience high angle waves occasionally, but are not dominated fully by low-angle nor high-angle waves (i.e. intermediate situations). Research results will ultimately contribute towards more effective predictions of nourishment performance.

1.3 Research question

The main research questions are defined as:

1. Does net nourishment migration play a significant role in coasts that experience occasional periods of high angle waves?
2. Do large scale nourishments impact the behavior of a coast exposed to high-angle wave conditions?

To answer the main questions, the following research sub-questions are defined:

- Under what conditions can nourishment migration occur?
- What approaches are suitable for assessing nourishment migration?

1.4 Approach

The research phases go as follows:

- Phase 1: literature review of high angle waves impact on beach nourishment (coastal salient or protuberances) and general nourishment evolution
- Phase 2: initial sediment transport analyses
- Phase 3: morphodynamic evolution of nourishments for time invariant wave conditions
- Phase 4: morphodynamic evolution of nourishments for time varying wave climate

Even though Delft3D is a valuable tool in coastal modeling capable of accounting for different hydrodynamic forcing like waves, tides, and wind, the main focus of this research is the influence of waves and the associated currents thus; the effects of tides and wind have been purposely excluded.

1.5 Thesis outline

The outline of this document follows the research approach described on the previous section. First, an introduction has been presented on the current chapter. Chapter 2 corresponds to Phase 1 and it includes a literature review of wave transformations, sediment transport, and the effect of high angle of wave incidence on coastal salients. Chapter 3 gives an overall description of Delft3D and the model settings used throughout the numerical simulations. Chapter 4 represents Phase 2 and it includes the findings corresponding to the initial sediment transport results including rates, gradients, and pertinent sensitivity analyses. Chapter 5 presents the results corresponding to Phases 3 and 4 where morphodynamic simulations of time invariant and time varying wave climates are analyzed. Finally, conclusions and recommendations are provided in Chapters 6 and 7.

2 Theoretical background

As a mean to mitigate beach erosion, beach nourishments are now-a-days employed with an increasing frequency around the world. In order to properly design, understand and predict their evolution, it is essential have a thorough understanding of the physical mechanisms that dictate their behavior. Such behavior is governed by the physical processes that take place in the nearshore region including wave transformations and sediment transport.

Because of the geometric characteristics, nourishments can be considered a protuberance or a salient in the alongshore direction. Previous studies have revealed the effect waves from different angles have on the reshaping of protuberances (Ashton, et al. 2001; List & Ashton, 2007; Van den Berg, et al. 2011). Thus, this chapter provides the necessary background on wave transformations, sediment transport, and a chronological recount on the studies related to high angle of wave incidence and nourishment reshaping.

2.1 Wave transformations

As waves travel from offshore to the nearshore region, they undergo different kinds of transformations such as shoaling, refraction, and wave braking. As Bosboom & Stive (2013) describe, the waves slow down because they are affected by the bottom when the water depth becomes approximately half the wavelength:

- Shoaling is the processes in which wave energy concentrates increasing the wave height; this phenomenon occurs because the first wave in a wave train decreases its speed while the wave behind it, which travels at a faster speed, reaches the front train causing an “energy bunching”.

- Refraction (Figure 2.1) is the change in wave direction due to changes in its propagating medium. For coastal waters sections of the crest at deeper parts travel faster than those in shallower sectors; in the shoaling region outside the breaker zone, the wave crests turn towards the depth contours causing the wave to bend. The direction of the waves rays changes proportionally to the wave propagation speed according to Snell’s law:

$$\frac{\sin\phi_2}{c_2} = \frac{\sin\phi_1}{c_1}$$

Equation 1: Snell’s Law, where φ_n is the wave angle with respect to the coastline and c_n is the wave celerity at location n

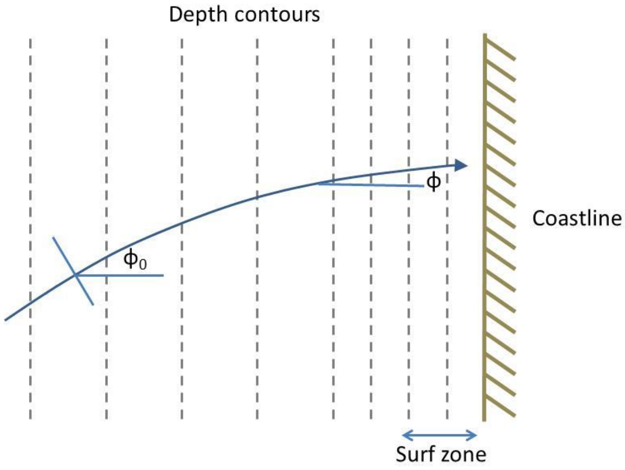

Figure 2.1 Schematization of oblique incidence waves refracting over uniform depth contours, (Bosboom & Stive, 2013)

Thus, along the wave ray sinφ/c is constant and equal to its deep water value sinφ_0/c_0 (Bosboom & Stive, 2013). Refraction is an important aspect of curved coastlines as it is the case of nourishments since the nourishment may acts as a shield resulting in refraction-induced energy concentration and spreading.

- Wave breaking is the physical processes in which waves dissipate energy. Shoaling increases the wave height; the wave crest becomes unstable and starts breaking when the particle velocity exceeds the velocity of the wave crest. In the near-shore area, wave breaking is depth induced since the limiting wave height is governed by a water depth limitation.

2.2 Sediment transport

Two main sediment transport mechanisms take place in the shoreface region: cross-shore and longshore transport; their schematic representation is shown on the Figure 2.2.

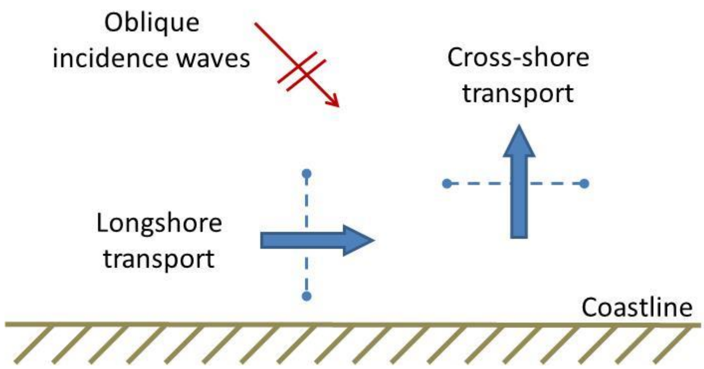

Figure 2.2 Schematization of longshore and cross-shore transports, (Bosboom & Stive, 2013)

Cross-shore processes are dominated by wave action and they are the main responsible agent of changes in the coastal profile. In addition, the response of the coastal profile to wave action is extremely depth-dependent, i.e. the shallower the depth, the faster the response (Bosboom & Stive, 2013). Therefore, it is important to define a limit at which no substantial morphological changes occur. This depth of closure concept was originally introduced by (Hallermeir, 1978) as the "seaward limit to appreciable sand level changes".

Cross-shore evolution is defined by different mechanisms which can either be on-shore or off-shore directed; such mechanisms include undertow, Longuett-Higgins, Stokes drift, and long-short wave interaction:

- **Undertow** is a return current seaward directed resulting from compensating the onshore directed flow above the wave trough water level; the undertow mass transport is larger under breaking waves and predominant under storm conditions.
- **Longuett-Higgins streaming** is an onshore directed mean current profile near the bottom; streaming takes place due to non-linarites in the wave boundary layer where out phase relationships between surface elevations induced pressure with the horizontal motion gives a net streaming.
- **Stokes drift** is net mass flux between wave trough and wave crest in the direction of wave propagation because the velocities under the wave crest are higher than the velocities under the trough. It is associated with orbital particle excursion and it is responsible for transport in the onshore direction.
- **Long-short wave interaction** produces a net off-shore sediment transport when the correlation between the short waves and the long wave is negative; when this correlation changes, the transport is on-shore directed increasing when shoaling and decreasing upon breaking.

Longshore sediment transport is the wave-driven net movement of sediment particles through a fixed vertical plane perpendicular to the shoreline. The direction of this transport is parallel to the shoreline; wave-driven longshore sediment transport depends on the hydrodynamics in the breaker zone and on the sediment properties (Bosboom & Stive, 2013). Therefore, the longshore transport depends on the sediment concentration and the longshore current velocity.

Since the longshore current is not constant, it is necessary to integrate over the cross-shore to assess the sediment transport rate. As a result, not only the sediment characteristics are responsible for the longshore transport but also forcing parameters such as, wave height, breaker type, wave steepness and period. Different transport formulations have been developed to estimate transport quantities. One of the pioneer sediment transport formula was developed in the 1940's by the Coastal Engineering Research Center (CERC) of the American Society of Civil Engineers; and its general form can be expressed as:

$$S = \frac{K}{16(s-1)(1-\mathrm{p})}\sqrt{\frac{g}{\gamma}}\sin(2\phi)\,\mathrm{H}_b^{2.5}$$

Equation 2: CERC formula, where K is a coefficient, s is the relative density of the sediment (ρ_s/ρ), p is the porosity, g is gravitational acceleration, γ is the breaker index, φ is the angle of wave incidence, and H_b is the wave height at breaking

As shown on Equation 2, the angle of wave incidence with respect to the depth contours is of vital importance in longshore transport which is deeply reflected on nourishment reshaping. "Given a relatively constant wave climate along a stretch of coast, alongshore variations in coastline orientation cause gradients in longshore sediment transport and hence cause the coastline orientation to change in time" (Bosboom & Stive, 2013). The S,ϕ-curve (Figure 2.3) illustrates the net longshore sediment transport rates as a function of deep water wave angle. As shown on the figure below, the maximum and minimum transport rates, as estimated by the CERC formula, occur for angles smaller than but close to 45° (critical angle) and for normally incident waves, respectively.

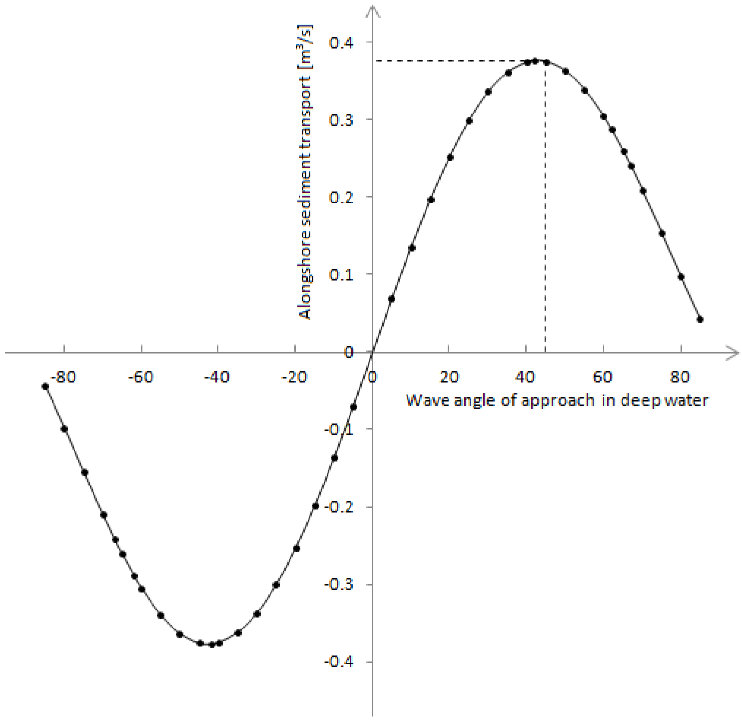

Figure 2.3 S,φ-curve: longshore transport rates (S) as a function of deep water wave angle (φ_0) calculated for an offshore wave height of 2 m and wave period 7s using the CERC formula, dotted line indicates ϕ_0=45° (Bosboom & Stive, 2013)

Due to the changes in concavity along the salient perimeter, as it is the case for large scale nourishments such as the Sand Motor, the approaching angle of the waves with respect to the salient curvature will vary along its perimeter independently of the wave incidence angle; therefore, different transport rates should be observed throughout the salient length.

The gradients in sediment transport are the responsible agent for changes in the shoreline such as, erosion and accretion. When there is a net export of sediment, erosion will take place in the given control volume; whereas, a net import will cause accretion.

2.3 Chronology of studies related to high angle of wave incidence

The classical evaluation of salient response to wave action is considered to be diffusing in character as described by the equation (Pelnard-Considere, 1956):

$$\overline{D}\frac{\partial x_s}{\partial t} = -\frac{\partial Q}{\partial y}$$

Equation 3: Diffusion equation according to (Pelnard-Considere, 1956), where Q is the total sediment transport rate in the y direction, t is the time, and the perturbed coastline is given by $x = x_s(y,t)$

However, “the traditional formulation set up by Pelnard-Considere (1956) just ignores the perturbation in wave transformation caused by the coastline changes. This is equivalent to keep the bathymetric contours being parallel to the unperturbed rectilinear coastline even if changes in coastline position occur” (Falqués & Calvete, 2005)

In 2001, Ashton et al. showed, by means of a numerical model and a comparison to land formations seen on the Sea of Azov, Ukraine and the Carolina coast, USA (Figure 2.4), the smoothing of a protuberance would only be valid for small angles of wave incidence with respect to the coastline orientation (θ) whereas; high angle waves would cause a protuberance to grow.

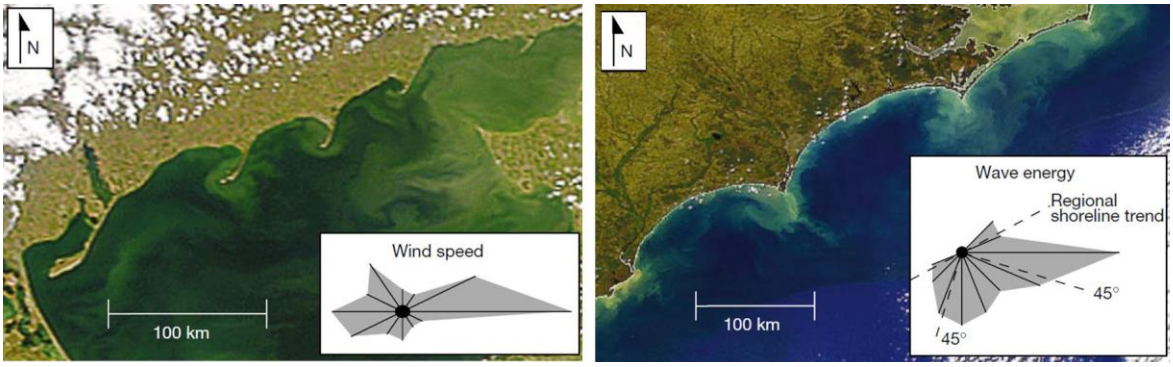

Figure 2.4 Satellite images showing naturally occurring large-scale shoreline features: Sea of Azov, Ukraine (left) and Caroline Coast (right). (Ashton, et al. 2001)

Consequently, following the S-ϕ curve, when the deep water angle of wave incidence is smaller than the critical angle, such as 15°, the transport increases (decreases) as the relative wave angle increases (decreases), which leads to a diffusive behavior eventually reshaping the protuberance into an alongshore uniform coastline. On the other hand, when the angle of wave incidence is larger than the critical angle, such as 65°, the transport decreases as the angle increases and vice versa. As a result, this mechanism would lead to deposition at the crest of the protuberance making it grow, also referred to as anti-diffusive behavior (Figure 2.5).

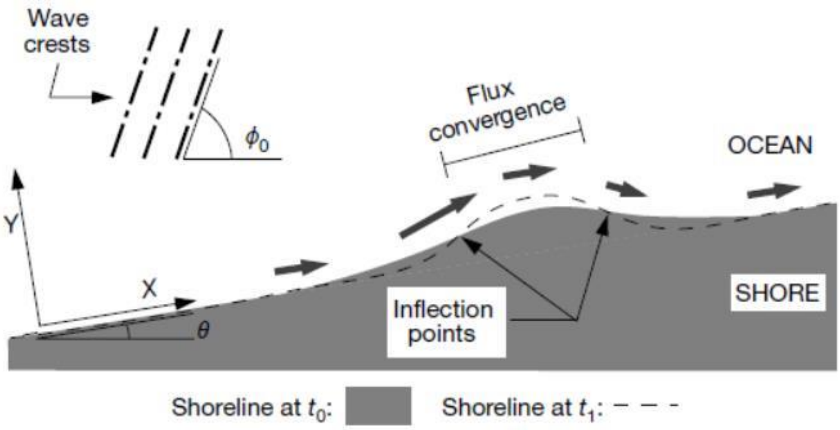

Figure 2.5 "The relative magnitude of the alongshore sediment flux, shown by the length of the arrows, and the consequent zones of erosion and accretion on a perturbation to a straight shoreline when the angle between the wave crests and the shoreline trend is greater than that which maximizes the sediment flux." (Ashton et al., 2001)

In 2005, Falques and Calvete evaluated the potential limits to the shoreline instability effect using a linear stability analysis and an analytical wave transformation model. Their study accounted for the curvature of the coastline as well as perturbations with finite cross-shore distances. The instability was found in agreement with Ashton et al (2001). However, the anti-diffusive character was inhibited by several factors including wave height, wave period, and gently sloping shorefaces. In addition, the size of the salient was also found to be a limiting factor: no instability was found if the protuberance was confined close to the coastline, and a minimum longshore length may be required for instability. Thus compared to Ashton, et al. (2001), Falques & Calvete's (2005) results appeared to be more representative of natural conditions seen in a coastal environment.

Ashton and Murray (2006a, 2006b) continued their line of work through a simple cellular modeling approach and the inclusion of Snell's law for wave transformations over shore-parallel contours (Figure 2.6). They found shoreline features migrating in the downdrift direction for asymmetrical wave climates, either as subtle alongshore sand waves or as ''flying spits'' depending on the proportion of high-angle waves. Furthermore, the relevance of refraction and the interdependent changes in breaking wave angle and breaking wave height were found to be a critical factor in the developing of shoreline instabilities. As shown on the Figure 2.7, differing amounts of refraction results in varying breaking wave height (H_b) and therefore, varying sediment transport (Q_s) along an undulating coastline.

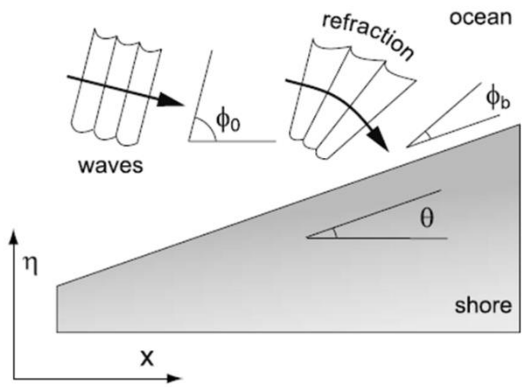

Figure 2.6 High wave angle instability and refraction in shorelines, *where φ_0 is the deep water wave angle, φ_b is the wave angle at breaking, and θ is the coastline orientation angle*. (Ashton & Murray, 2006a)

Thus, it was concluded the diffusion equation (Equation 3) should be replaced with a with either a function that accounts for predicted changes in breaking wave height due to refraction or with a function that is in terms of globally constant variables (Ashton & Murray, 2006a).

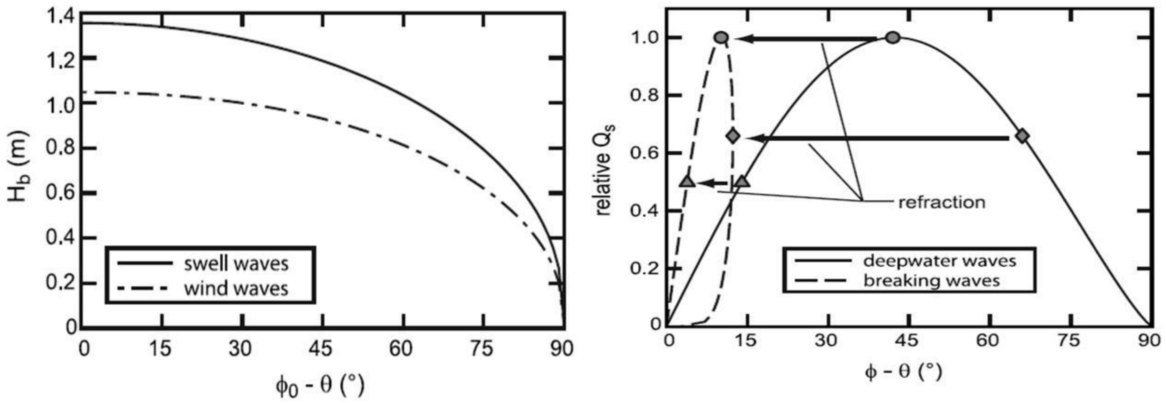

Figure 2.7 On left panel, H_b for waves refracted over shore-parallel contours as a function of (φ_o - θ), for representative wind (dash-dotted line, H_0 = 2 m T = 7 s) and swell (solid line, H_0 = 2 m T = 15 s) waves. Note that with higher-angle waves, H_b varies considerably as (φ_o - θ) is varied. On right, resultant alongshore sediment transport (Q_s) for swell waves in terms of deepwater ((φ_o - θ), solid line) and breaking ((φ_o - θ), dashed line) angles. (Ashton & Murray, 2006a)

In 2007, List and Ashton used the process-based wave, circulation, and sediment transport model Delft3D to assess whether instabilities would develop under wave conditions with high angle of wave incidence. Different salient dimensions were tested reaching cross-shore depths of 16m and 10m, and varying alongshore lengths between 1km and 8km. Their assessment was based on longshore sediment transports and sediment transport gradients without considering morphodynamic simulations. “[Their] results with coastal salients agree with previous findings that minimum salient length scales may be required for the instability effect to be active” (List & Ashton, 2007). Under the action of high angle waves, the results indicate salient translation in the downdrift direction for all tests; in addition, the sediment transport gradients predict salient growth (anti-diffusive response) when the salient length increased from 4km to 8km scale which also implies extending to a longer distance in the cross-shore direction reaching deeper contour lines.

Van den Berg, et al. (2011) used a non-linear model as an extension of the model used by Falqués & Calvete (2005) to investigate the effect high angle waves have on nourished beaches. The "model results suggest that due to high angle wave instability a nourishment or a borrow pit could trigger the formation of a shoreline sand wave train—alternating accretional and erosional zones (Figure 2.8). Its formation is a self-organized response of the morphodynamic system and can be seen as a spatial-temporal instability. New sand waves are formed downdrift while the old sand waves migrate downdrift and increase in amplitude and wavelength" (Van den Berg, et al., 2011).

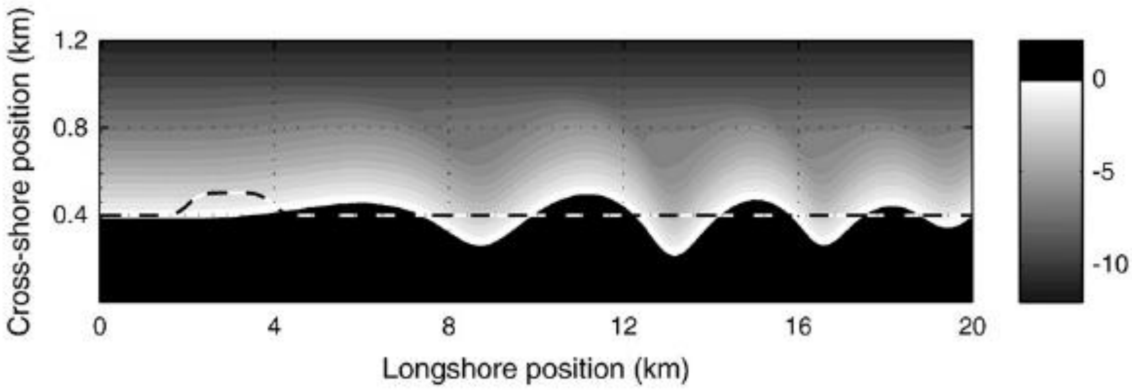

Figure 2.8 Bathymetry after 8 years for the beach nourishment with 60° angle of wave incidence, 1m wave height, and 6s wave period, taken from (Van den Berg, et al. 2011)

In addition, the research results revealed "instability develops only if the bathymetric changes related to shoreline perturbations extend to a depth where the wave angle is greater than the critical angle of 42°. The potential for coastline instability is therefore limited by the wave angle at the depth of closure and not by the wave angle at deep water as suggested in previous studies". The underlying statement is in agreement with previous studies where refraction has been stressed as a limiting mechanism for the perturbations to grow.

Lastly as an extension of their previous work, Van den Berg, et al. (2012) evaluated the effect of variable incidence wave angle required for a sand wave to grow. However, wave conditions used in the model were purposely set up in a manner that was to minimize the effect of chronology –time dependency of wave conditions. The study concluded the effect diffusive waves (low angle waves) have on shoreline dynamics has a bigger impact than the anti-diffusive effect of high angle waves. The simulation results indicate, contrary to previous studies, that instability requires a wave climate with a minimal proportion of high angle wave incidence of at least 80%. Moreover, "a wave climate with high wave angles alternating between opposite directions reduces shoreline instability and, in case the wave climate is completely symmetrical, the sand waves do not migrate and organize themselves with a constant wavelength" (Van den Berg, et al. 2012).

3 Modeling approach

Numerical models are a valuable tool used in coastal engineering to understand and predict coastal processes. In this research, the process-based model Delft3D was employed to assess the influence of high angle waves on nourishment migration. In Chapter 3, section 3.1 provides a description of the modeled scenarios used to achieve the research goal, the bathymetry, and the hydrodynamic forcing; section 3.2 gives a general description of Delft3D, and section 3.3 describes the model settings including: general parameters, grids, initial conditions, boundary conditions, and morphodynamic simulations settings.

3.1 Modeled scenarios

The current study aims at answering the research questions listed on section 1.3 by applying the scenarios described on Table 3.1:

1. Does net nourishment migration play a significant role in coasts that experience occasional periods of high angle waves?
2. Do large scale nourishments impact the behavior of a coast exposed to high-angle wave conditions?

Table 3.1 Description of modeled scenarios employed to answer the research questions

Scenarios	Features
I. Potential for reshaping of nourishments	▪ Aimed at obtaining quick insight in the potential for alongshore downdrift migration and instability formation ▪ Investigating the initial transport patterns (Chapter 4) ▪ Application of coast normal, mildly oblique, and very oblique waves (section 3.1.2) ▪ Two nourishment configurations of realistic proportions (section 3.1.1) ▪ Wide range of variations including (see section 3.1.2) - Wind and swell - Extra oblique waves - Highly energetic conditions - Mild and steep nourishment profiles
II. Morphodynamic evolution of nourishments	▪ Aimed at: 1. Verification of the quick approach with initial transport patterns 2. Potential impact of temporary periods with high angle wave conditions for alongshore migration and instabilities. ▪ Morphodynamic updating of the coast in time (section 5.2.1) ▪ Time varying combinations of very oblique and coast normal wave conditions (section 5.2.2)

3.1.1 Bathymetry

The model bathymetry was numerically generated by superimposing a Gaussian-shaped nourishment on an alongshore uniform coast given by Dean-Moore-Wiegel profile (DMW-profile); the bathymetries used in this research represent schematized synthetic nourishment scenarios following an ideal cross-shore profile (see Figure 3.1).

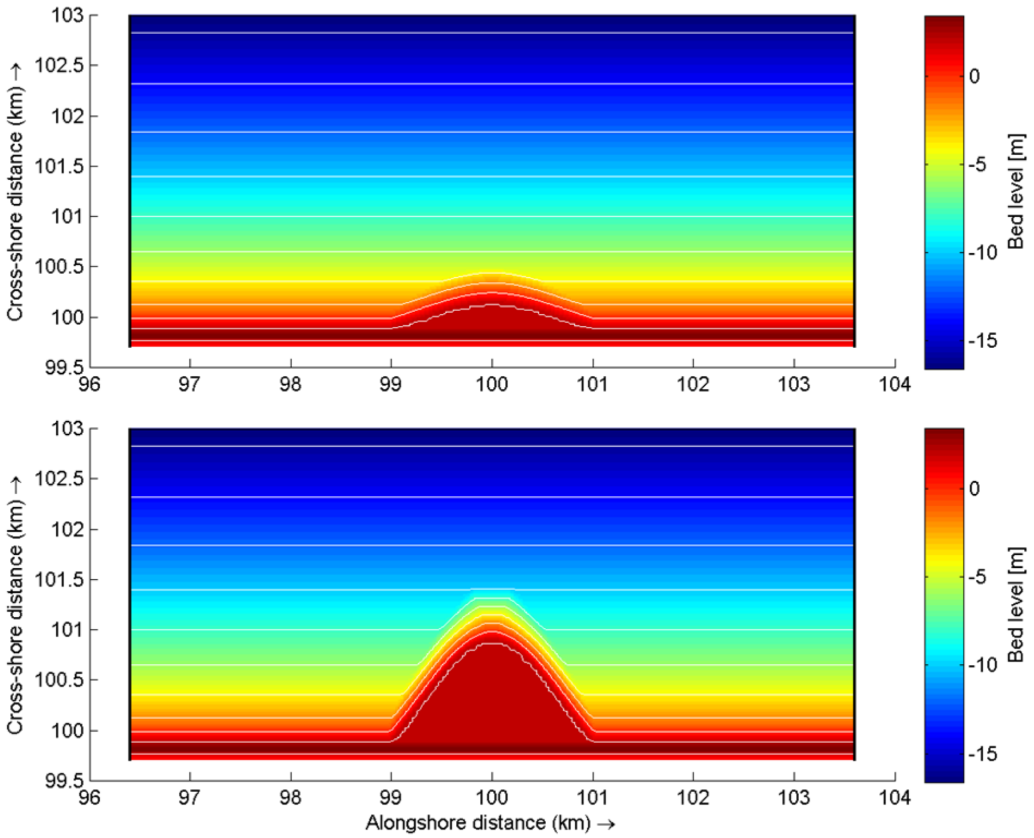

Figure 3.1 Plan view of initial, large (bottom) and small (top), Gaussian nourishment bathymetries

As shown on Figure 3.2, the DMW profile, as described by Stive, et al. (1992), is considered an "ideal" profile consisting of the Dean equilibrium profile with a grain diameter dependence in the proportionality constant. Near the waterline, a constant slope is adopted which is related to the grain diameter and the exposure of the coast following Wiegel (1964). When combined the DMW-profile formulation goes as follows:

$$D = Ay^{2/3} \text{ for } dD/dy \le \tan\beta$$
$$D = D^{*} - \tan\beta\left(y^{*} - y\right) \text{ for } dD/dy > \tan\beta$$

Equation 4: DMW profile, where D is the mean still water depth, y the cross-shore distance belonging to the Dean profile, tan β the beach slope, and A the proportionality constant. The parameters denoted with an asterisk (y and D*) are evaluated at dD/dx = tan β.*

The schematized nourishments were numerically designed purely using the Gaussian equation:

$$f(x,\mu,\sigma) = A\frac{1}{\sigma\sqrt{2\pi}}\exp\left[-\frac{(x-\mu)^2}{(2\sigma)^2}\right]$$

Equation 5: Gaussian equation, where μ is the mean or expected value, σ is the standard deviation, A is a scaling factor, and x is the alongshore distance

In order to adjust the nourishment dimensions in the alongshore and cross-shore directions, the Gaussian parameters were manipulated. For all nourishments, the mean was set to 100,000 meters, and the nourishment length was defined as two standard deviations away from the mean in both directions (east and west). Thus, nourishment length was not a variable considered in this study. Overall, two main nourishments were used; large and small (see Table 3.2). The large nourishment was numerically designed to resemble the Sand Motor initial alongshore and cross-shore dimensions. For all nourishments, the top contour line reached an elevation of +2 meters where the nourishment attached to the alongshore uniform coastline. For the base matrix, the seaward slope was set to 1:50 and for sensitivity analysis, two more large nourishments with a milder and a steeper slope were employed (see Figure 3.2).

Table 3.2 Geometric characteristics of nourishment configurations for bas matric and sensitivity analysis

Nourishment	μ [m]	σ [m]	A factor	2m depth alongshore Length [m]	2m depth cross-shore length [m]	Slope (y-z plane)	Volume [$10^6 m^3$]
Base matrix							
Small	0	500	500000	2000	252	1:50	1.49
Large	0	500	2000000	2000	1009	1:50	9.15
Sensitivity analysis							
Large steep	0	500	2000000	2000	1009	1:25	7.26
Large mild	0	500	2000000	2000	1009	1:100	14.2

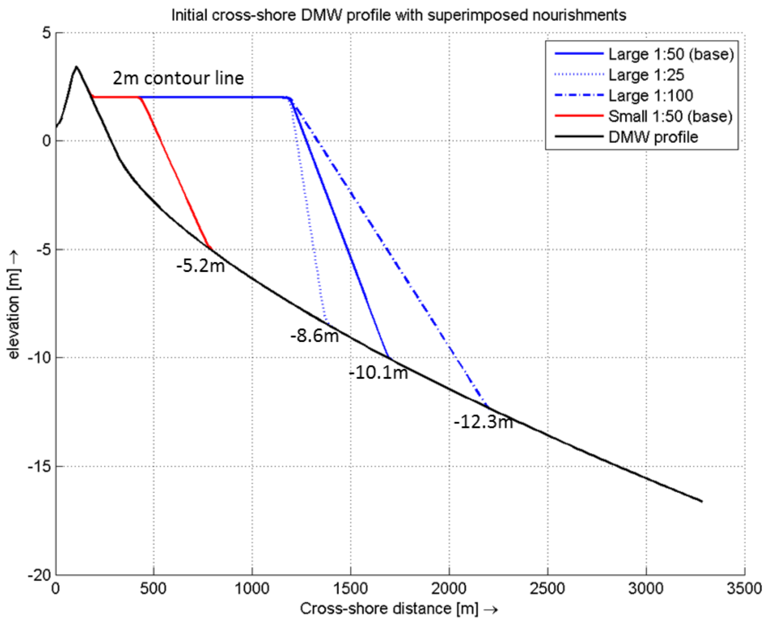

Figure 3.2 Initial DMW cross-shore profile with superimposed nourishments, notice the exaggerated scale on the elevation-axis

3.1.2 Hydrodynamic forcing

The focus of this study is to assess the reshaping mechanisms of nourishments due to influence of high angle waves. Hence, wave action is the only forcing agent taken into consideration, and the action of wind and tides has been purposely excluded. The hydrodynamic forcing used on the base matrix and sensitivity is shown on Table 3.3.

Table 3.3 Time invariant offshore wave conditions used in base matrix and sensitivity analysis

Description	Wave height [m]	Wave angle* [°]	Wave period [s] and directional spreading [cosine power]
		Base Matrix	
Coast normal	1.5 m	0°	6 s [4]
Mildly oblique	1.5 m	15°	6 s [4]
Very oblique	1.5 m	65°	6 s [4]
		Sensitivity analysis	
Extra oblique	1.5 m	80°	6 s [4], 12 s [40]
Energetic	4.0 m	0°, 15°, 65°	6 s [4]
Mild/steep slope	1.5 m	65°, 80°	6 s [4]
Swell	1.5 m	0°, 15°, 65°	12 s [40]

*Wave angles have been defined as positive from the north in a counterclockwise direction (waves enter the domain from the west toward the east boundary)

3.2 Delft3D model description

The Delft3D package is a process-based model composed of different modules which resolve complex processes including wave propagation and refraction, hydrodynamic flow, sediment transport, bed morphology, water quality and ecology. In this research, water quality and ecology have been omitted. The main module is the FLOW module which solves the unsteady shallow-water equation in either two or three dimensions, 1 layer or 2 (or more) layers, respectively.

The FLOW equations consist of the continuity equation, horizontal momentum equation, transport equation, and the turbulence closure model (Lesser, et al. 2004). In addition, the vertical momentum equation is reduced to the hydrostatic pressure relation since the vertical accelerations are small compared to the gravitational acceleration; this assumption allows the FLOW module to predict flow behavior in systems where the horizontal scale is considerably larger than the vertical

Waves are simulated in the WAVE module which employs SWAN (Simulating WAves Nearshore); SWAN computes the evolution of random wind-generated short-crested waves, and it includes the effects of refraction, depth-induced breaking, and dissipation due to bed friction. The FLOW and the WAVE modules can be coupled through a communication feedback where the output of one module constitutes the input of the other; this mechanism allows for the inclusion of the wave effects on the flow (currents) and vice versa.

The Delft3D morphological module runs simultaneously ("online") the hydrodynamics and sediment transport modules. Several transport formulations are available; gradients in sediment transport are employed to estimate the bed level or bathymetry changes. When changes on the bathymetry occur, the new bed levels are fed back into the wave calculations which in turn influence the magnitude and direction of currents. This approach thus allows for real time modeling with increased accuracy.

Two distinctive time scale are characteristics of coastal processes: hydrodynamic and morphological changes. As described in (Deltares, 2011), "one of the complications inherent in carrying out morphological projections on the basis of hydrodynamic flows is that morphological developments take place on a time scale several times longer than typical flow changes (for example, tidal flows change significantly in a period of hours, whereas the morphology of a coastline will usually take weeks, months, or years to change significantly)." One solution to overcome the phase difference between the two time scales is to employ the so-called "morphological time scale factor" or "MorFac". According to Lesser et al. 2004, changes in bed sediments are multiplied by a constant factor (MorFac) allowing the upscaling of morphological changes to match the rate of the hydrodynamic flows. The figure below illustrates the structure of the MorFac approach:

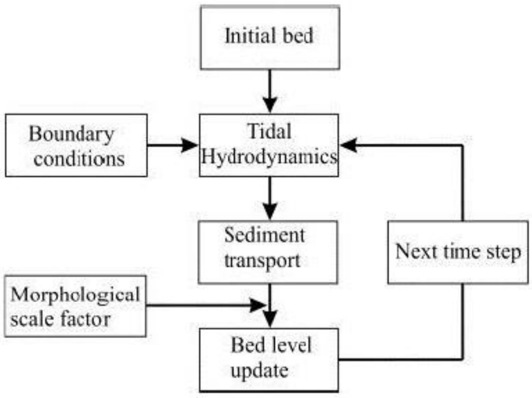

Figure 3.3 Schematic representation of Delft3D processing (Dissanayake, 2012)

"The implementation of the morphological time scale factor is achieved by simply multiplying the erosion and deposition fluxes from the bed to the flow and vice-versa by the MorFac factor, at each computational time-step. This allows accelerated bed-level updating scheme" (Deltares, 2011). The MorFac is calculated based on the following relation:

$$\mathrm{MorFac} = \frac{\text{Morphological time}}{\text{Hydrodynamic time} - \text{spin-up time}}$$

Equation 6: MorFac relation to different time scales

Delft3D uses finite numerical methods to solve the necessary partial differential equations therefore, it is imperative to discretize the domain. Domain discretization is done in grid cells which can either be rectangular or curvilinear. Each module (FLOW and WAVE) has an associated grid, the WAVE grid comprises a larger extent compare to the FLOW domain in order to minimize undesirable boundary effects as the waves enter the FLOW domain.

At an open boundary, the flow and transport boundary conditions are required; these conditions represent the influence of the outer world (area beyond the model which is not modeled). The choice of boundary condition to be used depends on the phenomena. Neumann boundary conditions are used to impose the alongshore water level gradient; they can only be applied on cross-shore boundaries in combination with a water level boundary at the seaward boundary, which is needed to make the solution of the mathematical boundary value problem well-posed (Deltares, 2011).

3.3 Model settings

3.3.1 General parameters

The numerical model used in this research is a depth-average (2D). The focus of this research consists on nourishment response to high angle of incidence waves in terms of net longshore migration; as a result, the area of interest is the horizontal plane as supposed to the vertical plane. Resolving the vertical profile of the flow does not constitute an area of interest in the current scope, and the two-dimensional model choice is justified.

As previously mentioned, one of the major features of Delft3D is the ability to couple the WAVE and the FLOW modules. The results presented on this report adhere to this feature. All simulations were performed using a full coupling of the WAVE and FLOW modules: the hydrodynamic results from the FLOW module, which include water level, current, and bathymetry, were used and extended in the WAVE module. The communication interval between the two modules was done every 20 minutes.

$$CFL = \frac{\Delta t\sqrt{gH}}{\{\Delta x, \Delta y\}}$$

Equation 7: CFL number, where Δt is the time step (in seconds), g is the acceleration of gravity, H is the (total) water depth, and {Δt,Δy} is a characteristic value (in many cases the minimal value) of the grid spacing in either direction (Deltares, 2011).

Generally, the Courant number should not exceed a value of ten; thus, the time step was chosen to be 12 seconds resulting in a CFL number less than 10 in the area of interest.

The FLOW module makes use of the roller model for wave calculations which obtains wave directions from SWAN. In the roller model, the wave breaking index (γ_w) is not set as a constant, but is being calculated by the expression of Ruessink, et al. (2003) where γ_w increases linearly with the product of the local wave-number and water depth. The roller model parameters are set to default values (Giardino, et al. 2011).

The sediment transport formulation used in this research is the TRANSPOR2004 (Van Rijn & Walstra, 2003; Van Rijn, et al, 2004) which is a combination between the original TRANSPOR1993 (Van Rijn, 1993), its successor TRANSPOR2000 (Van Rijn, 2000) and new approximation formulations (Van Rijn, 2002). "Only Van Rijn (1993) and Van Rijn et al. (2004) compute explicitly a wave-related transport component" (Deltares, 2011):

$$S_{total} = BED \times S_{\text{bedload current}} + BEDW \times S_{\text{bedload waves}} + BEDW \times S_{\text{suspended waves}}$$

Equation 8 Explicit current and wave related sediment transport components (Van Rijn, 1993; Van Rijn, et al. 2004)

In this research, multiplication factors for current and wave transport equal 1 and 0.2, respectively. The sediment characteristics used in all the simulations were constant in space and time having a sediment fraction size equal to 200µm, sand with a specific density of 2650 kg/m3, and dry bed density of 1600 kg/m3.

3.3.2 Model grids

As mentioned on section 3.2, Delft3D makes use of two computational grids: flow and wave. Both grids used in this study are rectangular and east-west oriented (Figure 3.4). In order to avoid undesired boundary effect within the FLOW module grid (from now on referred to as the "domain"), the WAVE module grid (18600 by 3600 meters) was set up to have longer dimensions in the cross-shore and alongshore direction than the FLOW grid (7200 by 3300 meters). In addition, since the wave conditions are westerly oriented (coming from the west) upon entering the domain, the FLOW grid was shifted with respect to the WAVE grid axis in order to ensure the parallel wave contour entrance of high angle waves as shown on Figure 3.5.

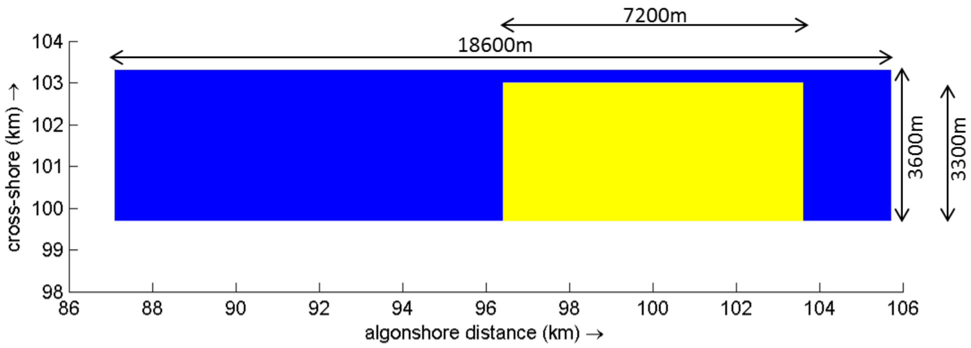

Figure 3.4 Delft3D-WAVE module grid (blue) and Delft3D-FLOW module grids

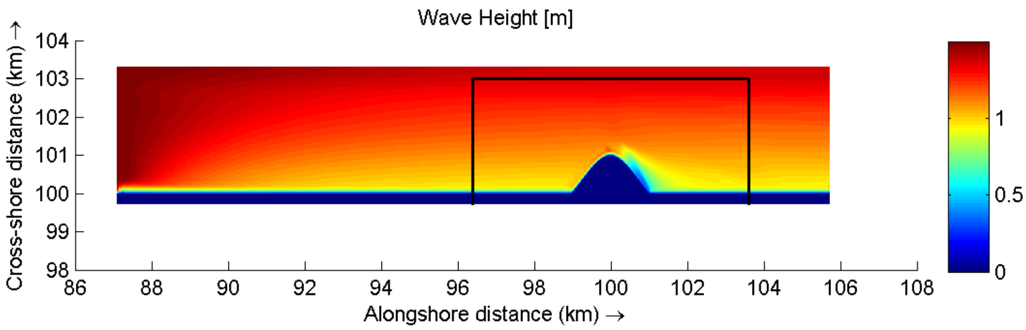

Figure 3.5 Example of parallel 80° wave contour lines entering the shifted FLOW domain enclosed by black rectangle avoiding the curved flow contours seen between 88km and 94km in the alongshore direction

The resolution in the FLOW domain was uniform in the vertical and horizontal directions with a grid size of 15 meters. The alongshore resolution in the WAVE grid (outside the FLOW domain) decreased smoothly reaching a resolution of 60 meters at the edge of the WAVE computational grid; no variations in grid resolution were imposed in the cross-shore.

3.3.3 Initial conditions and boundary conditions

Boundary conditions

Per Deltares (2011), Neumann boundaries were applied to the east and west cross-shore boundaries in combination with a water level boundary at the north (seaward boundary). This combination of boundary conditions is needed to make the solution of the mathematical boundary value problem well-posed. The Neumann boundaries are interpreted as gradient type of boundary conditions for water level as supposed to a fixed water level or flow velocity; such gradients are calculated based on the north boundary condition. As previously mentioned, the focus of this study lies on the exclusive effect of waves on nourishment reshaping; as a result, the seaward water level is also zero due to the absence of tide influence, and the gradient at the lateral boundaries is assumed to be zero.

In addition to maintaining a zero water level gradient at the boundary, a concentration gradient perpendicular to the open Neumann boundary is also equal to zero: "the flow should enter carrying the same concentration of sediment as computed in the interior of the model […]. By setting the sediment concentrations at the boundary equal to those just inside model domain, a near-perfectly adapted flow will enter the domain and very little accretion or erosion should be experienced near the model boundaries" (Deltares, 2011).

Initial conditions

The initial conditions of sediment concentration and water levels were set to zero.

A spin-up time equal to 6 hours was used for all simulations. Spin-up is the time required to reach a steady state by reducing the disturbances generated in the initial conditions through internal dissipation, such as bottom friction. The spin-up time of a model is dependent on the time-scale at which the transient solution dies out (Deltares, 2011).

3.3.4 Morphodynamic simulations settings

The results and conclusions pertaining to the morphological simulations (Chapter 5) were completed under the following model characteristics:

- Hydrodynamic time of 15.5 days
- MorFac of 60 [-]
- Morphodynamic time of 2.55 years (15.5days x 60 = 930 days = 2.55 years)
- FLOW grid resolution of 25 meter in longshore and cross-shore direction (see section 9.2 for discussion)
- Wave computations performed by SWAN using Battjes & Janssen, (1978) with γ=0.73 and α=1.0 (Roller model deactivated, see section 9.2 for discussion)

4 Initial sediment transport approach

By modeling the **Scenario I** shown on Table 3.1., initial sediment transport of time invariant wave conditions is employed to assess the potential for downdrift nourishment migration by means of (1) initial sediment transport gradients and (2) initial sediment transport distribution skewness. The overall aim of Chapter 4 is schematized in Figure 4.1.

Research questions:
Under what conditions does nourishment migration occur?
What approaches are suitable for assessing nourishment migration?

Method:
Approach 1: sediment transport gradients (Qualitative)
Approach 2: sediment transport distribution skewness (Quantitative)

Hypothesized results:
Large angle of wave incidence leads to nourisment migration
Approach 1 and Approach 2 should result in same reshaping mechanism

Figure 4.1 Schematization of initial sediment transport approach for assessing nourishment migration

Section 4.1 gives a description of the methods used for assessing nourishment migration, section 4.2 provides the results for each of the methods, section 4.3 gives a detailed analysis of the results, section 4.4 included sensitivity analysis, and the chapter concludes in section 4.5.

4.1 Approach

The first step required for assessing nourishment migration by means of (1) transport gradients and (2) transport skewness is to calculate the sediment transport rates. The sediment transport rates were calculated from Delft3D model results by integrating the total initial net longshore sediment transport over parallel cross-shore transects. Total transport is defined as the sum of bed load plus suspended transport, initial transport comprises steady state with no bathymetry updates, and net transport combines transport to the west (left) plus transport to the east (right). Pore volumes were not included in the results. The sign convention used in this research indicates positive transport to the east (updrift) and negative transport to the west (updrift). The transects were constructed in the following manner:

- Parallel to the nourishment center line (cross-shore axis)
- In the alongshore direction from the west to the east FLOW boundary
- In the cross-shore direction from +2 to -10.95 meters depth where transport was not significant for 1.5 meter wave heights
- With a distance separation of 50 meters between consecutive transects

4.1.1 Approach 1: longshore sediment transport gradients

This approach comprises the use of the longshore sediment transport gradients for the purpose of descriptively finding areas of erosion and accretion in the alongshore direction that would result in a potential for nourishment migration. It is therefore considered a qualitative approach.

Alongshore sediment transport gradients were calculated by means of numerical differentiation using the “forward” (one-sided) approximation of the first derivative; positive transport gradients indicate erosion and negative gradients indicate of accretion:

$$S'(x) \approx \frac{S(x+h) - S(x)}{h}$$

Equation 9: Forward differentiation scheme, where S is the cross-shore integrated net sediment transport, x is the distance in alongshore direction and x is the spacing between transects equal to 50m

The patterns of the resulting gradients provide information regarding the potential reshaping mechanism of the nourishment under a given wave condition. In this research, we look for the distribution of positive and negative gradients with respect to the nourishment centerline. Recalling oblique waves have an eastward direction (see section 3.1.2), Figure 4.2 schematizes the reshaping mechanisms deduced from the alongshore sediment transport gradients:

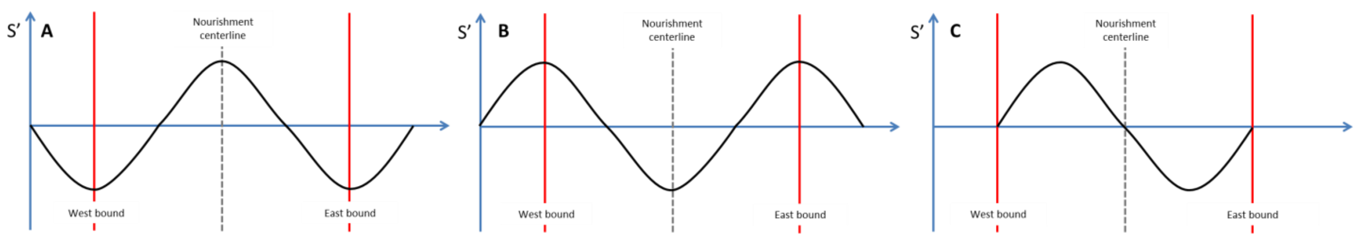

Figure 4.2 Schematic representation of diffusion (A), growth (B), and migration(C) of nourishment based on initial sediment transport gradients

- **Nourishment diffusion:** erosion at the nourishment centerline in combination with accretion at nourishment bounds
- **Nourishment growth:** accretion at the nourishment centerline, as described by List & Ashton, (2007)
- **Nourishment migration (translation):** updrift erosion in combination with downdrift accretion

Updrift and downdrift areas are defined west and east of the nourishment centerline, respectively.

4.1.2 Approach 2: longshore sediment transport skewness

This approach comprises the evaluation of the longshore sediment transport skewness for the purpose of quantitatively assessing the asymmetry of the sediment transport distribution. Highly asymmetric distributions result in a potential for nourishment migration. Approach 2 is therefore considered a quantitative approach.

Skewness "γ_1" is a statistical moment coefficient of a data set about its mean; in this case, the data set is the initial sediment transport distribution. It is a measure of shape, and it gives a precise evaluation of the departure from symmetry defined by:

$$\gamma_1 = \frac{\mu_3}{\mu_2^{3/2}}$$

$$\mu_3 = \frac{\sum_{i=1}^{n}(X_i - \bar{X})^3}{n}, \quad \mu_2 = \frac{\sum_{i=1}^{n}(X_i - \bar{X})^2}{n}$$

Equation 10 Skewness "γ_1", where μ_3 is the third central moment, μ_2 is the second central moment (variance), X is the cross-shore integrated sediment transport per transect and n is the number of transects

By definition, when skewness equals zero ($\gamma_1 = 0$), the distribution is symmetrical; the distribution is asymmetrical when skewness is larger ($\gamma_1 > 0$) or lower ($\gamma_1 < 0$) than zero. For positive skewness, bulk of the data is at the left and the right tail is longer, and for negative skewness, bulk of the data is at the right and the left tail is longer (Measures of Shape: Skewness and Kurtosis, 2012).

In this study, the skewness was calculated using the cross-shore integrated net sediment transport values between the west and east nourishment bounds (shown on red verticals lines on Figure 4.4), where the Gaussian-shaped nourishment reaches the +2 meter contour line (see section 3.1.1 for further description).

The corresponding skewness of initial sediment transport distribution provides information regarding the potential reshaping mechanism of the nourishment under a given wave condition. If the sediment transport distribution is asymmetric (skewness larger than 1), the nourishment is expected to reshape asymmetrically which implies migration; on the other hand, if the sediment transport distribution is symmetric (skewness equal to 0), the nourishment is expected to reshape symmetrically implying diffusion. In this research, we look for well-defined skewness values like 0 or 1 representative of the shape of the transport distribution. Figure 4.3 schematizes the reshaping mechanisms deduced from the alongshore sediment transport distribution skewness:

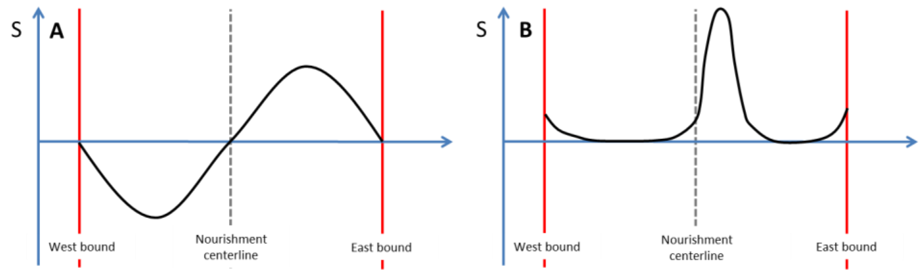

Figure 4.3 Schematic representation of (A) symmetric initial sediment transport distribution with skewness equal to 0 resulting in subsequent nourishment diffusion and (B) asymmetric initial sediment transport distribution with skewness larger than 1 resulting in subsequent nourishment migration

- **Nourishment diffusion:** initial sediment transport distribution skewness equal to or close to zero, $\gamma_1 \approx 0$
- **Nourishment migration (translation):** initial sediment transport distribution skewness greater than zero, $\gamma_1 > 1$

The added value of using the skewness as a metric for assessing the potential nourishment migration lies on the fact that skewness is a universal measure of shape which can be applied to any data set; therefore, skewness as an indicator for migration can be translated into different types of nourishment configurations aside from Gaussian.

4.2 Results

Figure 4.4 shows the initial sediment transport results employed to assess potential nourishment reshaping following Approach 1: longshore sediment transport gradients (section 4.1.1) and Approach 2: sediment transport distribution skewness (section 4.1.2). The corresponding research results are shown on sections section 4.2.1 and section 4.2.2.

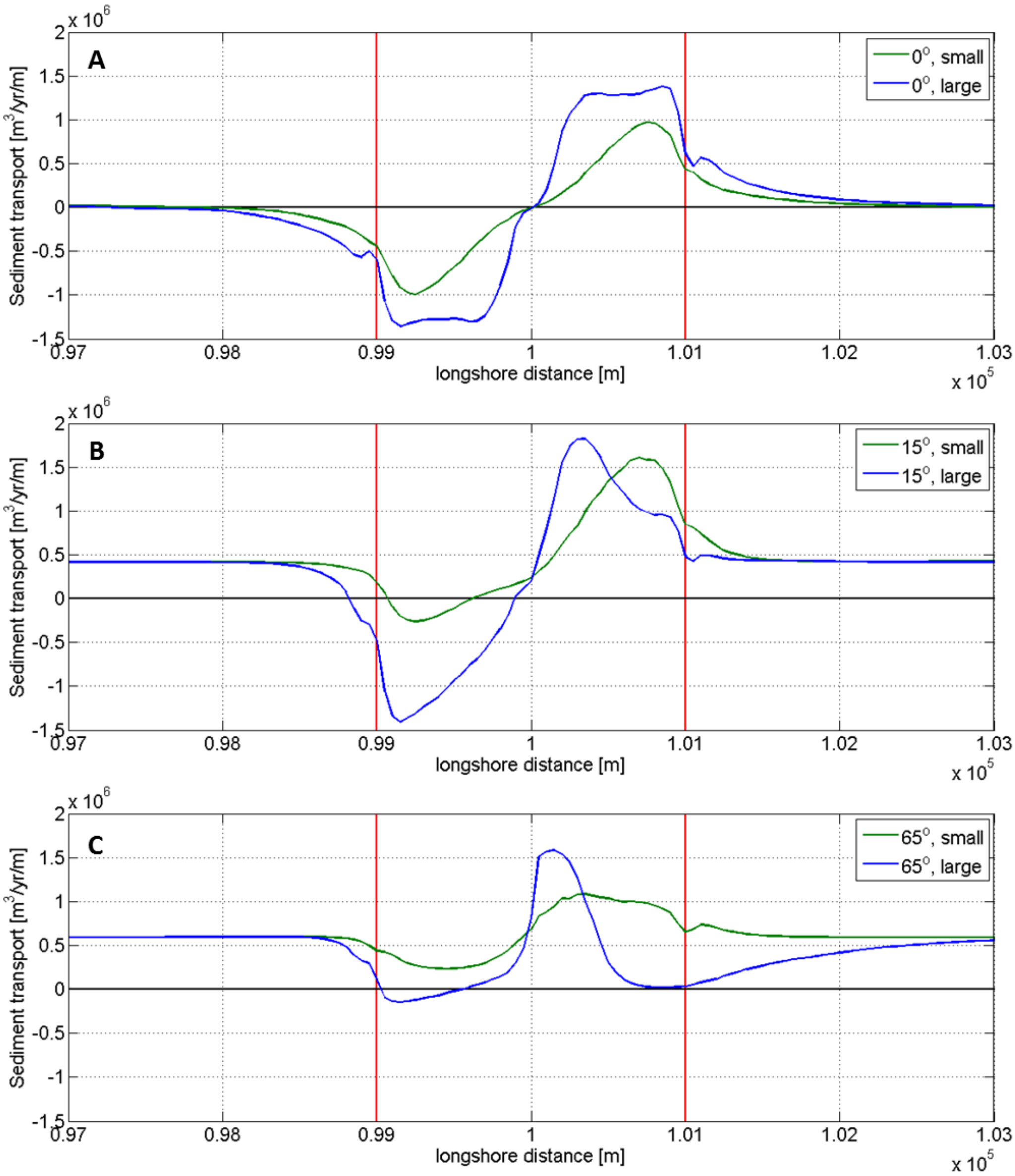

Figure 4.4 Initial net longshore sediment transport simulation results for 1.5m wave height and 6 second mean period: 0°, 15°, 65° angle of wave incidence respectively on A, B, and C panels. Small (green) and large (blue) nourishment plot on same window, nourishment bounds highlighted between red vertical lines, scales kept equal to facilitate comparison. Positive transport goes to the east (updrift) and negative transport goes to the west (updrift).

4.2.1 Results 1: longshore sediment transport gradients

As described in section 2.2, coastline changes occur under the presence of sediment transport gradients and/or sediment sinks or sources. In this research, no sinks or sources are considered hence; the gradients in sediment transport are responsible for accretion or sedimentation patterns influencing nourishment reshaping. Table 4.1 gives a summary of the reshaping mechanisms qualitatively found by inspecting the alongshore sediment transport gradients shown on Figure 4.5; the results indicate the following:

- Under very oblique waves, large nourishment transport gradients indicate downdrift migration; in addition to lee erosion and minor nourishment diffusion
- Under mildly oblique waves, large nourishment transport gradients indicate mixed behavior including diffusion and downdrift migration
- Diffusion is the reshaping mechanism of small nourishments for all angles of wave incidence including very oblique waves

Table 4.1 Approach 1 result summary table for base matrix (1.5 meter wave height, 6 second mean wave period)

Nourishment size	**Wave angle**	**Approach 1: Reshaping mechanism**
Small	0°	Diffusion
	15°	Diffusion
	65°	Diffusion
Large	0°	Diffusion
	15°	Diffusion + minor migration
	65°	Migration + minor diffusion

Looking at the transport gradients of the large nourishment under very oblique waves (panel C on Figure 4.5), the erosion at the nourishment crest is heavily localized having a significantly high and narrow peak that is immediately followed by a wide area of accretion; such gradient pattern depicts downdrift migratory character. On the other hand, the reshaping is not purely migratory because a smaller accretion area is also seen at the west nourishment bound which is characteristic of diffusion. When looking at the transport gradients downdrift of the east bound, a mild but extended area of lee erosion is observed; this erosional spot is neither observed for small nourishments nor for large nourishments under mild angle waves.

An important aspect to point out is the resulting lack of nourishment growth (convergence of sediment transport at nourishment centerline) when exposed to high angle of wave incidence as initially described by Ashton, et al. (2001). Per the present study, the salient growth instability itself is improbable and instead, it has taken on a translation form. Migration reshaping agrees with agree List & Ashton (2007) for the cases with similar nourishment configurations.

Looking at the transport gradients of the large nourishment under mildly oblique waves (panel B on Figure 4.5), the coexistence of accretion at the west bound, erosion surrounding the nourishment centerline, and a relatively wide area of accretion between the centerline and the east bound are representative of diffusion. However, the observed accretion downdrift of the nourishment centerline is believed to be wide enough to have the potential to exert some translation of the object. Therefore, a potential for diffusion in combination with downdrift migration results for large nourishment under mildly oblique waves.

The transport gradients associated with all small nourishments indicate a clear diffusive behavior. Independent of wave obliquity, erosion is always present at the nourishment centerline and its surroundings, and accretion results at both nourishment bounds. The gradient magnitudes vary depending on the angle of wave incidence; however, the diffusion pattern schematized on Figure 4.2 is well maintained in the alongshore direction throughout all the small nourishment simulations results.

In general, the nourishments exhibit diffusive behavior for all simulations, and the degree at which the diffusive mechanism is overcome by migration depends on nourishment size and angle of wave incidence. In small nourishments, diffusion is always the dominant reshaping mechanism; on the other hand for large nourishments, diffusion drastically decreases its effect as the wave angle increases until exhibiting a predominantly translation behavior for 65° waves.

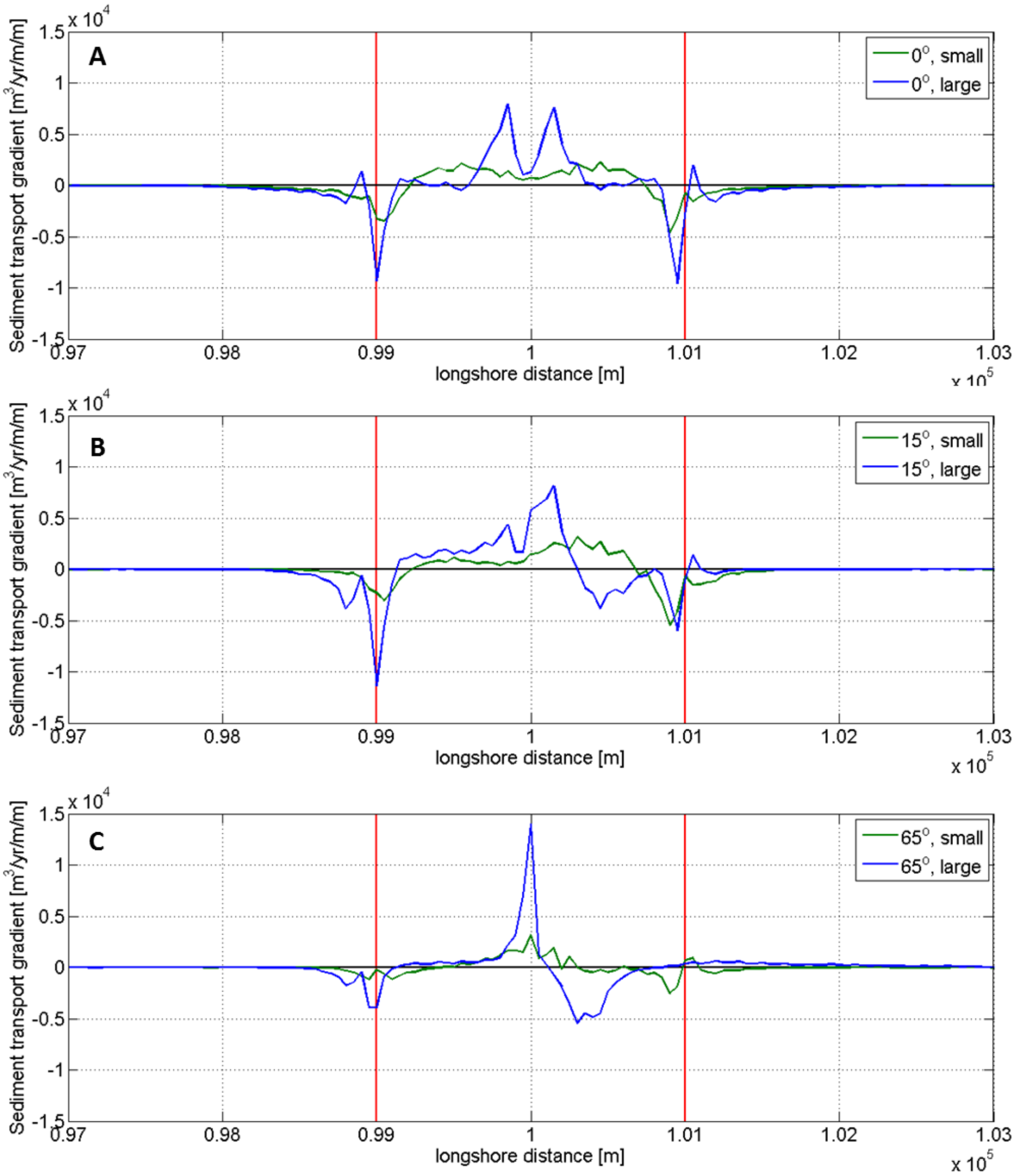

Figure 4.5 Initial net longshore sediment transport gradient for 1.5m wave height and 6 second mean period: 0°, 15°, 65° angle of wave incidence respectively on A, B, and C panels. Small (green) and large (blue) nourishment plot on same window, nourishment bounds highlighted between red vertical lines, scales kept equal to facilitate comparison. Positive transport gradients indicate erosion and negative gradients indicate of accretion

4.2.2 Results 2: longshore sediment transport skewness

As described in section 4.1.2, nourishment migration can be assessed by quantifying the level of asymmetry in the initial sediment transport distribution. Table 4.2 gives a summary of the reshaping mechanisms quantitative found by evaluating the skewness of the initial sediment transport distributions shown on Figure 4.4; the results indicate the following:

- Skewness larger than 1 resulted from the initial sediment transport distribution of large nourishment under very oblique waves only; such is indicative of asymmetric reshaping and downdrift migration
- Skewness values equal to 0 resulted from the initial sediment transport distributions of large and small nourishments under normally incident waves; such is indicative of symmetric reshaping and nourishment diffusion

Table 4.2 Approach 2 result summary table for base matrix (1.5 meter wave height, 6 second mean wave period)

Nourishment size	Wave angle	Skewness [-]	Approach 2: Reshaping mechanism
Small	0°	0.01	Diffusion
	15°	0.44	Diffusion
	65°	0.01	Diffusion
Large	0°	0.07	Diffusion
	15°	-0.03	Diffusion
	65°	1.36	Migration

A clear contrast between the transport distribution skewness for normally incident waves and very oblique waves was found for the large nourishment configuration: 0.07 and 1.36, respectively. Therefore, the differences between the shapes of the distributions were properly captured by the corresponding skewness values; the found contrast confirms the link between high sediment transport distribution skewness and asymmetric reshaping.

However, when comparing the calculated skewness under mildly oblique waves (15°) for small and large nourishments, 0.44 and -0.33 respectively, the results do not provide major insight in the potential nourishment reshaping mechanism; since such skewness values were close to 0, the given nourishment reshaping was assigned as diffusion, and no further details were derived at this point (see Table 4.2). For small nourishments exposed to 0° waves, skewness close to 0 properly quantified the symmetry in the sediment transport patterns; this result corresponds to transport divergence (erosion).

It is worth stressing the skewness approach had not been considered in previous literature. The present research study has proven the valuable insight a simple evaluation of transport distribution skewness has on predicting nourishment migration.

4.3 Analysis

In section 4.2, potential mechanisms for nourishment reshaping were obtained based on initial sediment transport gradients and skewness. These results are analyzed in section 4.3. Firstly, on section 4.3.1 the overall initial sediment transport behavior of large nourishment under very oblique waves is analyzed by employing the simulation wave and flow fields, followed by section 4.3.2 where a comparison between the two approaches is evaluated. In section 4.3.3 the differences between Delft3D and the bulk sediment transport equation are analyzed.

4.3.1 Why do large nourishments migrate under the influence of very oblique waves?

Potential downdrift nourishment migration was observed for large nourishments under the influence of very oblique waves, such as 65°. Section 4.3.1 explains why migration occurs under such conditions; the analysis includes the impacts of (**A**) shielding effects of large nourishments and (**B**) longshore current patterns. Referring to Figure 4.6, the analysis of large nourishment under high angle waves reflects on the patterns seen in the initial sediment transport distribution which includes the following impacts:

- **A.** Refraction-induced increase in wave height resulting in localized enhancement of sediment transport near the crest
- **B.** Decrease in net westward oriented transport related to updrift alongshore current

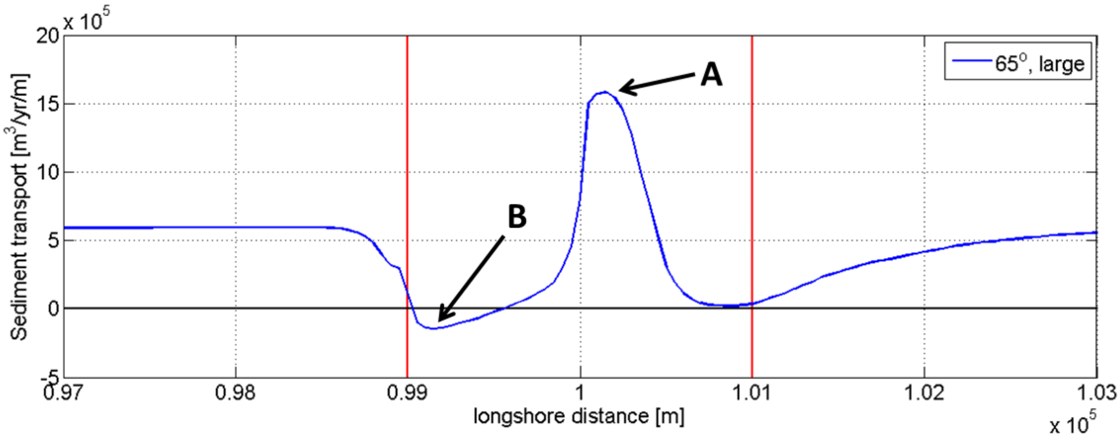

Figure 4.6 Initial net longshore sediment transport simulation results for 65°, 1.5m, 6s mean period waves. Nourishment bounds highlighted between red vertical lines. Positive transport goes to the east (updrift) and negative transport goes to the west (updrift). Effect of interest noted with A and B

A. Observed shielding effects of large nourishment

The size of the nourishment and the angle of wave incidence have a significant effect on the spatial distribution of wave heights. For the large nourishment, pronounced differences in wave heights between the updrift and downdrift nourishment sides were observed in the oblique wave simulations, both mild (15°) and high (65°) obliquity. The observed differences are attributed to the impact nourishment size has on wave refraction.

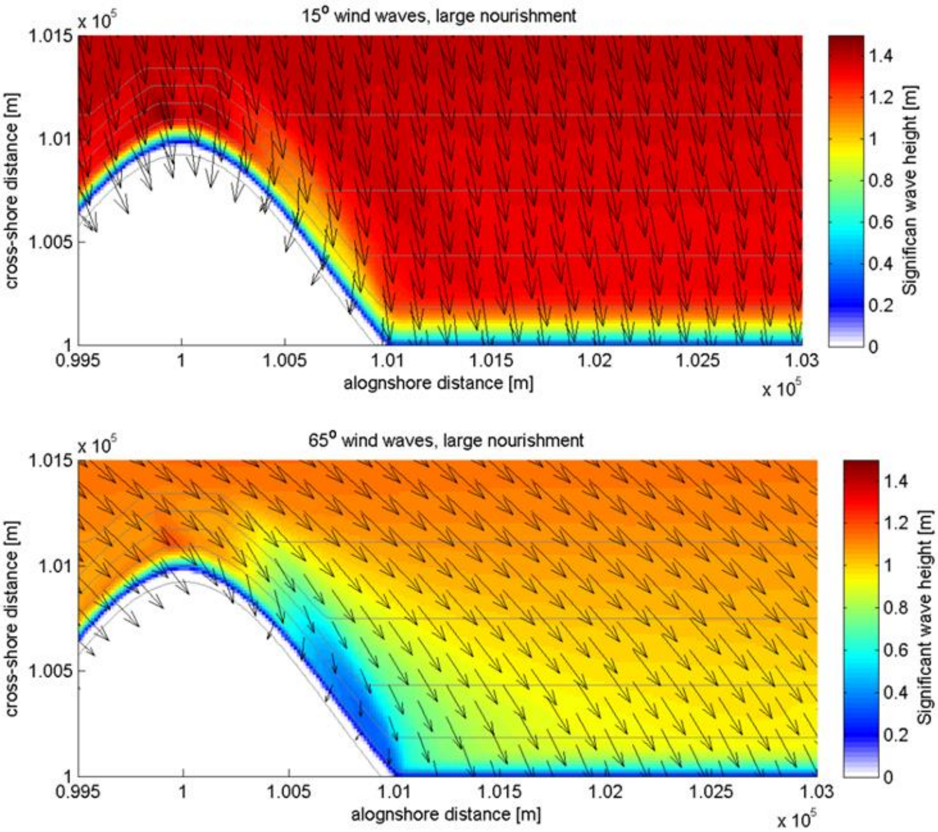

Figure 4.7 Detail of wave fields for 15° (top panel) and 65° (bottom panel) wind wave (6 second mean period) simulations, schematic representation of low energy apron enclosed by dashed black line

"As waves approach shore, they shoal […] increasing their heights. Waves approaching a coast at an angle also refract as they shoal, with their crests becoming more shore-parallel. This refraction, in turn, reduces wave heights as wave crests are stretched. As a result, breaking wave angle and breaking wave height are interdependent, a phenomenon that is particularly pronounced when waves approach with large deep water angles" (Ashton & Murray, 2006a). Consequently, refraction results on lower and higher wave heights on the lee side and at the nourishment crests, respectively (shown on Figure 4.7).

Attributed to the influence the large nourishment bathymetry has on nearshore wave refraction, large nourishments under the influence of oblique waves act as a wave shield causing (1) spreading of low wave energy on the lee side and (2) focusing of wave energy near the crest. Because the energy spreading and focusing was also observed on 15° wave simulations although at a smaller scale compared to the 65° case (see upper panel on Figure 4.7), the shielding effect is considered a characteristic of the large nourishment. Consequently, this refraction induced increment in wave height is the responsible agent for the localized peak in sediment transport rates on the lee side (see A on Figure 4.6).

On the contrary, the limited cross-shore extent of the small nourishment does not allow for shielding effects to take place, and the wave distribution appears to be uniform along the nourishment perimeter. In this case, waves have already refracted before reaching the small nourishment contours, indicating the unlikelihood of nourishment migration (List & Ashton, 2007); consequently, no refraction-induced wave energy increase is observed and no amplification of sediment transport occurs. Therefore, the limiting factor for nourishment migration is the combination of large nourishment and high wave obliquity.

It is noted, Ashton & Murray (2006a) define the low energy area as the region in the coastline shadowed from incoming waves when a protuberance extends seawards (see Figure 4.8). Their simplified numerical model and corresponding refraction assumptions "neglect the effects of the relatively small amounts of wave energy that could refract [...] into shadowed regions." Thus, contrary to Ashton & Murray's (2006a), the present results account for the impact of refraction-induced low wave energy areas, which contribute to the alongshore variations in the wave-driven sediment transport distributions.

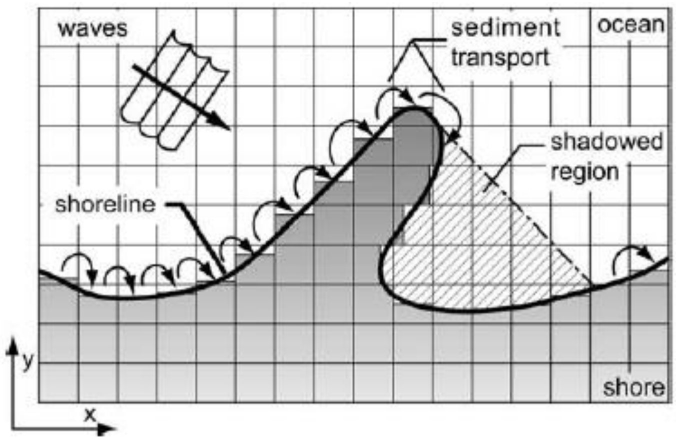

Figure 4.8 Plan view schematic of the model domain demonstrating the directions of sediment fluxes for a given wave approach angle and the region shadowed from incoming waves as described by Ashton & Murray (2006a)

B. Observed longshore current patterns

Different angles of wave incidence result in different alongshore current patterns, particularly in the nourishment updrift side. Under normally incident waves, an even distribution of flow velocities is observed along the large nourishment perimeter in which flow diversion occurs at the nourishment crest. For very oblique waves (65°), the flow symmetry vanishes: a return current develops on the updrift side, the flow diversion point moves away from the crest toward the west, and the strength of the updrift directed current decreases.

The decrease in strength of the updrift directed current for large nourishment under very oblique waves correlates with the updrift shifting of the flow diversion point (Figure 4.9) and with the decreases of gross sediment transport toward the west (see B on Figure 4.6). When comparing the large nourishment sediment transport curves for 15° and 65°, the sediment transport for 65° is mostly eastward directed, with the exception pointed out by B on Figure 4.6, resulting in the given distinctive transport distribution. For the 15° case, the updrift current is stronger and stretches over a longer distance and the corresponding transport on the updrift side is westward directed (see Figure 4.4 C panel) which leads to more symmetric transport distribution.

In the case of small nourishment under very oblique waves, the formation of the return current is inhibited by the size of the nourishment where the flow becomes unidirectional from west to east. Consequently, the longshore current behavior gives an explanation for the sediment transport patterns observed on the updrift side of the large nourishment.

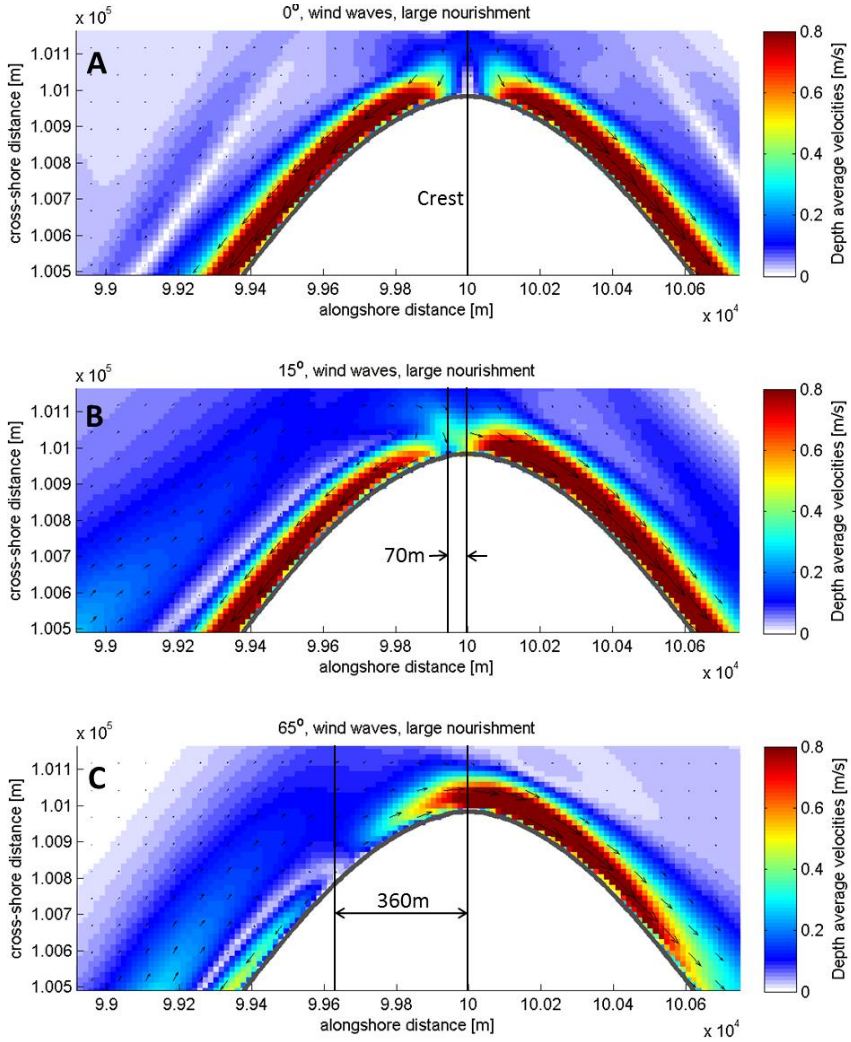

Figure 4.9 Detail of large nourishment crest velocity fields for 0° (A), 15° (B), and 65° (C) (6 second mean period, 1.5 meter wave height) simulations, distance between flow diversion point and crest noted between back lines

4.3.2 How does skewness compare to flow diversion location and downdrift erosion?

Section 4.3.2 is employed to assess how the initial sediment transport distribution skewness compares to the flow diversion and downdrift erosion locations.

Updrift flow diversion location

As shown on section 4.3.1, the flow diversion location has been defined as the alongshore distance from the nourishment centerline to the point of flow diversion (low flow or cero velocities) on the updrift side of the nourishment (see Figure 4.9). Such value was measured from the unfiltered flow velocity fields (see Appendix 9.4). Updrift flow diversion location is not intended to be used as a method for predicting nourishment reshaping but as proxy that can give insight in the understanding of nourishment migration: the closer (further) the updrift flow diversion location is to the nourishment centerline, the more of a diffusion (migration) character the nourishment is expected to exhibit.

Downdrift accretion location

The downdrift accretion location has been defined as the alongshore distance from the nourishment centerline to the point where sediment transport gradients turns from erosion (positive) to accretion (negative). This value was measured from the initial sediment transport gradient curves (Figure 4.5). Downdrift accretion location is not intended to be used as a method for predicting nourishment reshaping but as proxy that can give insight in the understanding of nourishment migration: the closer (further) the downdrift accretion location is to the nourishment axis, the more (less) of a migration character the nourishment is expected to exhibit.

Table 4.3 Result summary table for base matrix (1.5 meter wave height, 6 second mean wave period) indicating relationship between flow diversion location, downdrift accretion location, Approach 1 (gradients), and Approach 2 (skewness)

Nourishment size	Wave angle	Flow diversion location [m]	Downdrift accretion location [m]	Approach 1: Reshaping mechanism	Approach 2: Skewness [-]
Small	0°	0	740	Diffusion	0.01
	15°	130	680	Diffusion	0.44
	65°	-	310	Diffusion	0.01
Large	0°	0	830	Diffusion	0.07
	15°	70	300	Diffusion + minor migration	-0.03
	65°	360	110	Migration + minor diffusion	1.36

As shown on Table 4.3 the initial sediment transport distribution skewness for normally incident waves (0°) and very oblique waves (65°) properly correlates with the flow diversion location, downdrift accretion location, and reshaping mechanisms found through the transport gradients.

For skewness larger than one, the downdrift accretion location draws near to the nourishment centerline, and the flow diversion point moves further updrift; the opposite applies for skewness close to zero since the downdrift accretion location shifts downdrift, and the flow diversion point moves closer to the nourishment axis.

Mixed parameters indicating diffusion and migration are seen for large nourishment under 15° waves. Diffusion is represented by low skewness values (-0.03) plus close proximity of the flow diversion location to the nourishment centerline (70 meters), and migrations is represented by the close proximity of the downdrift accretion location to the nourishment centerline (300 meters). In such cases, it is therefore recommended to further look into the sediment transport gradients because they provide a more complete description for the potential for nourishment migration.

For small nourishments under very oblique waves, skewness values close to 0 properly agree with the location of downdrift accretion. In this case, the flow diversion is does not apply since the sediment transport is directed toward the east throughout the domain.

Aside from calculating the initial sediment transport distribution skewness, the initial sediment transport cumulative sum was also explored as method for evaluating transport distribution asymmetry; the results qualitatively indicated the alongshore location where symmetry disappears. However the results were not considered as valuable as the quantitative contribution of the skewness; thus such findings have been excluded from the report.

4.3.3 Why bulk sediment transport equation cannot cope with nourishment migration?

In this section, the difference in nourishment reshaping predictions between process-based model Delft3D and bulk sediment transport is explored.

In section 2.2, an example of the S,ϕ-curve was introduced by changing the angle of wave approach with respect to a fixed longshore uniform coastline; here, the opposite situation is presented. The corresponding bulk sediment transport, resembling S,ϕ-curves, was calculated for a fixed angle of wave incident and a varying coastline angle associated with the Gaussian nourishment shape. This is the basic principle of coastline modeling (Bosboom & Stive, 2013).

The bulk sediment transport curves (also referred to as "theoretical transport") were estimated by evaluating the $\sin 2\varphi$ (from Equation 2) using offshore angles of wave incidence (0°, 15°, and 65°) and the varying coastline orientation angles along the nourishment perimeter. The curves were then adjusted to match the Delft3D undisturbed sediment transport value (upstream of the nourishment at 98.0 kilometer). The resulting curves are shown on Figure 4.10. It is evident the bulk sediment transport curves fail at the nourishment bounds, as shown on the sharp vertical gradients, which result from the angle at which the nourishments attaches to the longshore uniform coast () see section 3.1.1).

When nearshore wave refraction does not play a crucial role in the spatial distribution and variations of wave heights, as it is the case for normally incident waves, the bulk sediment transport matches the Delft3D results with a high level of precision since the two curves slightly deviate from each other. This is particularly the case for the large nourishment configuration (upper right panel on Figure 4.10) because the bulk sediment transport curve is able to properly mimic the two peaks observed on the updrift and downdrift sides.

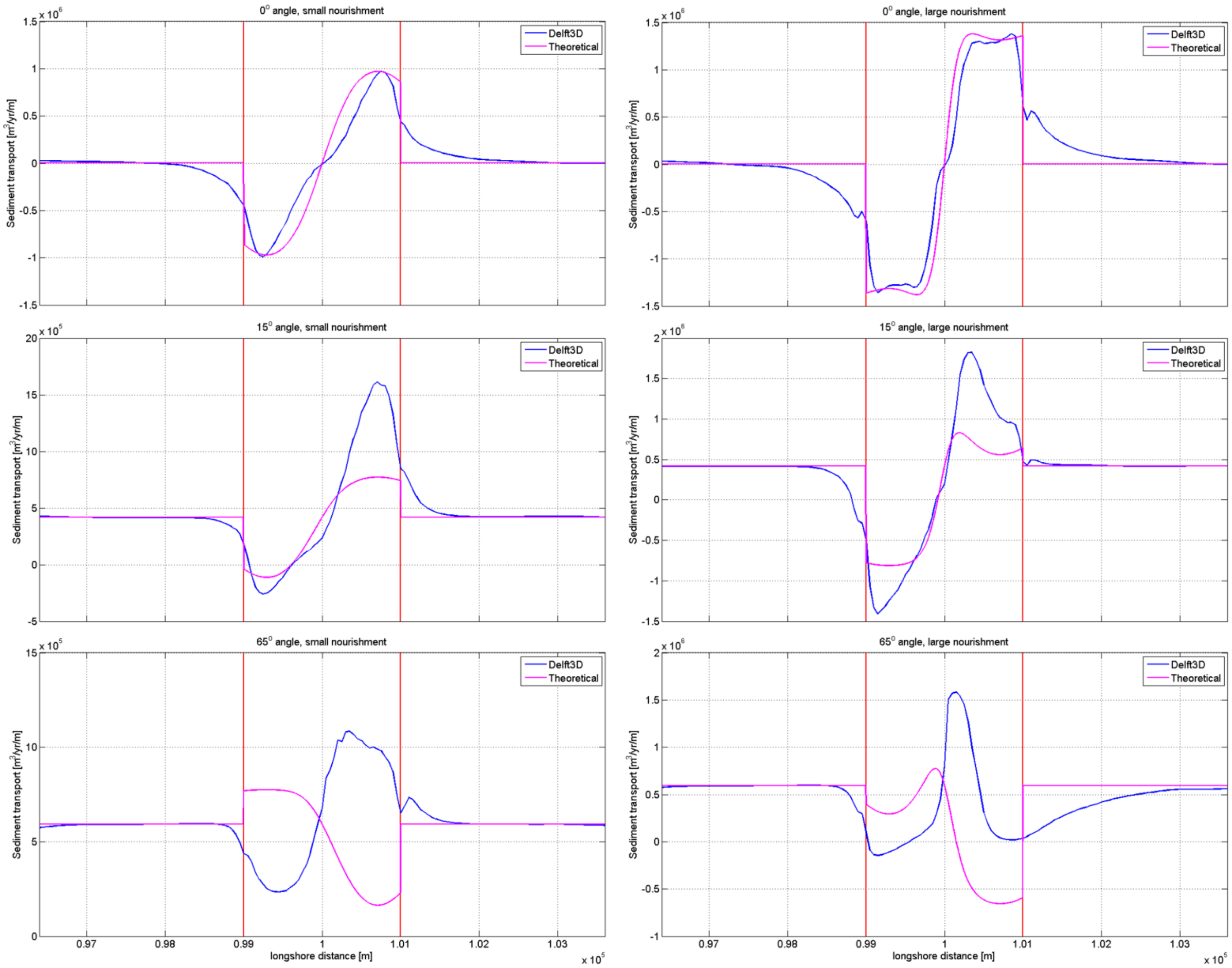

Figure 4.10 Comparison of Delft3D results of cross-shore integrated instantaneous net longshore sediment transport for 1.5 meter wave height and 6 second period waves in blue versus adjusted theoretical longshore transport corresponding to sin(2Φ) in magenta. Nourishment bounds highlighted between red indicators

As the angle of wave incidence increases, wave refraction affects the sediment transport distributions and the deviation between the two methods becomes evident. For 15° waves (middle panels on Figure 4.10), the theoretical transport measures up to the Delft3D results in areas close to the nourishment crest but as the distance away from the crest increases, the theoretical transport cannot represent the refraction-induced transport peaks seen on Delft3D results. However, the bulk sediment transport curve can capture the transport asymmetry between updrift and downdrift sides;

hence, the non-linearity of the *sin2φ* to some degree can capture sediment transport patterns for low angle waves.

For high oblique waves, the bulk sediment transport curves completely fail to represent the Delf3D results. The misrepresentation of theoretical sediment transport is attributed to assumptions behind the *sin2φ curves*: (1) parallel contour lines and (2) wave angle at breaking equal to offshore angle of wave incidence. In cases when the angle of wave incidence is very oblique (lower panels on Figure 4.10), the transport decreases as the angle increases and vice versa (see Figure 2.3); as a result, the bulk sediment transport curves lead to accretion at the crest indicative of nourishment growth.

In reality, bathymetric contours are reoriented in the cross-shore direction and the trajectory of a wave ray adjusts according to the bed levels; this behavior is captured by Delft3D. Presumably, an accurate sediment transport distribution could be attained if the nearshore wave angles and wave heights were extracted from Delft3D and used as input in a coastline model.

As pointed out by Van den Berg, et al (2012), “in the context of one-line shoreline modeling, Ashton et al. (2001) showed that the existence of a maximum in the alongshore transport rate curve, could lead to shoreline instability and the growth of shoreline perturbations. The actual growth of a shoreline undulation however depends on the particular transport gradients along the undulation, which are driven by the gradients in the wave height and the relative wave angle at breaking.” Therefore, the inclusion of nearshore processes (i.e. wave refraction) by utilizing process based model Delft3D provides a more complete analysis of the corresponding sediment transport gradients and nourishment reshaping.

4.4 Sensitivity analysis

The analyses presented on section 4.3.1 have demonstrated the impact nearshore wave refraction has on the wave driven sediment transport distribution which leads to nourishment migration. Four different sensitivity analyses were performed to evaluate the potential variations in nourishment reshaping due to changes in nearshore wave refraction under: (section 4.4.1) different wave periods (wind waves/swell), (section 4.4.2) extra wave obliquity, (section 4.4.3) energetic conditions, and (section 4.4.4) variations in beach slope.

Shielding effects and associated skewed sediment transport are characteristic of large nourishments as supposed to small scale nourishments therefore; the sensitivity analysis was performed on the large nourishment configuration exclusively.

In general, sensitivity analyses indicate (1) no essential difference between wind waves and swell, (2) downdrift translation stability for high oblique waves since no nourishment growth is observed, (3) decrease skewness and potential migration for energetic conditions, and (4) increase in skewness and potential migration for steeper nourishment slopes.

4.4.1 Wave period (sea/swell)

As shown on Figure 4.11, swell waves (12 second mean period) result in larger localized transport magnitudes through peak enhancement than wind waves (6 second mean period). For swell, the updrift maximum transport is magnified while maintaining the spatial distribution of the transport patterns: minimum and maximum occur at similar alongshore locations for wind waves and swell.

The differences in transport magnitudes between wind and swell are associated with wave refraction. The nearshore refraction of swell is more pronounced than in wind waves (Figure 4.12); as the water depth decreases, swell becomes more shore-normal than wind waves in the region of increased transport. Also, shoaling of swell is more intense than for wind waves irrespective of nourishment size (see Figure 4.13 and Figure 4.14); consequently, the resulting accentuated increment in wave height for swell leads to the magnification of sediment transport. These observations are consistent with Falques (2003) and Ashton & Murray (2006a).

Since the corresponding amplification of sediment transport does not generate changes in the spatial distribution of transport gradients, the nourishment reshaping patterns under swell or wind waves are expected to be the same. In fact, changes in magnitudes are only associated with the time needed to mobilize the sediment: larger (lower) transport magnitudes require less (more) time for nourishment reshaping.

Overall, the nourishment reshaping is independent of wave period since the sediment transport patterns do not vary in space—essentially there is no major distinction for nourishment migration with respect to wave period. It is important to mention the present results disagree with Falqués & Calvete (2005) where “instability (migration) is inhibited by high waves with long periods and gently sloping shorefaces so that in this case the coastline may be stable for any angle;” further discussion regarding the nourishment slope is included in section 4.4.4.

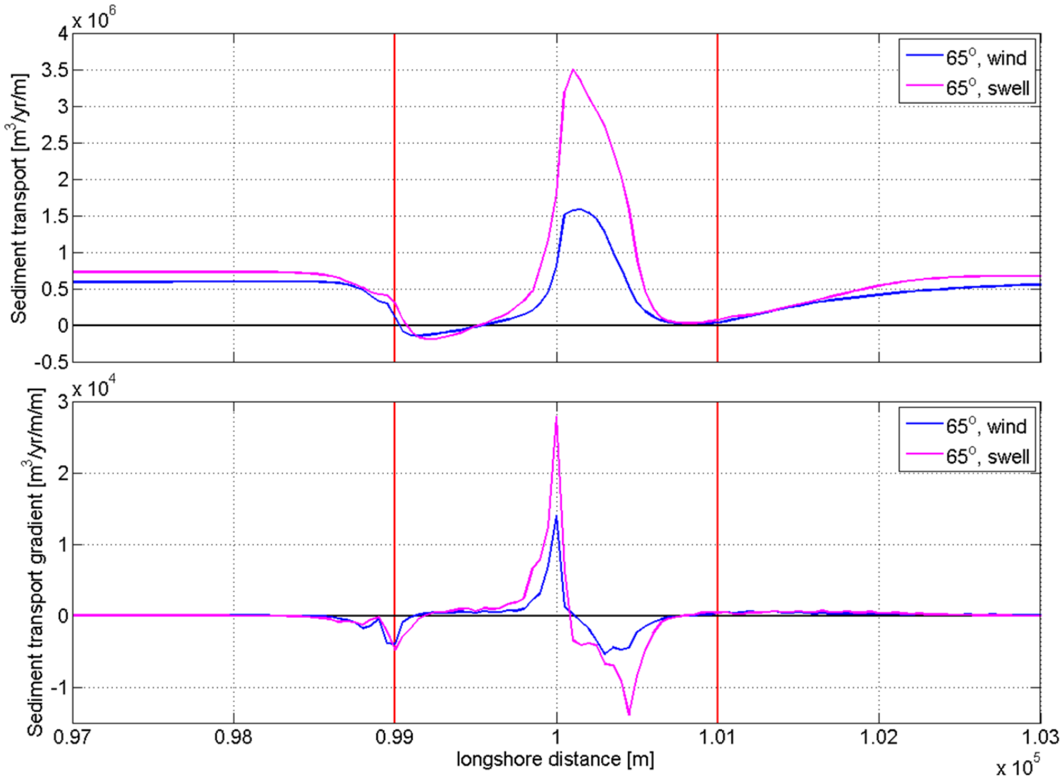

Figure 4.11 Comparison of cross-shore integrated instantaneous net longshore sediment transport (top panel) and gradients (bottom panel) of large nourishment under 1.5 meter wave height, 65° waves with 6 and 12 second mean wave period. Nourishment bounds highlighted by red indicators

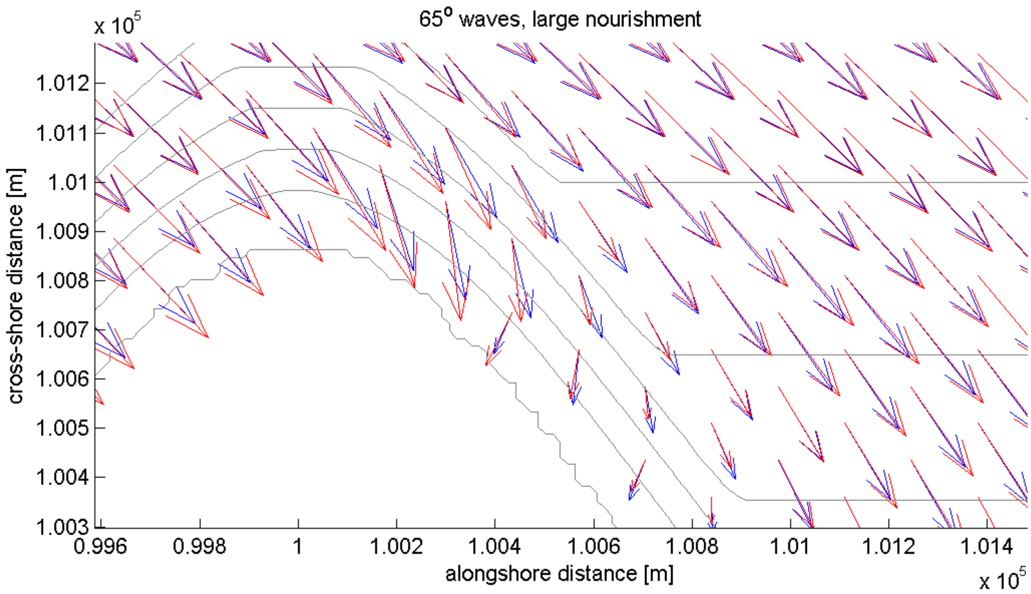

Figure 4.12 Detail of wave field for large nourishment under 65° angle of wave incidence, swell waves (12 second mean period) in red and wind waves (6 second mean period) in blue

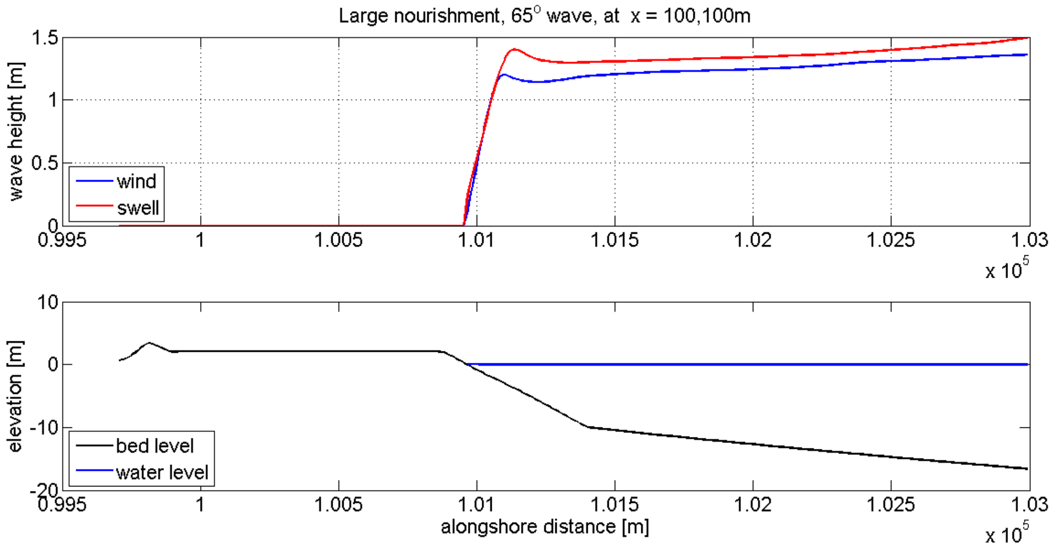

Figure 4.13 Large nourishment cross-shore profile at maximum longshore transport location (x=100,400m), 1.5m wave height and 65° offshore angle of wave incidence. Upper panel: wave height [m] profile for wind (6s mean period) and swell (6s mean period) waves. Bottom panel: corresponding bed level and water depth

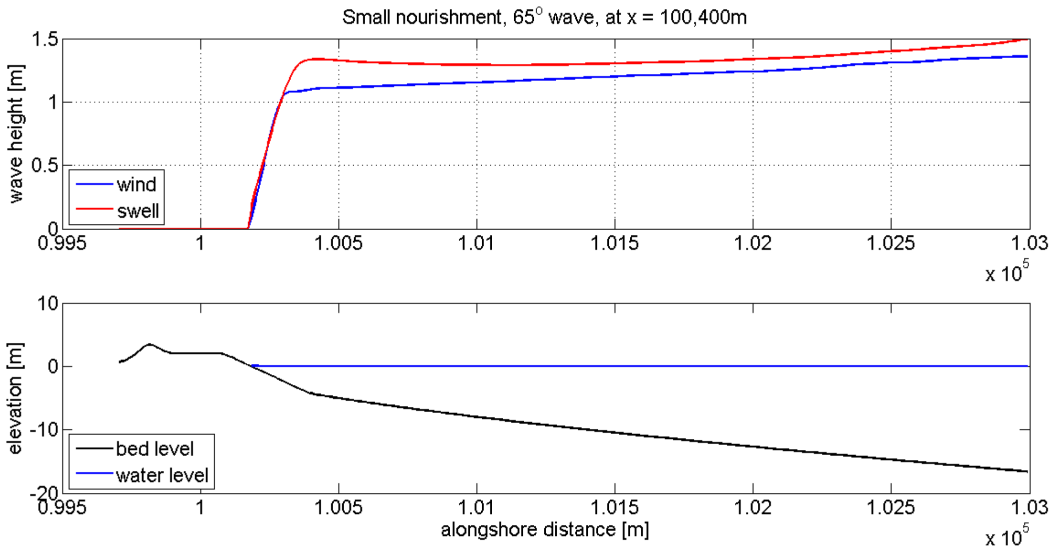

Figure 4.14 Small nourishment cross-shore profile at maximum longshore transport location (x=100,400m), 1.5m wave height and 65° offshore angle of wave incidence. Upper panel: wave height [m] profile. Bottom panel: corresponding bed level and water depth

4.4.2 Extra oblique waves

In section 4.2, large nourishment under 65° waves resulted in downdrift migration and no growth at the crest; thus, it is of interest to evaluate the nourishment reshaping, in terms of gradient and sediment transport skewness when the angle of wave incidence is considerably oblique equal to 80°. Results are shown on Table 4.4. Overall, no significant difference is observed between 65° and 80° waves; alongshore sediment transport and sediment transport gradients indicate same expected reshaping for 65° and 80° waves: downdrift migration and no nourishment growth. Thus, the reshaping mechanism of the given large nourishment reaches equilibrium when exposed extra oblique waves.

Looking at the upper panel of Figure 4.15, similar transport patterns are maintained in space for 65° and 80° waves; the 80° wave simulation results in lower sediment transport magnitudes having a yet sharper maximum transport; such observation is quantitatively reflected on a higher skewness value. In addition on the lower panel of Figure 4.15, a clear sign of translation is observed based on the wide accretion area updrift of the nourishment centerline.

Using Delft3D, List & Ashton (2007) performed simulations using 80° angle of wave incidence, they concluded 4 kilometer long coastal salient would translate in the downdrift direction however; this mechanism would be reverted from salient erosion at the crest to salient growth when the salient spatial scale shifts from 4 to 8 kilometers. As previously mentioned, in this study the nourishment length is not considered a variable of interest because realistic nourishment proportions, i.e. 2 kilometer long and a cross-shore extent of 250 or 1000 meters, wanted to be evaluated. Remarkably, sensitivity analysis does not show nourishment growth despite the 80° wave condition because the waves have already refracted outside the flow domain. The angle at which the waves reach the nourishment (see Figure 4.16) is not oblique enough to shift the focal point of sediment transport form the downdrift to the updrift side of the crest, which would be the required condition for nourishment growth. Furthermore, the refraction-induced change in wave height is already present upon entering the FLOW domain (see Figure 4.17), which causes lower wave heights for the 80° than for 65° waves resulting in a reduction of sediment transport rates.

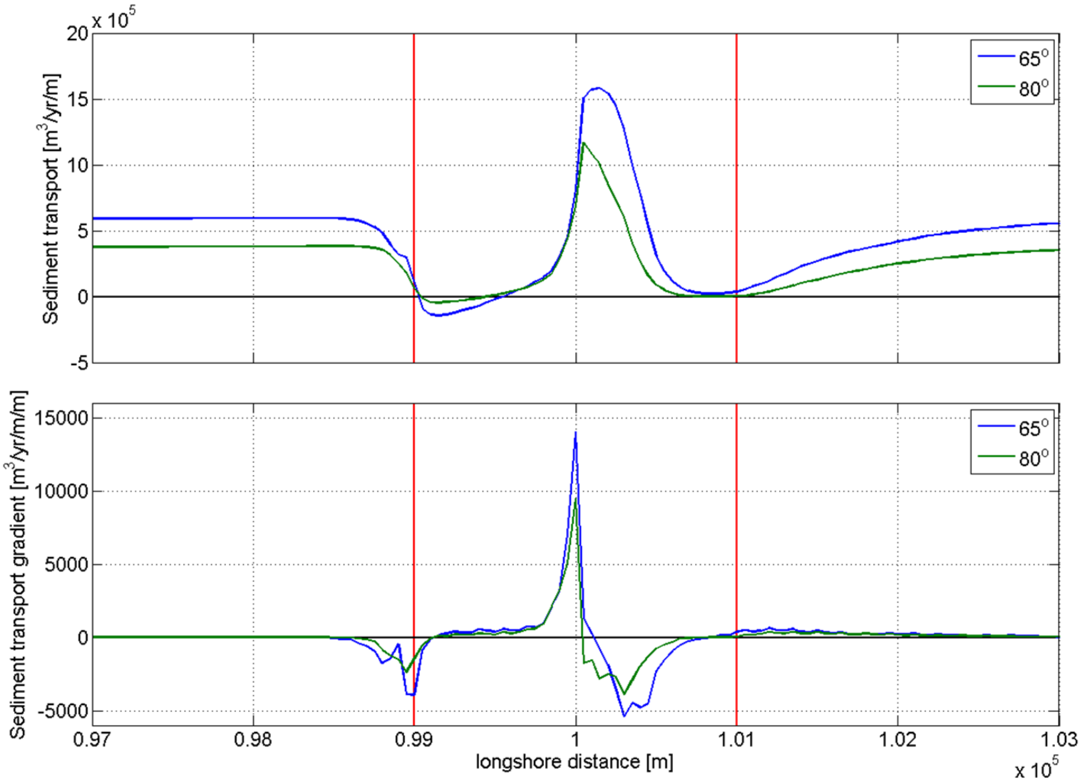

Figure 4.15 Comparison of cross-shore integrated instantaneous net longshore sediment transport (top panel) and gradients (bottom panel) for large nourishment under 1.5 meter wave height, 6 second mean wave period, 65° and 80° high angle of incidence. Nourishment bounds highlighted by red indicators

Table 4.4 Result summary table for sensitivity analysis of large nourishment under extra oblique waves with 1.5 meter wave height. Includes relationship between flow diversion location, downdrift accretion location, Approach 2 (skewness), and Approach 1 (gradients)

Simulation description	Flow diversion location [m]	Downdrift accretion location [m]	Approach 1: Reshaping mechanism	Approach 2: Skewness [-]
Wind waves, 80°	460	40	Migration + minor diffusion	1.64
Swell, 80°	580	40	Migration + minor diffusion	1.69

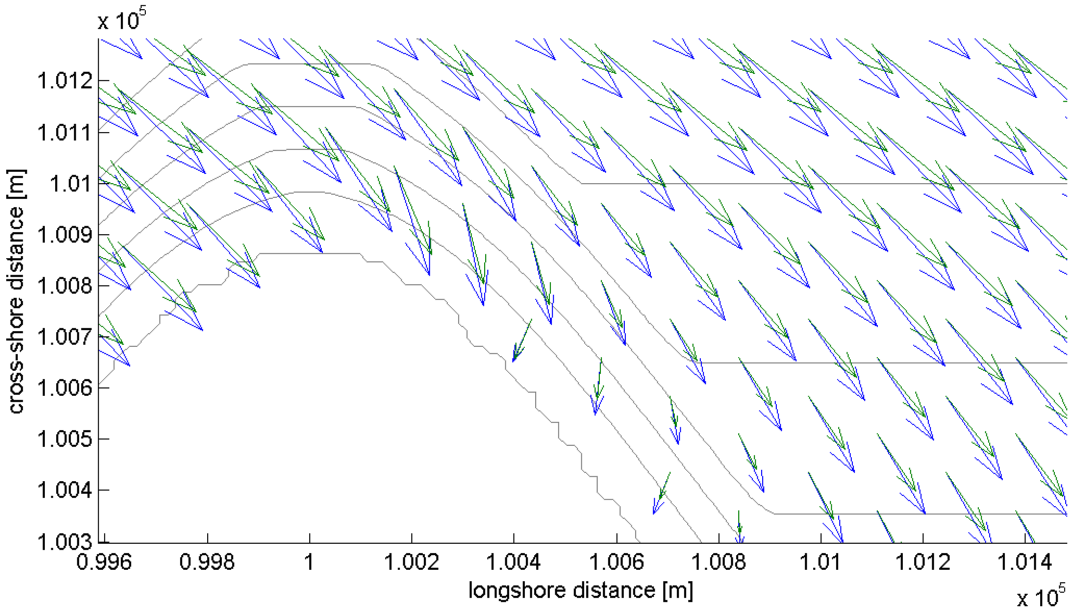

Figure 4.16 Detail of wave field for large nourishment under 1.5 meter wave height and 6 second mean period, 65° angle of wave incidence in blue and 80° angle of wave incidence in green

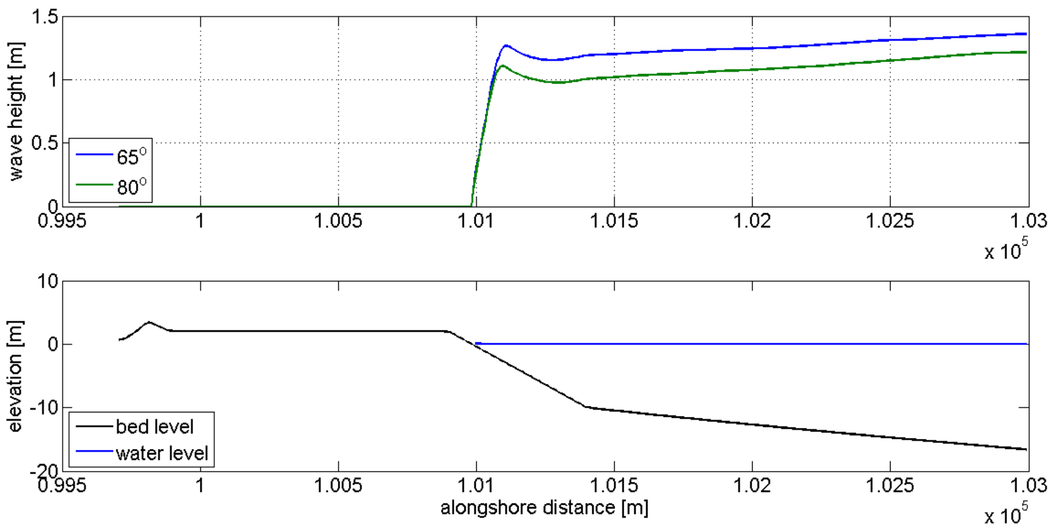

Figure 4.17 Large nourishment cross-shore profile at crest where maximum gradient occurs for 1.5m wave height and 6 second mean period. Upper panel: wave height [m] profile for 65° and 80° angle waves. Bottom panel: bed level and water depth

4.4.3 Highly energetic waves

In order to fully cover the parameter spcae, simulations were performed with a wave height equal to 4.0 meters, which resembles energetic conditions seen in the Dutch coast (Kaji, 2013). Results are shown on Table 4.5.

The simulations of large nourishment under energetic very oblique waves indicated the potential for migrating downdrift; no potential for nourishment growth is observed. Figure 4.18 shows the significant increase in wave driven longshore transport magnitudes for 4.0 meter wave heights.

The general distribution of sediment transport is maintained in the alongshore direction. Nevertheless higher energy waves cause the localized increase in wave-driven transport to spread over a longer distance along the nourishment perimeter (see upper panel on Figure 4.18 and right panel on Figure 4.19) resulting in a wider sediment transport peak; hence, a decrease in skewness: from 1.36 to 1.00 for 1.5 and 4.0 meter wave heights, respectively (see Table 4.2). Even though the skewness decreases, based on transport gradient (see lower panel on Figure 4.18) the nourishment is still expected to migrate because of the wide accretion area observed downdrift of the centerline. In addition, a small downdrift accretion location equal to 120 meters and significant distance between flow diversion and the centerline (300 meter) properly correlate to the downdrift migration potential.

When comparing the 1.5 and 4.0 meter significant wave height simulation results, nourishment translation appears to be favored by a less energetic (1.5 meter wave height) but prolonged 65° angle wave event than a single event of 65° waves and 4.0 meter high, i.e. a storm. Since such hypothesis is based on the comparison of longshore sediment transport simulation results, it would need to be verified via morphodynamic simulations. Moreover, the observed reduction in skewness could be compared to the results from Falqués & Calvete (2005) where computations indicated that for very high waves (5.0 meters), there is no growth of coastline protuberances for quite oblique wave incidence.

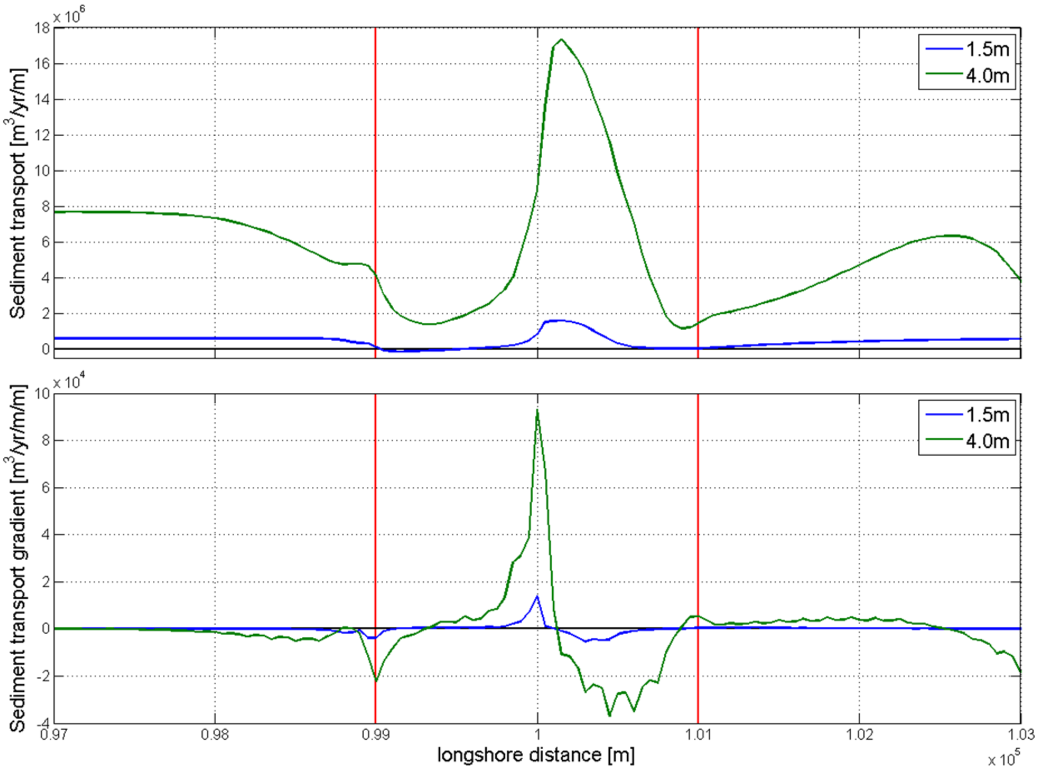

Figure 4.18 Comparison of cross-shore integrated instantaneous net longshore sediment transport and gradients for large nourishment under 65° angle waves, 6 second mean wave period, 1.5 and 4.0 meter wave height. Nourishment bounds in red

Table 4.5 Result summary table for sensitivity analysis of large nourishment under highly energetic conditions (4.0 meter wave height, 6 second mean wave period). Includes relationship between flow diversion location, downdrift accretion location, Approach 2 (skewness), and Approach 1 (gradients)

Simulation description	Flow diversion location [m]	Downdrift accretion location [m]	Approach 1: Reshaping mechanism	Approach 2: Skewness [-]
4.0 m, 0°	0	570	Diffusion	0.01
4.0 m, 15°	30	540	Diffusion + minor migration	0.04
4.0 m, 65°	300	120	Migration + minor diffusion	1.00

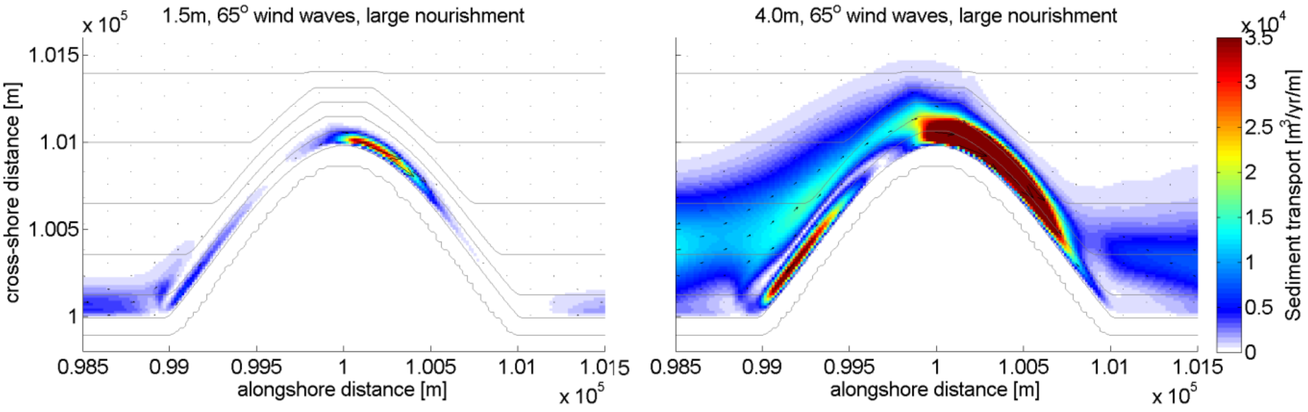

Figure 4.19 Comparison between instantaneous sediment transport fields of 1.5 (left panel) and 4.0 (right panel) meter wave height for large nourishment configuration under 65° angle of wave incidence and 6 second mean wave period. Notice the spread of sediment transport for the 4.0 meter wave height simulation

4.4.4 Effect of beach slope

Wave refraction depends on the bathymetry. Mild profiles are more prone to refraction since the depth contours reach longer cross-shore distances forcing the waves to turn further offshore; by the same token, steeper profiles poorly conduct refracting waves since the depth contours are closely packed. The results presented on section 4.2 show the impact nearshore wave refraction has on nourishment reshaping. Falqués & Calvete (2005) also explain the dependence of the instability (nourishment growth) on the equilibrium topographic profile where steeper shorefaces are more conducive to instability than gently sloping ones. Section 4.4.4 evaluates the impact on nourishment migration due to changes in beach slope (nourishment profile).

Sensitivity to beach slope was assessed by comparing results for the large nourishment with mild (1:100) and steep (1:25) profiles under the influence of oblique angle waves; results are shown on Table 4.3. Based on the sediment transport gradients (Approach 1), nourishments with mild and steep slopes maintain a general downdrift migration with no nourishment growth. Moreover, the initial sediment transport distribution skewness accurately represents the sediment transport variations induced by bathymetry changes. The steeper profile with a large skewness corresponds to a heavily localized transport downdrift of the nourishment centerline while the milder profile with lower skewness corresponds to a wider transport distribution.

A decrease in nourishment slope, 1:100 to 1:50 to 1:25, and the associated reduction in wave refraction result in lower skewness values equal to 0.64, 1.36, and 2.80, respectively. Consequently, it is presumed that a balance, meaning skewness equal to one, can be found for a large nourishment with a slope of approximately 1:80. In addition, a similarity was observed between nourishment reshaping corresponding to (a) 1:50 nourishment slope under 4.0 meter wave height and (b) 1:100 mild nourishment slope under 1.5 meter wave height. In both scenarios, the sediment transport spreads over a long distance along the nourishment perimeter on the lee side resulting in lower skewness when compared to their counterpart base scenario results; although the differences in net transport rates are significant, both configurations are expected to reshape in a similar fashion.

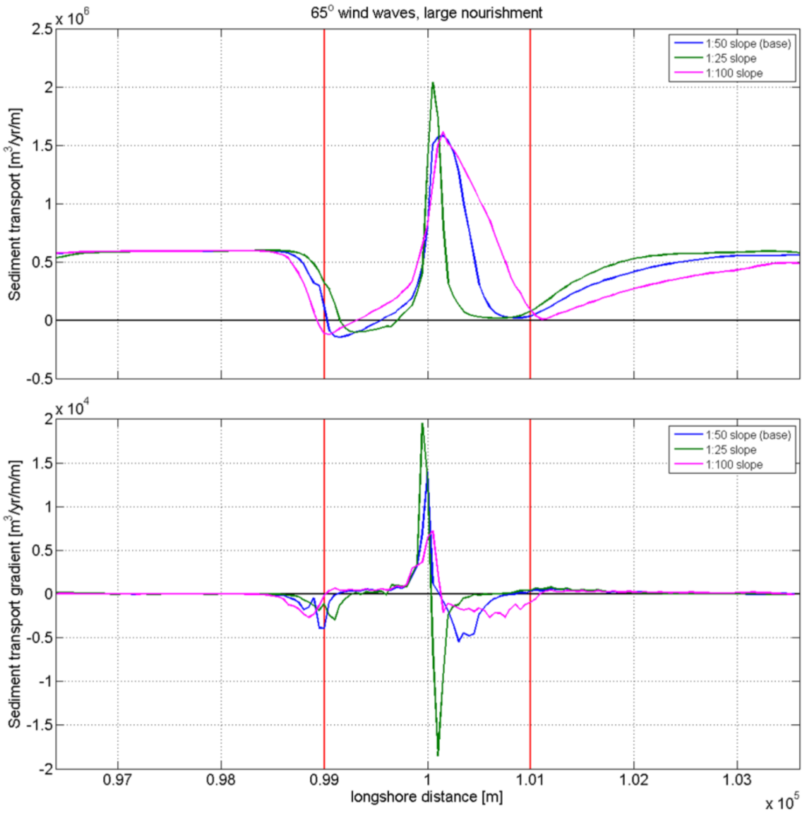

Figure 4.20 Comparison of cross-shore integrated instantaneous net longshore sediment transport (top panel) and gradients (bottom panel) of base (1:50), steep (1:25), and mild (1:100) slopes for 1.5 meter wave height, 65° angle of incidence, and 6 second mean wave period. Nourishment bounds highlighted by red indicators

Table 4.6 Result summary table for sensitivity analysis of large nourishment with mild (1:100) and steep (1:25) beach slopes under highly and extra oblique waves (1.5 meter wave height, 6 second mean wave period). Includes relationship between flow diversion location, downdrift accretion location, Approach 2 (skewness), and Approach 1 (gradients)

Simulation description	Flow diversion location [m]	Downdrift accretion location [m]	Approach 1: Reshaping mechanism	Approach 2: Skewness [-]
65°, 1:25	550	30	Migration + minor diffusion	2.80
80°, 1:25	550	30	Migration + minor diffusion	3.00
65°, 1:100	450	130	Migration + minor diffusion	0.64
80°, 1:100	580	100	Migration + minor diffusion	0.83

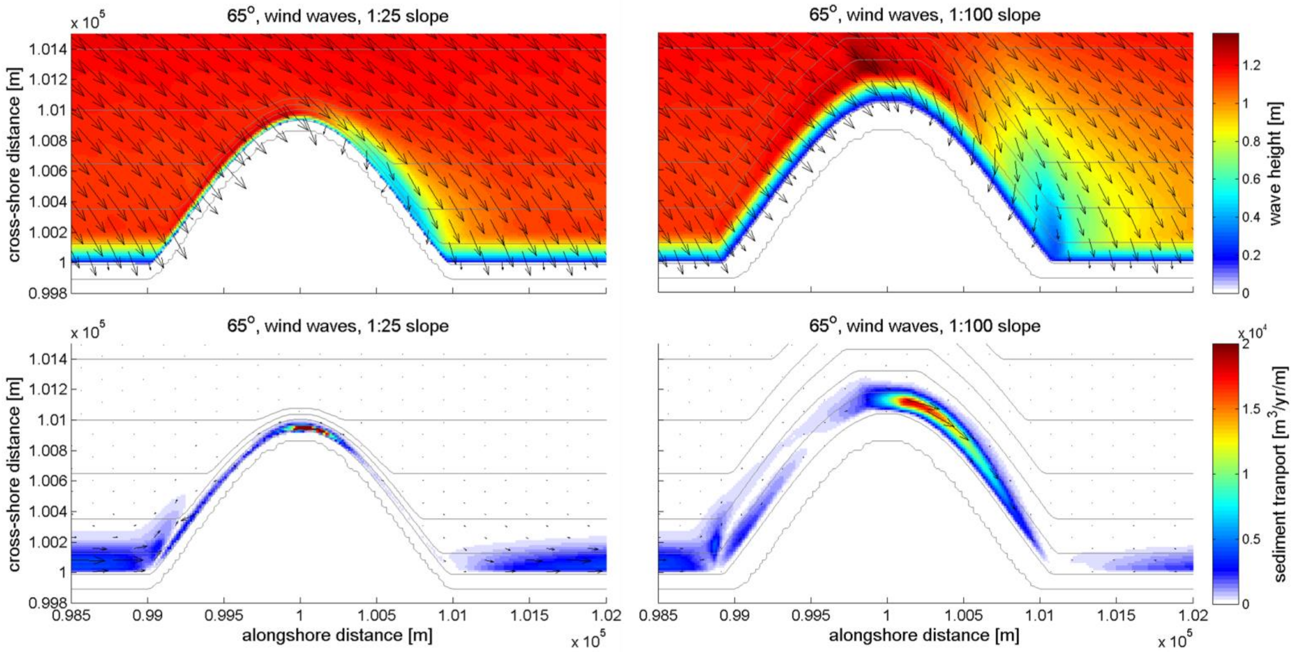

Figure 4.21 Comparison between steep (1:25, left panels) and mild (1:100, right panels) slope for large nourishment configuration under 1.5 meter wave height, 65° angle of wave incidence, and 6 second mean wave period. Wave fields on upper panels and instantaneous sediment transport fields on lower panels

4.5 Conclusions

A numerical experiment using Delft3D was undertaken to evaluate the potential for nourishment migration. Different scenarios were explored including the influence of high and low angle waves and large and small nourishment configurations of realistic proportions. The analysis was accomplished via (1) initial longshore sediment transport gradients, and (2) initial longshore sediment transport distribution skewness. The following conclusions were drawn from the model results:

From base matrix:

- Under the influence of very oblique waves such as 65°, large nourishment have the potential to migrate downdrift and to result in an area of lee erosion
- Initial sediment transport gradients (Approach 1) can provide qualitative information regarding the (a) diffusion, (b) migration, and (c) potential mixed reshaping between diffusion and migration of nourishments
- A proper quantification of the degree of downdrift migration can be obtained from the skewness in the initial alongshore sediment transport distribution (Approach 2):
    - Skewness values large than one (γ_1>1) have the potential for asymmetric nourishment response by means of downdrift migration (translation)
    - Skewness close to zero (γ_1≈0) have the potential for symmetric nourishment response with a more classical diffusive behavior

- Skewness is not able to assess nourishment reshaping where minor migration can also be of influence. In such cases, e.g. large nourishment under mildly oblique waves, it is necessary to refer to the transport gradient results

- Large nourishments act as a shield to non-normally incident waves creating an area of low wave energy on the lee side of the nourishment and a corresponding focal area of refraction-induced wave energy increase near the nourishment centerline; such localization of wave energy results in an enhancement of wave-driven sediment transport. This phenomenon is present in large nourishments under mild and very oblique waves but it is particularly pronounced for large angle such as 65°
- Irrespective of angle of wave incidence, small nourishment have the potential for classical diffusive reshaping mechanism. Translation is not predicted for small nourishments under high wave obliquity because the corresponding limited cross-shore extent reaches shallow depths upon which waves have already refracted hence; shielding effects and subsequent refraction-induce sediment transport increase cannot take place
- Process-based models (i.e. Delft3D) should be employed over coastline models for assessing the potential of nourishment migration because they properly account for nearshore wave transformation which is key for nourishment migration. The bulk sediment transport equation fails to predict sediment transport rates as Delft3D for high wave obliquity because it uses the off-shore wave properties and coastline angle ignoring the effects of refraction.

From sensitivity analysis:

- No major difference in potential nourishment reshaping is found between wind waves and swell. Nonetheless, swell is found to refract and shoal more than wind waves resulting in larger localized transport magnitudes, but the spatial distribution of sediment transport is independent of wave period
- Large nourishment migrate under extra oblique waves (80°) upon which no growth is observed; thus, the reshaping of large nourishment reaches an equilibrium
- Highly energetic waves result in potential migration of the nourishment and an observed decreases in transport distribution skewness due to the corresponding spread of sediment transport along nourishment downdrift side
- Changes in beach slope affect the nearshore wave refraction which is reflected on changes in the sediment transport distribution. The stepper profile results in heavily localization of sediment transport near the nourishment centerline whereas the mild profile results in the spreading of sediment transport; such behaviors were properly quantified by respectively high and low values of transport distribution skewness

Because the concluding remarks are solely based on the initial sediment transport computations where no bed level updates are considered, it is of uttermost interest to verify the nourishment reshaping predictions by means of morphological simulations. Such findings are presented in the next chapter.

5 Morphodynamic approach

Based on initial alongshore sediment transport, morphological outcome predictions were made in Chapter 4 for a given beach nourishment configuration under certain time invariant wave condition; therefore, the next step is to simulate shoreline evolution by including the feedback between the evolving morphology and the hydrodynamics.

In Chapter 5, **Scenario II** shown on Table 3.1 is modeled by means of bed level updates which serve the following purposes: (1) to verify whether the nourishment reshaping mechanisms predicted by the instantaneous transport gradients are reflected on the resulting bathymetry and (2) to assess the impact on nourishment migration of occasional high angle wave periods with alternating high and low angle wave conditions. The overall aim of Chapter 5 is schematized in Figure 5.1.

Research questions:

Does net nourishment migration play a significant role in coasts that experience occasional periods of high angle waves?

Do large scale nourishments impact the behavior of a coast exposed to high-angle wave conditions?

Method :

Approach 1: Assess morphodynamic response of time invariant conditions

Approach 2: Assess morphodynamic response of occasional high angle wave periods with alternating high and low angle wave conditions

Insight into / Hypothesised results :

(1) Morphodynamic results agree with potential nourishment reshaping predictions based on initial sediment transport reults

(2) Wave chronology and persistance of high angle waves have an impact on nourishment migration

Figure 5.1 Schematization of morphodynamic approach for assessing nourishment migration

It is worth stressing the caveat of List & Ashton (2007) research study as the lack thereof morphodynamic simulations and the inherited inability to evaluate the morphodynamic changes in time; consequently, the present study intends to bridge such knowledge gap.

5.1 Approach

5.1.1 Approach 1: Morphodynamic response of time invariant conditions

Morphodynamic simulations of time invariant wave conditions are intended to verify the nourishment reshaping mechanisms as predicted by the instantaneous transport gradients shown on Table 4.1 and Table 4.2. The morphodynamic simulations presented on section 5.2.1 were completed using process-based model Delft3D following the model settings described on section 3.3.4 and the time invariant hydrodynamic forcing (wave conditions) described on Table 3.3.

The results are presented in two different ways: (1) by qualitatively assessing the time evolution of the bathymetry via observed changes in bed level contours and (2) by quantitatively assessing the net cross-shore volumetric changes.

The net cross-shore volumetric changes were calculated by integrating the volumes in the cross-shore direction for every alongshore grid cell for the initial (t=0 years) and final (t=2.55 years) nourishment bathymetries. The volumetric percent change was then calculated by dividing the difference between final and initial volumes by the initial volume result (see Equation 11); positive percent change indicates accretion while negative percent change indicates erosion of the bed. Such indicator serves as a metric for assessing net sediment losses in the longshore direction exclusively; it does not have the capability to distinguish between the deformations at various depths

$$\%change = \frac{Volume_{final} - Volume_{initial}}{Volume_{initial}} \times 100$$

Equation 11 Net cross-shore volumetric percent change, where final and initial volumes are calculated by integrating the volumes in the cross-shore direction

5.1.2 Approach 2: Morphodynamic response of occasional high angle wave periods with alternating high and low angle wave conditions

Morphodynamic simulations of time varying wave conditions are intended explore the nourishment migration implications based on (1) the moment in time at which high angle wave events take place and (2) the persistence (timespan) of the high angle waves within the wave climate.

The time varying wave climate (wave chronology) morphodynamic results presented on section 5.2.2 were completed using process-based model Delft3D following the model settings described on section 3.3.4. Since potential nourishment migration was predicted for the large nourishment configuration only (see section 4.2), the wave chronology effects were exclusively investigated for the large nourishment configuration. In order to incorporate the effect of wave chronology, synthetic wave time series were created.

The 2.55 year total (morphodynamic) simulation time used in section 5.1.1 was divided into four equal segments after the exclusion of spin-up time. The synthetic time series included variation of high (65°) and low (0°) angle waves; they were set up by shifting the high angle wave event throughout the four different time segments and by increasing the event duration from 25% to 50% and 75% of the total simulation time. To avoid abrupt changes in the wave climate and undesired model instabilities, a smooth transition was achieved by having three time steps equivalent to 2.5 days (morphodynamic time) in between wave conditions. A total of eight synthetic time series were evaluated; the notation reads the wave condition in percent of total simulation time in chronological order, for instance: 25% 0°, 25% 65°, 50% 0° time series indicates the first quarter of the time the wave angle is 0°, the second quarter of the time the wave angle is 65°, and the last 2 quarters (50%) of the time the wave angle is 0°. The simulations scenarios go as follow:

- 25% 65°, 75% 0°
- 25% 0°, 25% 65°, 50% 0°
- 50% 0°, 25% 65°, 25% 0°
- 50% 65°, 50% 0°
- 75% 0°, 25% 65°
- 75% 65°, 25% 0°
- 25% 0°, 75% 65°
- 50% 0°, 50% 65°

Similar to section 5.1.1, the results are presented in two different ways: (1) by qualitatively assessing the time evolution of the bathymetry via observed changes in bed level contours and (2) by quantitatively assessing the net cross-shore volumetric changes using Equation 11.

5.2 Results

5.2.1 Results 1: Morphodynamic response of time invariant conditions

Section 5.2.1 is intended to assess the morphological evolution of nourishments under the influence of a constant wave condition. The aim of this section is to verify the reshaping mechanisms predicted by the initial sediment transport distribution analyses (see section 4.2). The main findings go as follows:

- Resulting bed level updates properly match the potential nourishment reshaping predictions based on the initial sediment transport distribution results (Table 5.1)
- Large nourishment migration includes three distinctive components: crest translation, downdrift protuberance formation, and lee erosion

Table 5.1 Nourishment reshaping result summary table for base matrix (1.5 meter wave height, 6 second mean wave period)

Nourishment size	Wave angle	Gradient approach	Skewness approach	Morphology approach
Small	0°	Diffusion	0.01	Diffusion
	15°	Diffusion	0.44	Diffusion
	65°	Diffusion	0.01	Diffusion
Large	0°	Diffusion	0.07	Diffusion
	15°	Diffusion + minor migration	-0.03	Diffusion + minor migration
	65°	Migration + minor diffusion	1.36	Migration + minor diffusion

In general for a constant wave condition in time, the overall nourishment reshaping seen on the morphological simulations mimics the predictions obtained from the transport gradients and skewness. The sediment transport gradients properly predict all nourishment reshaping, including the mixed behavior of large nourishment under mild oblique waves. Meanwhile, the sediment transport distribution skewness predictions correlate to the well-defined diffused and translated nourishments, but not to the cases where minor translation has an influence on nourishment reshaping.

Nourishment diffusion results from small and large nourishments under normally incident waves; diffusion is characterized by the spreading of sediment from the crest in the outward direction; as predicted by the sediment transport gradients (Table 4.1), the bathymetry updating for all small nourishment simulations resulted in diffused bed levels. Based on model bathymetry results, large nourishment downdrift migration (see Figure 5.2) comprises the following features: downdrift migration of the crest at deep water, protuberance development at shallow water, and downdrift erosion outside nourishment bounds in shallow water.

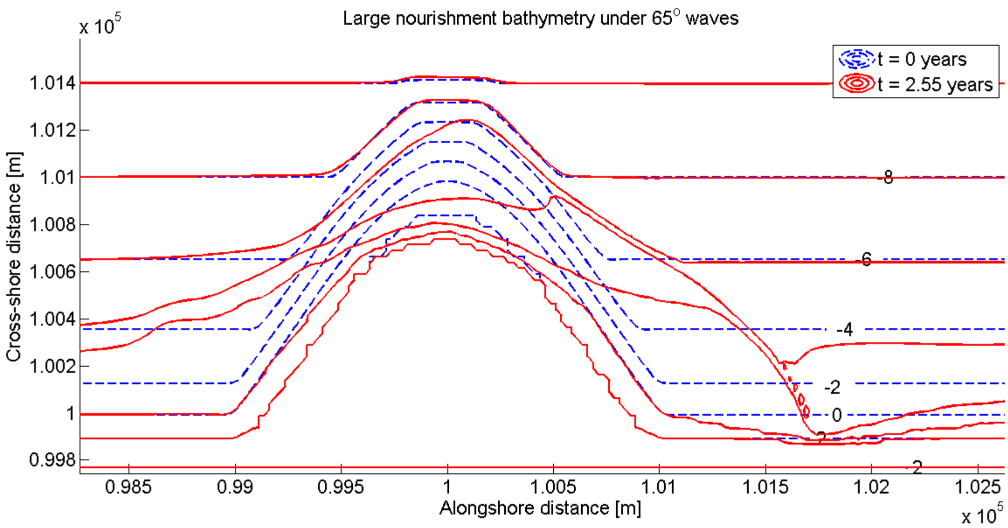

Figure 5.2 Detailed view of bed level changes for large nourishment under 1.5 meter wave height, 65° waves, 6 second mean wave period for initial (0 years) and final (2.55 years) conditions. Nourishment migration includes deep water crest translation, protuberance growth at shallow water, and lee erosion

5.2.2 Results 2: Morphodynamic response of occasional high angle wave periods with alternating high and low angle wave conditions

In section 5.2.1, the evolving nourishment morphology is driven by a time invariant angle of wave incidence, which could be considered an average wave climate. However in reality, waves vary in time and the corresponding chronology of wave conditions may have an effect coastline morphological evolution thus, on nourishment reshaping.

Section 5.2.2 is dedicate to numerically explore the implications of (1) the moment in time at which high angle wave events take place and (2) the persistence (timespan) of the high angle waves within the wave climate. The main findings go as follows:

- The final wave condition leaves an imprint on the nourishment bathymetry while the more persistent wave condition has an effect on the net volume change
- Periods of low-angle waves can rapidly wipe out the instabilities of high-angle wave situations and thus result in a diffusive pattern
- Long periods with high angle waves result in smaller net losses from the nourishment area at the expense of lee erosion

When high angle wave events have a long duration, the net sediment gain due to nourishment migration is maintained in the vicinity of the object (the nourishment). Following a high angle wave event, normally incident waves can in fact dissipate the translation signals (downdrift protuberance and lee erosion) very effectively particularly in shallow water. On the other hand, when the high angle wave event occurs in the end of the simulation after an extended low angle wave period, lee protuberance forms and the eroded sediment from the diffused nourishment crest is more evenly spread throughout the domain.

The closer high angle wave event occurs to the beginning of the simulation, the more symmetric the bathymetric contours are with respect to the nourishment centerline, and the more similar the behavior is to normally incident waves. As the high angle wave event shifts closer to the end of the simulation, translation imprints develop in the bathymetry; the greater the shift, the more pronounced the translation signals.

5.3 Analysis

Section 5.2 presented the results pertaining to nourishment reshaping based on morphodynamic simulations. These results are analyzed in section 5.3 by looking at the time evolution of nourishment under a constant wave condition (section 5.3.1) and by assessing the impact wave chronology has on nourishment reshaping (section 5.3.2).

5.3.1 How does nourishment bathymetry evolve in time under a constant wave climate?

For large nourishment under 65° waves (see Figure 5.2), asymmetry is clearly present and as predicted by the transport gradients and skewness, downdrift migration is the dominant reshaping mechanism. There is a clear distinction between the updrift and downdrift bed levels. The nourishment reshaping is depth dependent: protuberance formation, downdrift migration of the object, and lee erosion occur at -2 and -4 meter contour lines, and crest translation is observed at -4 and -6 meters. It was noted as the time increased, the protuberance kept migrating downdrift, which resulted in the displacement and enhancement of the lee erosion toward the east boundary. Diffusion was observed at 0 and +2 meter depths where crest retreat occurred. Imperceptible bed level changes are seen at or beyond the -8 meter depth.

For the large nourishment under the influence of 15° angle waves (Figure 5.3), downdrift migratory characteristics appear on the bathymetric contours however; it is observed the extent of the migration varies as a function of depth. Initially, the nourishment reshapes by diffusing the crest and by translating the lee side of the nourishment; this initial behavior is localized at shallow depths (0 and -2 meters); as time increases, the migratory features are enhanced and reach deeper water (-4 and -6 meters). Near the end of the simulation, the migratory character seen in shallow water vanishes giving a symmetric and diffused bed levels, but the slight translation condition seen on deeper regions remains unchanged. Overall, the morphodynamic nourishment reshaping of the large nourishment under 15° waves agrees with the mixed predictions of transport gradient being diffused and slightly migrated; however, a reshaping depth dependency is observed since the nourishment diffuses at shallower depths while the diffused footprint translates.

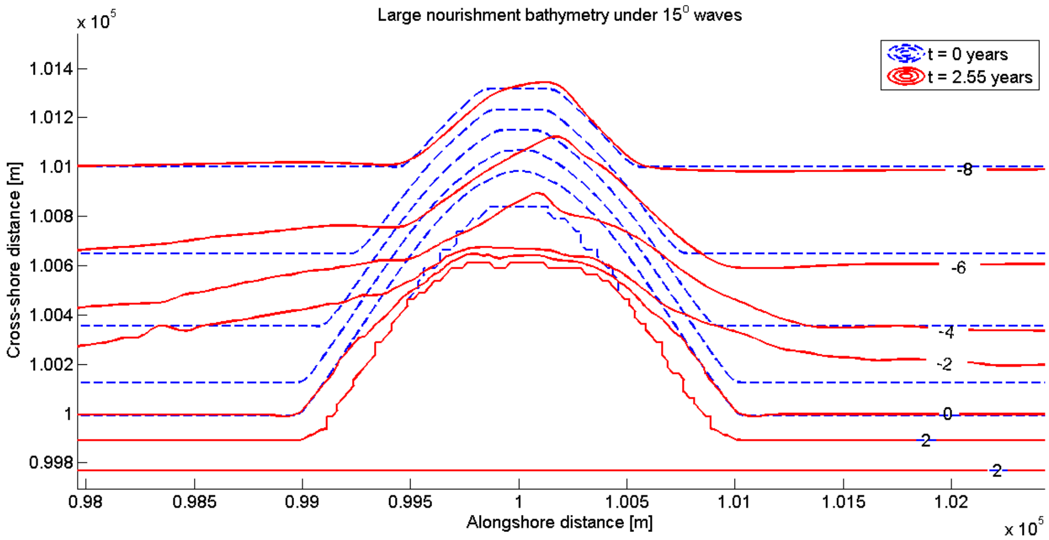

Figure 5.3 Detailed view of bed level changes for large nourishment under 1.5 meter wave height, 15° waves, 6 second mean wave period for initial (0 years) and final (2.55 years) conditions. Mild nourishment migration occurs at the crest on deep water

The morphodynamic simulations corresponding to large nourishment under normally incident waves as well as the small nourishment under 0°, 15°, and 65° waves results in a diffusive behavior which agrees with the initial sediment transport gradient predictions.

Aside from qualitatively describing beach nourishment reshaping as a function of depth, deformation is quantitatively evaluated by calculating the net cross-shore integrated volumetric changes (see Figure 5.4).

The net volume changes of 65° waves indicate the sediment is maintained within the nourishment bounds, when compared to the normally incident wave curve, but a pronounce erosion is observed in the downdrift side. For the 15° wave results, a net sediment gain is observed on the updrift nourishment side which in fact agrees with the sediment transport gradients (also see Figure 5.3); however, translation did occur at deep water (not captured by cross-shore integrated volumes) since the -6 and -4 meter contours took a saw-tooth like shape. Lastly, the cross-shore integrated volume percent change curve for normally incident waves as expected is symmetrical displaying heavy erosion at the crest and even accretion outwardly of nourishment bounds.

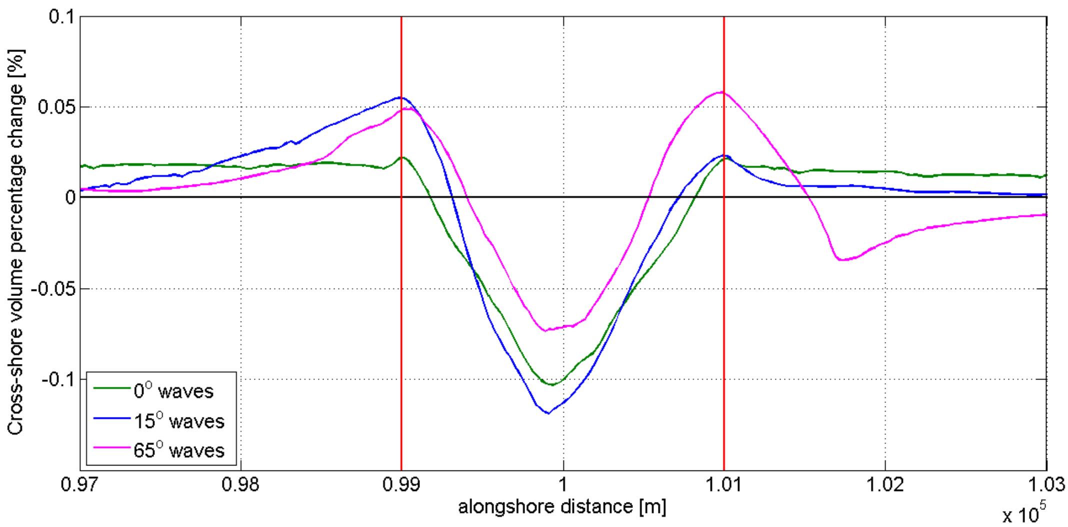

Figure 5.4 Cross-shore integrated volume percent change for large nourishment time invariant wave conditions with constant mean wave period of 6 second and constant wave height of 1.5 meter. Nourishment bounds shown in red vertical lines

5.3.2 How does wave chronology impact volume and bathymetry changes?

Results showed that a short duration (25% of total simulation time) of low-angle waves can rapidly smooth out the instabilities (protuberance like features) resulting from high-angle wave situations which leads to a diffusive pattern; however, a longer period (50% or more of total time) of high angle wave event results in lower net sediment losses within the nourishment area at the expense of downdrift erosion.

Persistence of high angle wave in time

Figure 5.5 shows how the persistence of a high angle wave condition impacts the net volume changes in a nourishment. When high angle wave event is more persistent (longer duration) in the wave climate compared to the low angle waves, the migration character is manifested in a larger net sediment gain within the nourishment vicinity: volume losses at the crest are small and the volume gains at the bounds are large; however, such volume retention comes at the expense of lee erosion (see 25% 0°, 75% 65° simulation). On the other hand, when low angle wave event is more persistent compared to the high angle wave event (see 50% 0°, 25% 65°, 25% 0° simulation), the diffusive character is manifested in a larger net sediment gain outside the nourishment bounds; such volume gain realtes to the sediment losses observed at the nourishment centerline.

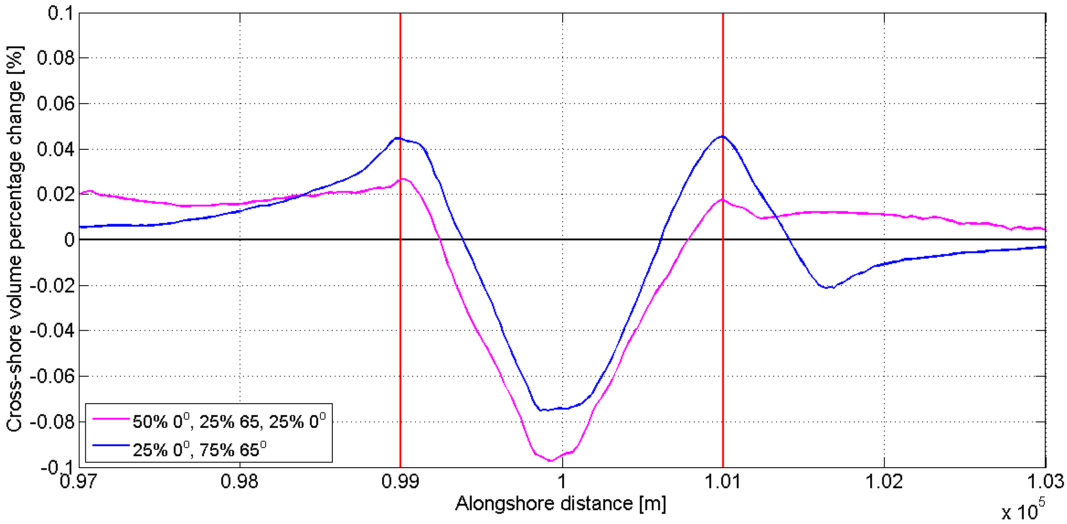

Figure 5.5 Cross-shore integrated volume percent change for representative time varying wave climate simulations: 50% 0° 25 % 65° 25% 0°, and 25% 0° 75% 65° with constant mean wave period of 6 second, and constant wave height of 1.5 meter. Nourishment bounds shown in red vertical lines

Although the results presented hereto pertain to nourishment reshaping and not to the development of large scale shoreline sand waves, the current results -indicating the need of a prolonged high angle wave event to have an imprint on net volume changes- are in partial agreement with Van den Berg, et al (2012). Their analysis found a minimum contribution of high incidence angles of about 80% is required for the spontaneous formation of sand waves where "apparently the contribution of the diffusive effect of the low angle waves to the shoreline dynamics was relatively stronger than the anti-diffusive effect (growth) of the high angle waves" (Van den Berg, 2012).

Moment in time at which high angle wave event occurs

Regarding the order of wave conditions, if high angle wave event is followed by normally incident waves (see Figure 5.6), 0° waves can smooth the distinctive protuberance and lee erosion; such smoothing varies throughout the depth contours since it is heavily pronounced in shallow water and more mild in deeper water. The final result is a more symmetric bathymetric pattern characteristic of diffusion.

A close look at the time evolution of wave and sediment transport fields reveals an abrupt increase in nearshore wave height and wave energy associated with the transition from high oblique to normally incident waves. Recalling highly oblique waves are prone to refraction upon entering the domain which causes the wave crests to stretch resulting in a reduction of wave height; on the contrary, normally incident waves are able to more efficiently maintain the offshore wave height which results in higher wave energy at the breaker zone and thus, larger sediment transport magnitudes. The change in wave orientation causes the spreading (along the nourishment perimeter) of the initially focused sediment transport (section 4.3.1); consequently, normally incident waves can rather rapidly stabilize the translation features seen near the breaker zone but not at deeper water where translation features remain.

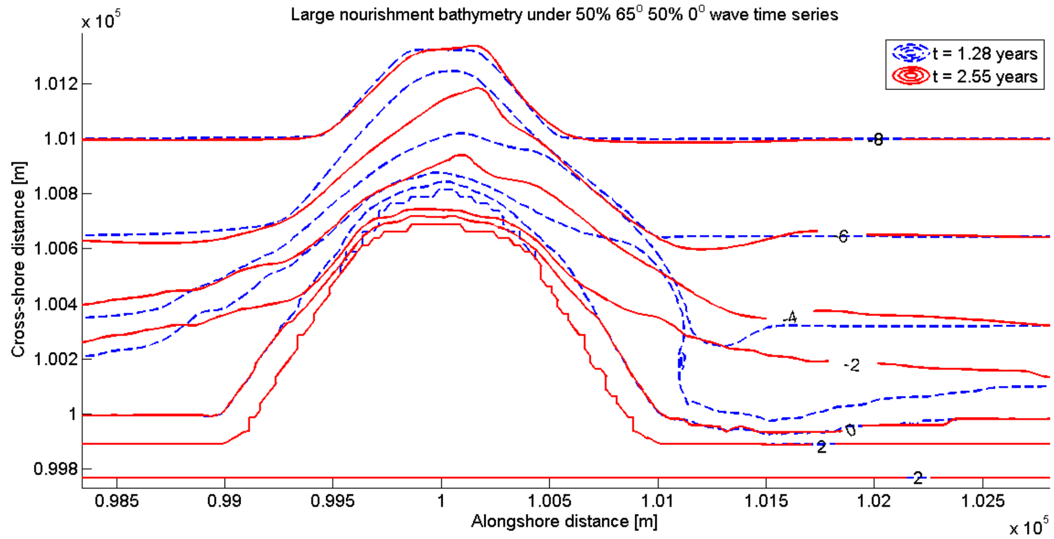

Figure 5.6 Detailed view of bed level changes for large nourishment under 1.5 meter wave height, 6 second mean wave period for half-time (1.28 years) and final (2.55 years), 50% 65° 50% 0° wave time series. Normally incident wave able to smooth out high angle wave protuberance

On the other hand, when the high angle wave event follows after normally incident waves (see Figure 5.7), two translation signals are observed at shallow water: (1) protuberance growth at nourishment right bound (similar to instability from Ashton, et al 2001) and (2) minor lee side erosion. Even though the nourishment had experienced sediment losses through the action of normally incident waves, the high angle waves can still imprint translation features on the object.

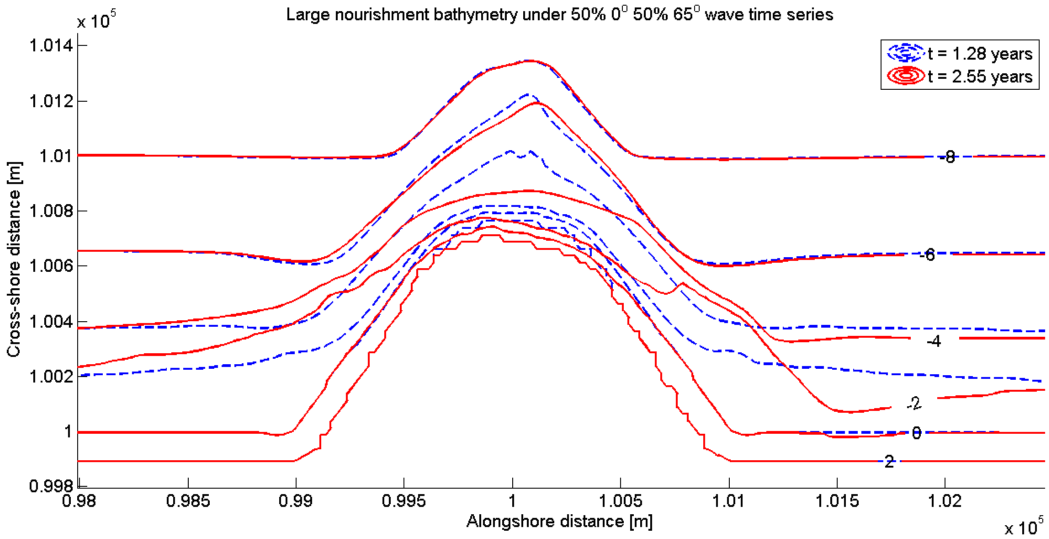

Figure 5.7 Detailed view of bed level changes for large nourishment under 1.5 meter wave height, 6 second mean wave period for half-time (1.28 years) and final (2.55 years), 50% 0° 50% 65° wave time series. Nourishment migration imprinted on protuberance formation

5.4 Conclusions

A Gaussian nourishment of large scale was set up in Delft3D to simulate the reshaping processes which include the interaction of waves and currents in the bed level updates. Constant and time varying wave conditions were simulated to evaluate the relevance of wave chronology on nourishment evolution.

The following conclusions are drawn from the time invariant wave climate model results:

- Morphodynamic simulations of time invariant wave conditions properly correlate to the reshaping predictions obtained from the initial sediment transport gradients and skewness for small and large scale nourishments
- Large nourishment under normally incident waves results in a symmetric and diffusive response displaying more pronounced cross-shore diffusivity at shallower depths. For 15° waves, a reshaping depth dependency is observed because the large nourishment diffuses at shallower depths and the initially diffused crest translates at deep water. Under 65° waves, the nourishment reshapes asymmetrically including the following translation features: (1) downdrift translation of the crest at deep water, (2) protuberance growth on object at downdrift side, and (3) lee erosion

The following conclusions are drawn from the time varying wave climate model results:

- Wave chronology has an impact on beach nourishment reshaping, and there is a distinction between (1) the duration and (2) the moment in time at which high angle wave events take place: the final condition has stronger signal on the reshaping (deformation) of bathymetric contours, but the more persistent condition produces a stronger effect on the net volume change

- Prolonged high angle wave events create a net sediment gain in the nourishment and its vicinity at the expense of lee side erosion. On the other hand, if normally incident wave events are prolonged, the crest retreat is evident and the corresponding eroded sediment is evenly and outwardly spread
- If a high angle wave event is followed by normally incident waves, the migration signals in shallow water (downdrift protuberance and lee erosion) are effectively smooth out but the migration signals in deep water (crest translation) remain preserved. When the high angle wave event occurs at the end of the simulation after nourishment diffusion, a downdrift protuberance can still develop at shallow depths despite the initial retreat
- Normally incident waves can effectively smooth out instabilities caused by prolonged high angle wave events in a short period of time because of the resulting increment of wave height (wave energy) and spreading of wave driven sediment transport associated with the transition from high to low wave angles

6 Conclusions

The goal of this research was to evaluate whether there can be net longshore migration of nourishments for areas which experience high angle waves occasionally, but are not dominated fully by low-angle nor high-angle waves. The goal was achieved by means of numerical simulations using process based model Delft3D in which the influence of high angle waves on nourishment of realistic proportions were tested. This analysis distinguished the following phases: initial sediment transport of time invariant wave climate, evolving nourishment morphology under constant wave conditions, and evolving nourishment morphology under time varying wave climate. Following the approach described on section 1.4 and the findings presented in Chapters 4 and 5, conclusions are drawn providing answers to the research questions stated in section 1.3:

Potential for nourishment reshaping

Asymmetric and symmetric nourishment reshaping are respectively defined as downdrift migration and diffusion. While all tests indicated nourishment diffusion at different levels, the degree at which the diffusive mechanism is overtaken by downdrift migration depends on nourishment size and the angle of wave incidence:

- Large nourishments under the influence of very oblique waves exhibit a predominantly downdrift migratory character
- Large nourishments under the influence of mild oblique waves exhibit diffusive and migratory mixed characters
- Diffusion is always dominant reshaping mechanism in small nourishments irrespective of wave angle

Ability of models to compute correct transport rates and predict migration

- Initial sediment transport gradients provide qualitative information regarding the (a) diffusion, (b) migration, and (c) potential mixed reshaping between diffusion and migration of nourishments
- Downdrift migration is quantitatively measured from the skewness in the initial alongshore sediment transport distribution. Skewness large than one (γ_1>1) result in asymmetric nourishment reshaping through downdrift migration; skewness close to zero (γ_1≈0) result in symmetric nourishment response with a more classical diffusive behavior.
- Skewness is not able to assess nourishment reshaping where minor migration can also be of influence. In such cases, e.g. large nourishment under mildly oblique waves, it is necessary to refer to the transport gradient results
- To understand and predict beach nourishment behavior under high angle of wave incidence, processed-based models such as, Delft3D should be chosen over coastline models, i.e. S,ϕ-curve. Because of the assumption behind the S,ϕ-curve (parallel contour lines and wave angle at breaking equal to offshore angle of wave incidence), theoretical transport fails to

predict sediment transport rates for high wave obliquity since it does not account for the refraction-induced transport peaks seen on Delft3D

Processes affecting nourishment reshaping

- Downdrift migration is the consequence of wave-driven sediment transport gradients having a pattern of updrift erosion and downdrift sedimentation. Such gradients are associated with the significant localization of sediment transport downdrift of the crest, which results from the refraction-induced focusing and spreading of wave energy
- Refraction-induced wave energy increase is a direct consequence of the nourishment size. Large nourishments act as a shield to oblique waves creating an area of low wave energy on the nourishment lee side and an adjacent area of wave energy increase downdrift of the crest. Shielding effects cannot take place in small nourishments even under high wave obliquity because the limited cross-shore extent does not allow for localization of wave energy thus; the subsequent transport gradients do not lead to translation, and diffusion is the dominant mechanism

Verification of nourishment reshaping predictions

The resulting bed levels properly mimic the reshaping mechanisms predicted via initial sediment transport gradients and skewness. For large nourishments, the reshaping process is depth dependent since the extent of diffusion and/or translation varies in space:

- Downdrift migration of large nourishment encompasses the following features: (1) translation of the crest at deep water, (2) protuberance development on object at downdrift side, and (3) lee erosion
- Irrespective of wave angle, diffusion always predominates in shallow water. For the mixed reshaping predictions (i.e. large nourishment under 15°), diffusion is more pronounced at shallow depths and crest translation occurs at deep water

Nourishment migration on coasts that experience occasional periods of high angle waves

Time varying wave climate simulations showed the morphological response of the considered nourishments depends on (1) the moment in time at which a high angle wave event takes place and (2) the persistence of the high angle waves within the wave climate:

- Prolonged normally incident wave events result in large net sediment losses (as observed from the evident crest retreat) on the nourishment itself but a net gain outside the nourishment bounds where sediment is evenly spread. On the contrary, prolonged high angle wave events result in net sediment gains within the nourishment bounds and its vicinity but at the expense of lee side erosion.
- If a high angle wave event occurs after a nourishment has been diffused, downdrift protuberance can still develop at shallow depths despite the initial retreat. On the other hand, if a high angle wave event is followed by normally incident waves, the migration

signals (downdrift protuberance and lee erosion) are effectively dissipated in shallow water but are well preserved in deep water.

- A short period of normally incident waves can effectively smooth out instabilities caused by antecedent high angle wave events because of the difference in wave height decay and wave energy spreading between 0° and 65° waves. Normally incident waves do not undergo refraction-induced wave height decrease as obliquely incoming waves do. On the contrary; normally incident waves maintain a higher wave height over a broader area along the nourishment perimeter

7 Recommendations

A deeper understanding of physical processes that drive nourishment reshaping is very much needed. The findings presented in this report provide insight for future research work; the following recommendations are intended to include study scenarios closer to natural processes and potential model improvements.

- **Inclusion of additional hydrodynamic forcing**

Beach nourishments are dynamic and complex systems driven by several natural processes. In the present study, the exclusive influence of waves was proven to be decisive in nourishment reshaping; nonetheless, other hydrodynamic forcing such as tides (vertical and horizontal) and wind exert an influence in sediment transport (Kaji, 2013). Hence it is recommended to assess the influence of tides and wind on the initial sediment transport gradients and skewness as well as subsequent morphodynamic simulations. The inclusion of more realistic scenarios will contribute to the improvement of beach nourishment reshaping predictions for better and more optimum designs.

- **Further initial sediment transport analyses**

In the present study, representative low and high wave obliquities were used to assess nourishment reshaping. Respectively for large nourishment under 15° and 65° angle waves, the calculated skewness were -0.03 and 1.36; therefore, it is believed a transition wave angle upon which the initial sediment transport skewness becomes one (γ_1=1) and the reshaping changes from mainly diffusive to translation exists between 15° and 65°. It is recommended to perform initial sediment transport analyses for various increasing wave angles in order to evaluate under what wave obliquity the reshaping transition occurs. Based on the present results and previous studies (Ashton, et al. 2001; Ashton & Murray, 2006), there is a potential for the transition to occur close to 45°.

- **Further morphodynamic simulations**

The analysis presented on section 9.2 indicates the sensitivity of morphodynamic model results to the cross-shore component in the TRANSPOR2004 sediment transport formula. Even though the exclusion of the wave related transport component does not cause significant changes on the initial longshore sediment transport distribution skewness, it does affect the resulting bed level updates at (1) deep water on the crest and at (2) the west domain boundary. Therefore it is recommended to assess the contribution of cross-shore transport; the effect of the undertow was not accounted in this study since the model used in was depth averaged (see section 3.3). In order to properly evaluate the contribution of wave related transport, a three-dimensional model setting is recommended where potential reshaping mechanisms can be further explored.

- **Improvements on Neumann boundary conditions**

As shown on appendix 9.2, the cross-shore component in the TRANSPOR2004 formula resulted in unexpected developments of spurious solutions at the Neumann boundary. It is highly recommended to evaluate and make the necessary adjustments to the interaction between the Neumann boundary and the wave related transport component in the TRANSPOR2004 formulation, particularly the bed load and suspended load factors, BedW and SusW. Such adjustments are considered essential for evaluating the contribution of cross-shore transport in nourishment morphology.

- **Comparison with data from sand engine**

Hindcasting of high angle wave events in the Sand Motor and evaluation of corresponding sediment transport skewness is recommended to assess the potential downdrift migration of the Sand Motor given an actual large scale beach nourishment proportion. It is also of interest to compare the potential cross-shore variability of diffusivity and translation in the Sand Motor under low angle waves versus the depth dependency of nourishment reshaping observed on the morphodynamic simulations.

8 References

Ashton, A., & Murray, A. (2006a). High-angle wave instability and emergent shoreline shapes: 1. Modeling of sand waves, flying spits, and capes. *ournal of Geophysical Research: Earth Surface (2003–2012), 111(F4)*.

Ashton, A., & Murray, B. (2006b). High-angle wave instability and emergent shoreline shapes: 2. Wave climate analysis and comparisons to nature. *Journal of Geophysical Research, 111*.

Ashton, A., Murray, B., & Arnoult, O. (2001). Formation of coastilne features by large-scale instabilities induced by high-angle waves. *Nature, 414*, 296-300.

Battjes, J., & Janssen, J. (1978). Energy loss and set-up due to breaking of random waves. *Proceedings 16th International Conference Coastal Engineering, ASCE*, (pp. 569-587).

Bosboom, J., & Stive, M. (2013). *Coastal Dynamics I.* Delft: VSSD.

Davis, R., Wang, P., & Silverman, B. (2000). Comparison of the performance of three adjacent and differently constructed beach nourishment projects on the Gulf pensinsula of Florida. *Journal of Coastal Research 16*, 396-407.

Deltares. (2011). *Delft3D-FLOW: Simulation of multi-dimensional hydrodynamic flows and transport phenomena, including sediments. User manual, version 3.15.* The Netherlands.

Deltares. (2014). *Delft3D-WAVE: Simulation of short-crested waves with SWAN User Manual.* Delft, Netherlands.

Dissanayake. (2012). Modelling morphodynamic response of a tidal basin to an anthropogenic effect: Ley Bay, East Frisian Wadden Sea – applying tidal forcing only and different sediment fractions. *Coastal Engineering, 67*, 14-28.

Falques, A. (2003). On the diffusivity in coastline dynamics. *Geophysical Research Letters, 30(21)*.

Falqués, A., & Calvete, D. (2005). Large-scale dynamics of sandy coastlines: Diffusivity and instability. *Journal of Geophysical Research: Oceans, 110(C3)*.

Giardino, A., Brière, C., & Van der Werf, J. (2011). *Morphological modelling of bar dynamics with Delft3D. The quest for optimal parameter settings.* Delft: Deltares.

Grunnet, N., Ruessink, B., & Walstra, D. (2005). The influence of tides, wind and waves in the redistribution of noursihed sediment at Terschelling, The Netherlands. *Coastal Engineering 52*, 617-631.

Hallermeir, R. (1978). Uses for a calculated limit depth to beach erosion. *Coastal Engineering Proceedings (1) 16.*

Hamm, L., Capobianco, M., Dette, H., Lechuga, A., Spanhoff, R., & Stive, M. (2002). A summary of European experience with shore nourishment. *Coastal Engineering 47*, 237-264.

Hartog, W., Benedet, L., Walstra, D., Van Konigsveld, M., & Stive, M. (2008). Mechanisms that influence the performance of beach nourishment: a case study in Delray Beach, Florida, USA. *Journal of Coastal Research*, 1304-1319.

Kaji, A. (2013). *Assesment of variables influencing sediment transport at the Sand Motor. Master Thesis.* Delft University of Technology.

Leonard, L., Clayton, T., & Pilkey, O. (1990). An analysis of replenished beach design parameters on U.S. east coast barrier islands. *Journal of Coastal Researh 6*, 15-36.

Lesser, G., Roelvink, J., van Kester, J., & Stelling, G. (2004). Development and validation of a three-dimensional morphological model. *Coastal Engineering, 51*, 883-915.

List, J., & Ashton, A. (2007). A circulation modeling approach for evaluating the conditions for shoreline instabilities. *Coastal Sediments' 07*, (pp. 327-340).

Measures of Shape: Skewness and Kurtosis. (2012, December 27). Retrieved from http://www.tc3.edu/instruct/sbrown/stat/shape.htm#Skewness

NOAA. (2014). Retrieved from www.csc.noaa.gov/archived/beachnourishment

Pelnard-Considere, R. (1956). Essai de theorie de l'evolution des formes de rivage en plages de sable et de galets. *4th Journees de l'Hydraulique, Les Energies de la Mer, 3(1)*, 289-298.

Reniers, A., Roelvink, J., & Thornton, E. (2001). Morphodynamic modeling of an embayed beach under wave group forcing. *Journal of Geophysical Research: Oceans (1978–2012), 109(C1)*.

Rijkswaterstaat. (2013). Retrieved from www.dezandmotor.nl

Ruessink, B., Walstra, D. J., & Southgate, H. (2003). Calibration and verification of a parametric wave model on barred beaches. *Coastal Engineering, 48(3)*, 139-149.

Stive, M., De Vriend, H., & Capobianco, M. (1992). Shore nourishment and the active zone: A time scale dependent view. *Coastal Engineeringn Proceeding, 1(23)*, (pp. 2464-2473).

Van den Berg, N., Falqués, A., & Ribas, F. (2011). Long-term evolution of nourished beaches under high angle wave conditions. *Journal of Marine Systems, 88(1)*, 102-112.

Van den Berg, N., Falques, A., & Ribas, F. (2012). Modeling large scale shoreline sand waves under oblique wave incidence. *Journal of Geophysical Research, 117*.

Van Rijn, L. (1993). *Principles of sediment transport in rivers, estuaries and coastal seas.* Amsterdam: Aqua publications.

Van Rijn, L. (2000). *General view on sand transport by currents and waves. Report Z2899.20-Z2099.30-Z2824.30.* Delft, The Netherlands: WL Delft Hydraulics.

Van Rijn, L. (2002). *Approximation formulae for sand transport by currents and waves and implementation in DELFT-MOR. Report Z3054.20.* Delft, The Netherlands: WL Delft Hydraulics.

Van Rijn, L., & Walstra, D. (2003). *Modelling of sand transport in Delft3D-ONLINE. Report Z3624.* Delft, The Netherlands: WL Delft Hydraulics.

Van Rijn, L., Walstra, D., & Van Ormondt, M. (2004). *Description of TRANSPOR2004 and implementation in Delft3D-ONLINE. Report Z3748.10.* Delft, The Netherlands: WL Delft Hydraulics.

9 Appendices

9.1 Model grid sensitivity

In this section, a reflection is made regarding the numerical modeling aspect related to grid sensitivity relevant fort his research.

In order to optimize model results, the sensitivity of 15 m, 25m, and 50m squared grid resolutions was tested for two different scenarios: 0° and 65° waves for the same large nourishment bathymetry. The corresponding instantaneous net longshore sediment transport integrated over the cross-shore shown on Figure 9.1.

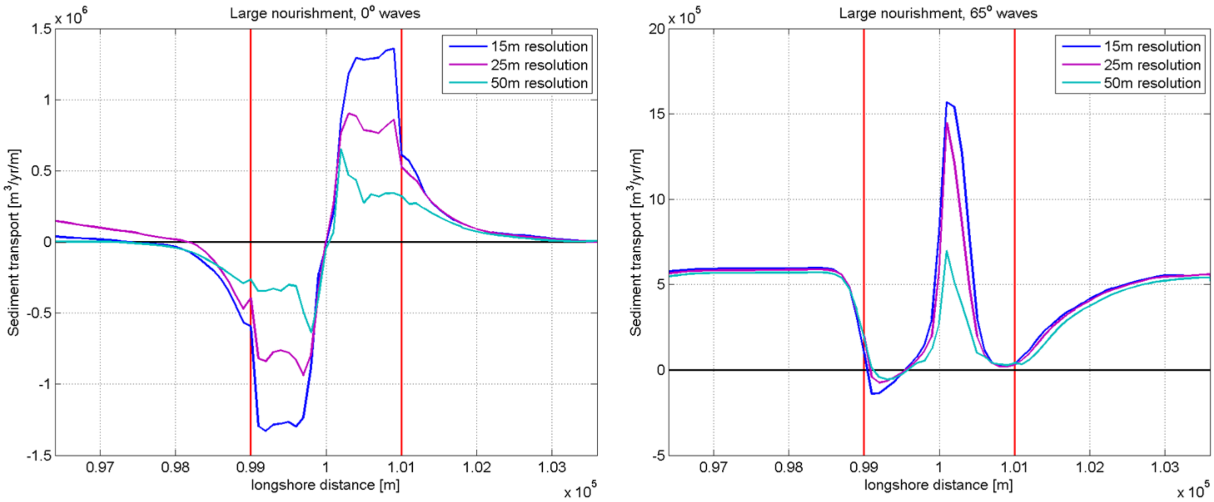

Figure 9.1 Grid resolution optimization results for large nourishment: instantaneous net longshore sediment transport corresponding to 0 degree waves and 65 degree waves at left and right panels, respectively

When looking at the deviations between the different resolutions for 65° angle of wave incidence sediment transport results, the 15m and 25m grid resolution result in similar patterns and magnitudes compared to the 50m grid resolution. Those similarities disappear under normally incident wave conditions however; the sediment transport distribution is maintained in space.

To counteract the difference in results, 12.5m grid was tested but the computational time increased exponentially. Therefore, a compromise between computational time and grid resolution was attained by selecting the 15m grid, and the 25m grid resolution was disregarded and considered coarse for wave propagation. The 15m grid resolution is believed to affect the normally incident wave results; nonetheless, 15m wave grid is considered appropriate for evaluating nourishment migration which occurs under the influence of very oblique waves. It is also noted the grid resolution used in (List & Ashton, 2007) is lower than the grid used in this study since it equaled 25m in the flow domain.

9.2 Notions on the application of the current Delft3D model for simulating the morphodynamic response of nourishments

Ideally, morphodynamic simulations should be performed following the parameters used in the initial sediment transport simulations provided model stability (free of spurious solutions). In an extensive series of preliminary simulations, spurious solutions developed at the west boundary where unwanted sediment accreted for all test runs. Different parameters and model features were tested in order to determine the cause of the model instability. Among those, the influence of the Roller model was tested by having the WAVE (SWAN) module perform the wave computations. "[The SWAN] option means to model the energy dissipation in random waves due to depth induced breaking, the bore-based model of Battjes & Janssen (1978) is used. In this option a constant breaker parameter is to be used: α (coefficient for determining the rate of dissipation) equal to 1.0 and γ (the value of the breaker parameter defined as ratio of wave height to depth) equal to 0.73" (Deltares, 2014). The Roller model was then deactivated resulting in successful 2.55 year morphodynamic time equivalent simulations; such results are presented in Chapter 5.

Morphodynamic simulations included the variables listed on the base matrix (Table 3.3); however, bed level updating results proved sensitive to wave period since sediment accumulation prevailed at west boundary when swell waves (12 second mean period) were used as the hydrodynamic loading. Wind waves simulations were completed properly without affecting the area of interest; consequently, wind wave simulations exclusively are presented in Chapter 5. To maximize productivity, additional changes had to be made due to associated contingencies faced while performing morphodynamic simulations; the grid size resolution was then decreased from 15 to 25 meters throughout the domain in order to optimize computational time. For grid resolution discussion see section 9.1.

In an effort to address the development of model instability at the boundary, additional model runs were performed including the effect of wind as a forcing agent. On model results corresponding to 80° waves with a period of 6.0 seconds, it was noted a time and space invariant wind load of 6.0 meters per second (intended to generate a littoral drift aside from the wave driven longshore current) was able to dissipate the sediment accumulation at the boundary.

Overall after the appropriate and necessary model adjustments were made (see model settings on section 3.3.4), the results corresponding to the morphodynamic simulations were considered stable and suitable for analysis.

Impact of roller model

The roller model “allows the modeling of the effect of short-wave groups on long waves. This effect is caused by spatial variations in the radiation stresses and causes long waves to travel along with groups of short waves” (Deltares, 2011). In the model “only the wave energy on the group scale [..] is modeled and is [and it] propagates shorewards. Wave energy released at wave breaking is first transferred to roller energy prior to dissipation causing a spatial lag between the location of wave breaking and the actual dissipation” (Reniers, et al., 2001).

Simulations were performed to evaluate the impact of the roller model. The findings presented on this section are based on the comparison between the implementation of the roller model and SWAN (using Battjes & Janssen, 1978). The roller model implementation resulted on:

- Significantly higher bed shear stresses (see Figure 9.2)
- Higher depth average velocities (see Figure 9.3)
- Higher sediment transport (see Figure 9.4)

Although the magnitudes of the bed shear stress seen on the roller model results tripled the magnitudes of the SWAN simulation, no spatial differences in the cross-shore distribution were observed. The increment in shear stresses properly correlates to the higher depth average velocities and higher wave heights. Overall, no spatial lag was observed when compared to the SWAN results.

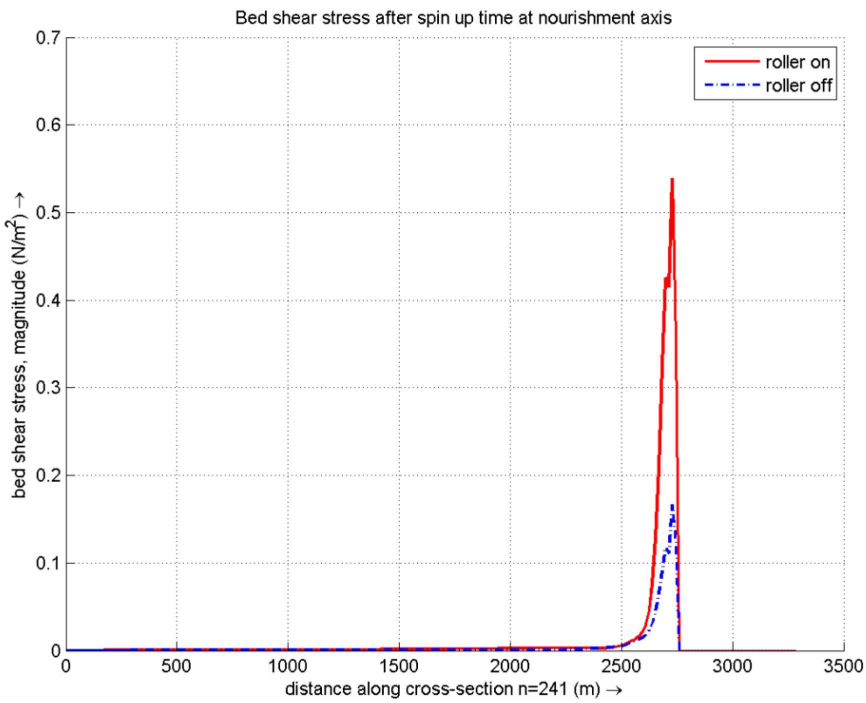

Figure 9.2 Cross-shore distribution of bed shear stress after spin-up time for large nourishment under 65 waves

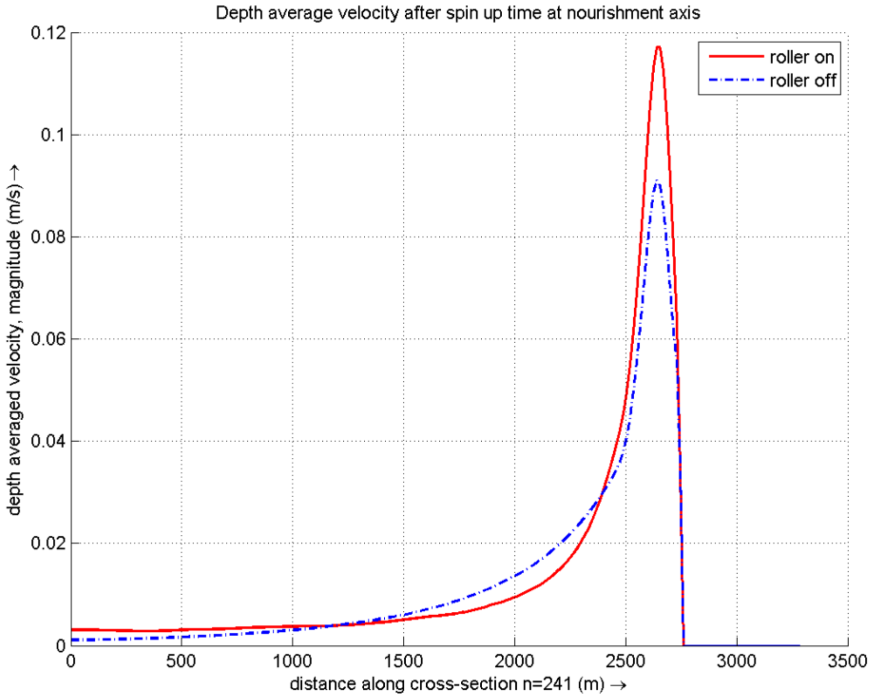

Figure 9.3 Cross-shore distribution of depth average velocities after spin-up time for large nourishment under 65 waves

Infragravity waves are expected to play a role in the transport of sediment; in fact, higher transport rates are observed when using the roller model (see Figure 9.4). Preliminary morphodynamic simulations results (Figure 9.5) indicate a better defined downdrift protuberance for large nourishment under the influence of 65° waves; it can be concluded, the roller model causes the smoothing of bathymetric features.

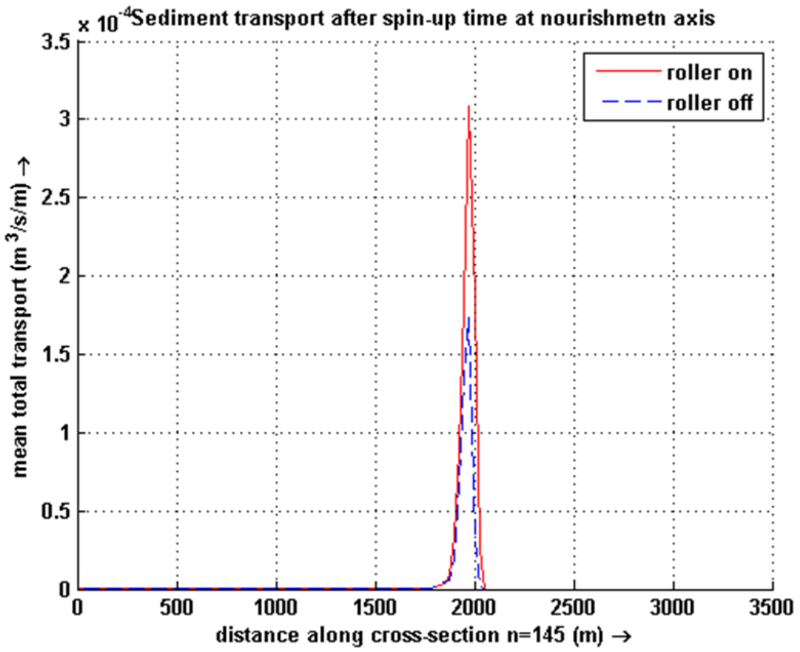

Figure 9.4 Cross-shore distribution of sediment transport after spin-up time for large nourishment under 65 waves

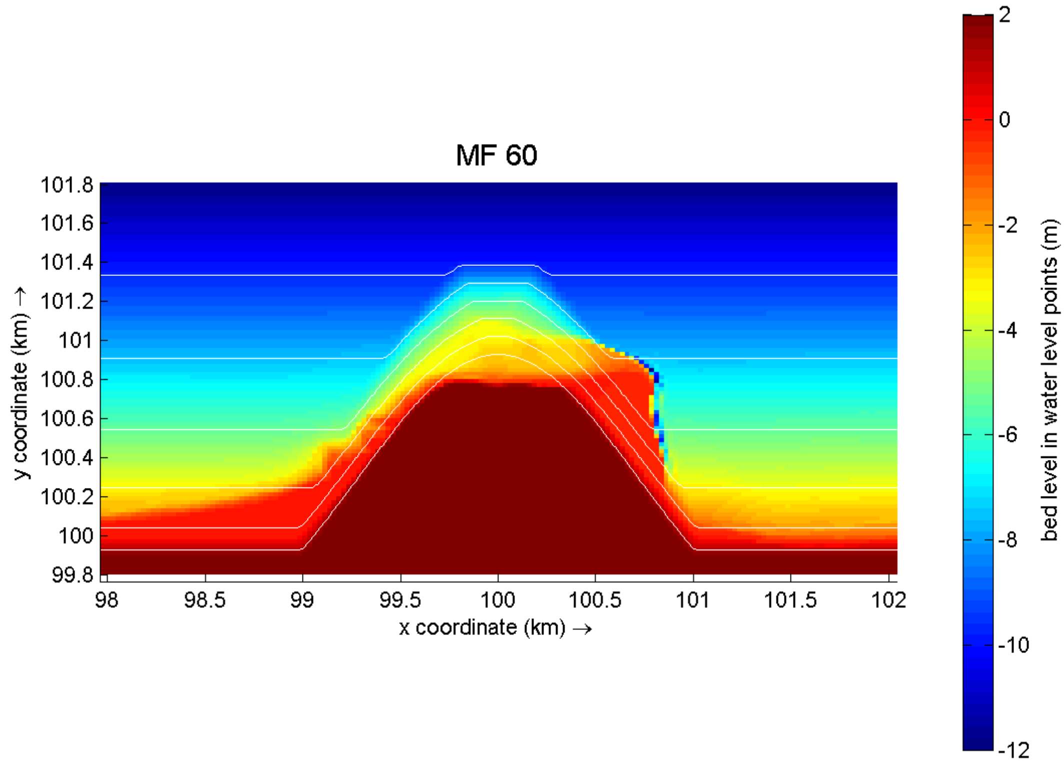

Figure 9.5 Preliminary results for morphodynamic simulation of large nourishment under the influence of 65 waves using the roller model

Impact of cross-shore sediment transport in nourishment reshaping

Results shown on section 5.2 indicate the downdrift migration of the large nourishment exposed to 15° waves occurs at deep water while diffusion takes place at shallow water. Further analysis was performed to assess the model sensitivity to the cross-shore contribution of sediment transport in the TRANSPOR2004 formula (e.g. the wave-related bed load and suspended load factors, BedW and SusW). Comparisons between the inclusion (BedW=0.2 and SusW=0.2) and exclusion (Bed=0 and SusW=0) of the wave related transport component were achieved via initial sediment transport distribution and skewness, morphodynamic simulations, and cross-shore integrated volume percentage change.

Figure 9.6 shows minor magnitude deviation between the initial sediment transport curves when including and excluding the wave-related transport component. As expected, excluding the wave related transport component results in lower transport magnitudes; the transport reduction occurs at the peaks and at the alongshore uniform areas. Consequently, the skewness calculations results in minor variations: -0.03 and -0.02 when including and excluding cross-shore transport, respectively.

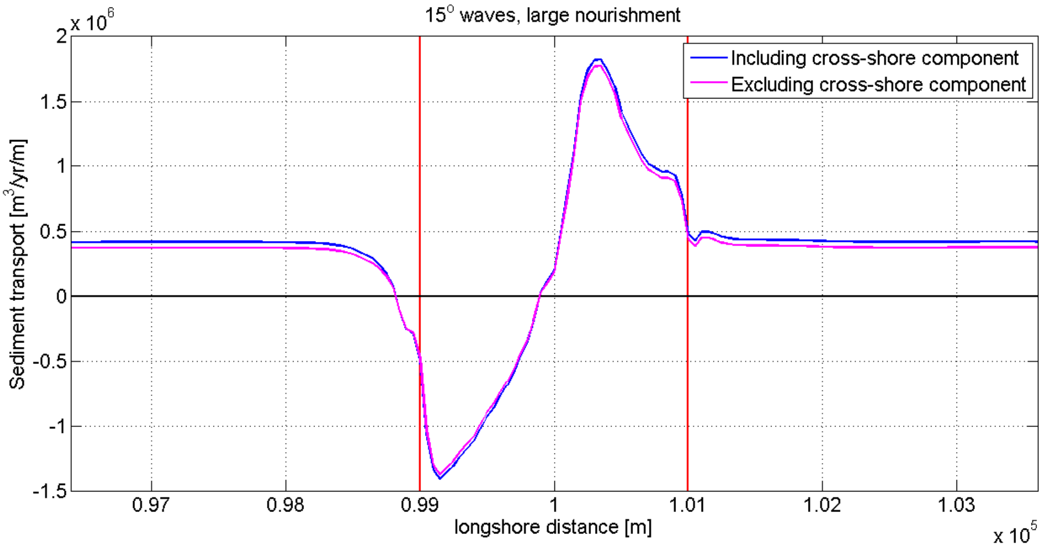

Figure 9.6 Instantaneous net longshore sediment transport through cross-shore transects for large nourishment under 15° wind waves, 6 second mean period, 1.5m wave height. Sensitivity analysis to the impact cross-shore sediment transport component

The impact cross-shore transport has on nourishment reshaping can be better appreciated on the morphodynamic simulations (see Figure 9.7). The results do exhibit similarities particularly at shallow depths where diffusion dominates; the deviations become notorious on the crest at deep water (-4 and -6 meter depth). In the absence of wave related transport, minor deep water crest retreat (shown on cross-shore integrated values Figure 9.6) and more symmetrical crest deformation are observed. Nonetheless, translation features appear: the deep water crest slightly migrates downdrift and the reduction of crest retreat compensates with downdrift erosion at -4 meter depth. When the cross-shore transport component is included, the deep water crest translation is more pronounced and the contours lines are smoother; hence, the downdrift migration of the object is attributed to the sediment transport contribution of waves.

What is striking about the morphological simulation results is the resolution of the sediment accumulation instability at the west boundary. Figure 9.7 indicates model stability when the cross-shore transport component is excluded from the simulations; therefore, the interaction between the Neumann boundary and the wave-related transport component results in the development of spurious solution. The necessary model adjustments fall out of this scope of work; pertinent recommendations are included in Chapter 7.

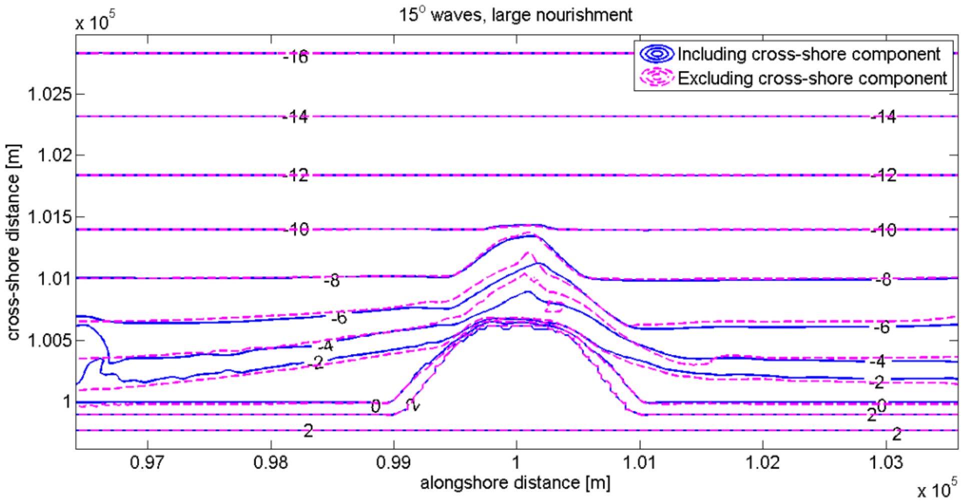

Figure 9.7 Detailed view of bed level changes before and after 2.55 years for large nourishment under 15° angle, 1.5 meter wave height, and 6 second mean wave period. Sensitivity analysis to the impact cross-shore sediment transport component

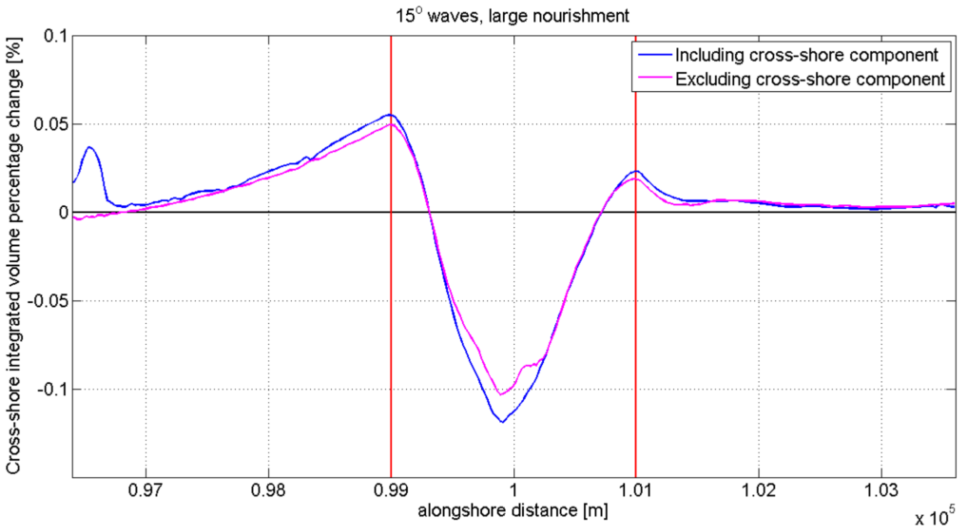

Figure 9.8 Cross-shore integrated volume percent change for large nourishment under constant wave condition: 15° angle of wave incidence, mean wave period of 6 second, and wave height of 1.5 meter. Nourishment bounds shown in red vertical lines.

9.3 Wave fields

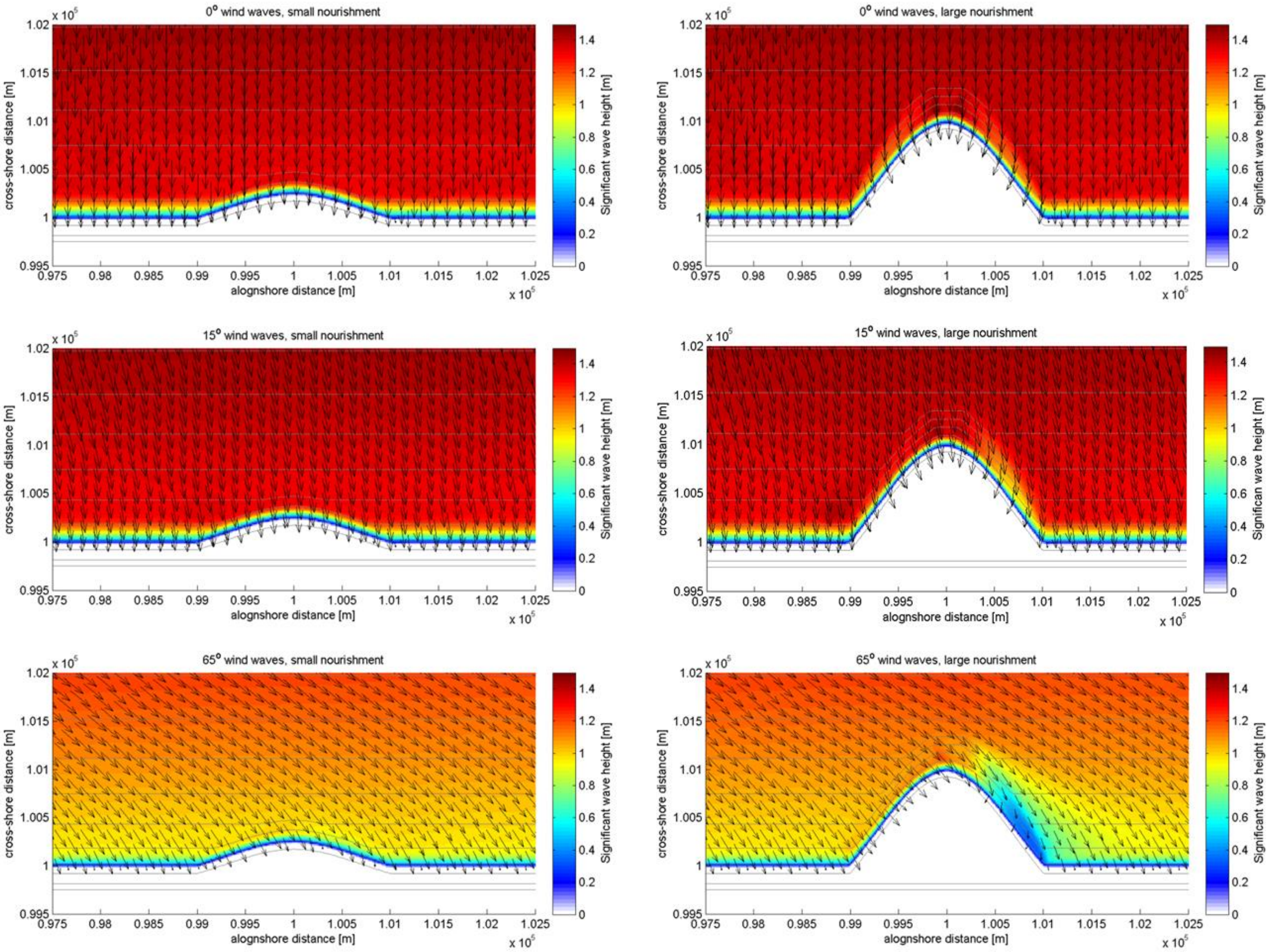

Figure 9.9 Wave fields for wind waves (6 second mean period) simulations: small nourishment on left panels, large nourishment on right panels, increasing angle of wave incidence (0°, 15°, 65°) from top to bottom panels. Color bar and scales kept constant to facilitate comparison

9.4 Longshore current fields

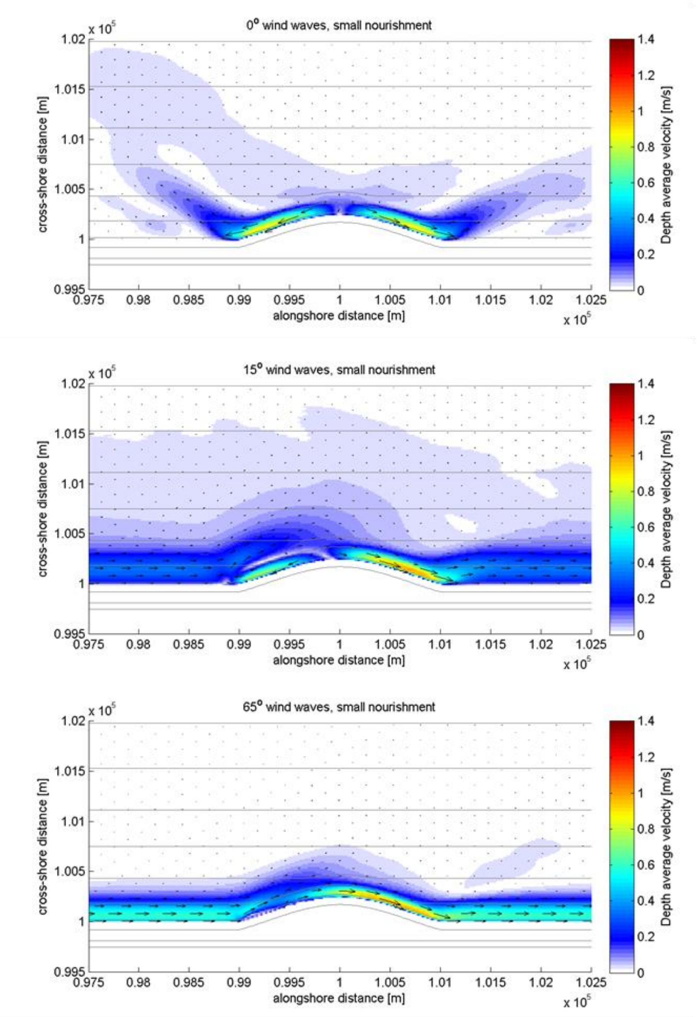

Figure 9.10 Depth average velocities field for wind waves (6 second mea period, 1.5m wave height) simulations: small nourishment on left panels, large nourishment on right panels, increasing angle of wave incidence (0°, 15°, 65°) from top to bottom panels. Color bar and scales kept constant to facilitate comparison

9.5 Sediment transport fields

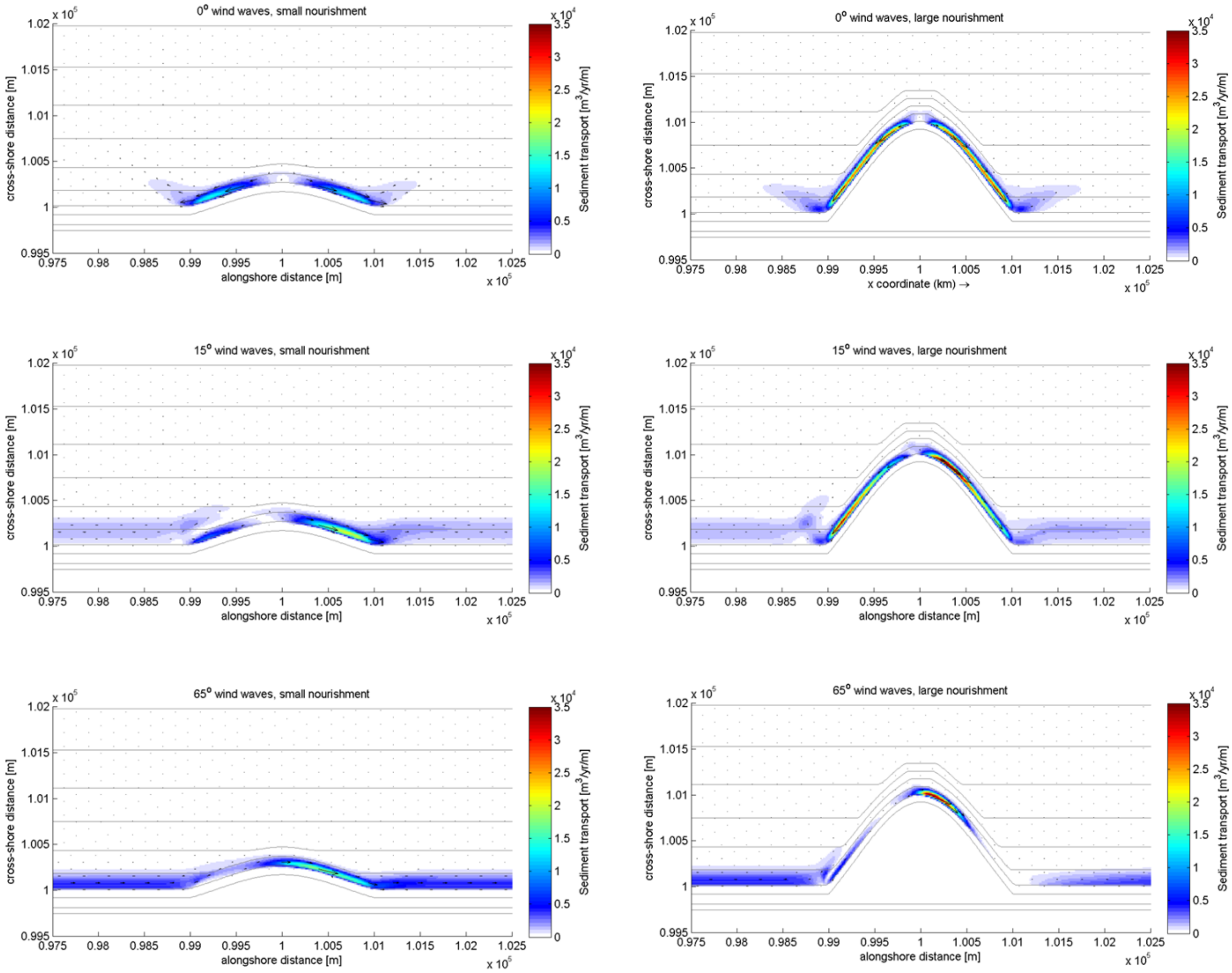

Figure 9.11 Instantaneous total sediment transport field (suspended and bed load transport) for wind waves (6 second mean period, 1.5m wave height) simulations: small nourishment on left panels, large nourishment on right panels, increasing angle of wave incidence (0°, 15°, 65°) from top to bottom panels. Color bar and scales kept constant to facilitate comparison

9.6 Results for time varying wave conditions

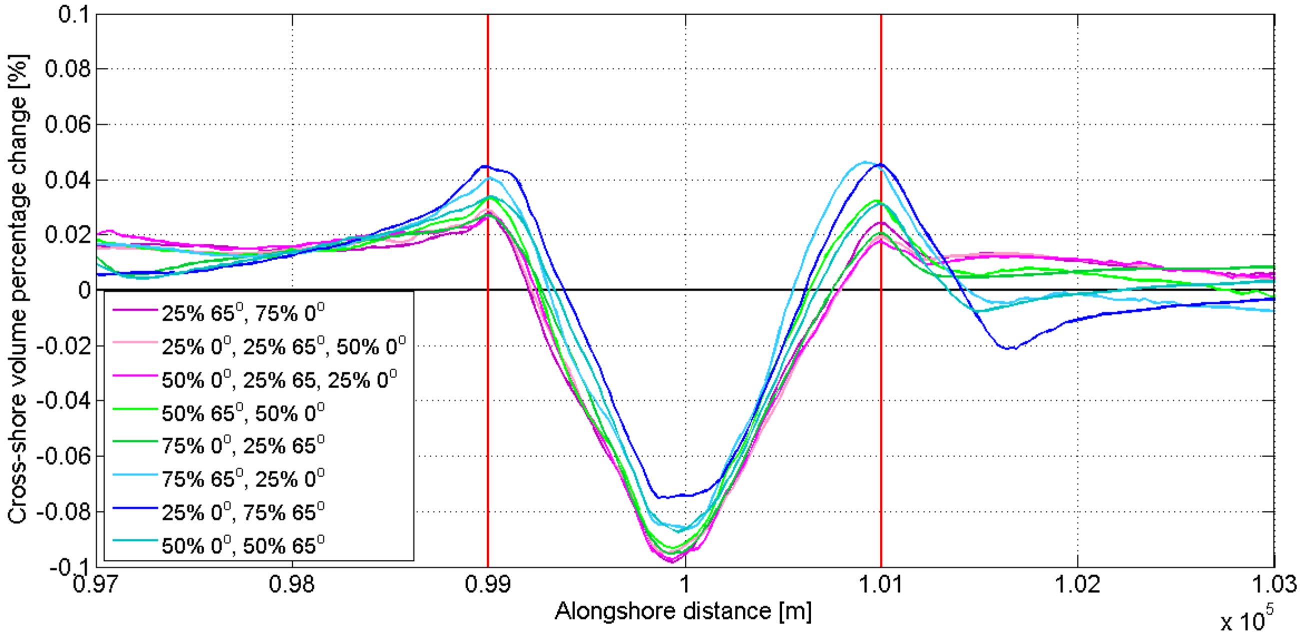

Figure 9.12 Cross-shore integrated volume percent change for time varying wave climate simulations with constant mean wave period of 6 second, and constant wave height of 1.5 meter. Nourishment bounds shown in red vertical lines